REPAIR OF FOCAL DEFECTS IN THE ANNULUS FIBROSUS USING AN *IN SITU*-PHOTOCROSSLINKABLE COLLAGEN HYDROGEL

A Dissertation

Presented to the Faculty of the Graduate School

Of Cornell University

In Partial Fulfillment for the Requirements of the Degree of

Doctor of Philosophy

By

Brandon Hayden Borde

January 2017

Repair of Focal Defects in the Annulus Fibrosus using an *In Situ*-Photocrosslinkable Collagen Hydrogel

Brandon Hayden Borde, PhD

Cornell University 2017

The intervertebral disc (IVD) is a cartilaginous structure in the spinal column comprised of the inner nucleus pulposus (NP) and the outer annulus fibrosus (AF). With untreated damage to the AF, the pressure forces the nucleus out into the surrounding disc space causing pain and, eventually, degenerative disc disease (DDD). Once an IVD has fully degenerated, treatment options are limited to full disc replacement or spinal fusion, and as such, research groups have begun to develop methods for tissue engineering repair and regeneration of damaged IVDs including repair of defects in the AF. This study evaluates an injectable, photocrosslinkable collagen hydrogel for the mechanical and biological repair of annulus fibrosus defects.

Collagen hydrogels for biomedical applications are often limited due their weak bulk mechanical properties. In order to increase their mechanical strength, researchers can increase the density of collagen in the final gel, crosslink the fibers of the resulting collagen gel, or both. The first aim observed the effects of collagen gels at different densities and degrees of riboflavin crosslinking on the repair of annulus fibrosus defects of different sizes in an *in vitro* rat caudal AF repair model. We observed improvements in the effective mechanical behavior of damaged IVDs with increasing collagen density and riboflavin concentration.

After establishing the collagen gel as a possible AF repair technology mechanically, we transitioned from an *in vitro* model to an *in vivo*, rat caudal model of

annular repair to better assess biological healing. The second aim centered on the use of both uncrosslinkined and crosslinked collagen gel formulations from aim 1 in an in vivo rat tail puncture model. We observed increased disc height and NP hydration, two markers of disc degeneration, in all treated groups. The highest improvement was exhibited in rats treated with the riboflavin-crosslinked collagen gels.

The third, and final aim discussed in this dissertation employed the same athymic rat tail puncture model to understand the effect of cell-seeded collagen gels on AF repair. Primary ovine AF cells were isolated and added to the crosslinked collagen gel formulations before injection into an *in vivo* AF defect. We observed greater disc height and NP hydration in animals treated with the cell-seeded collagen gel. Furthermore, cell-seeded gels exhibited integration with surrounding native AF tissue. These experiments establish that riboflavin-crosslinked collagen hydrogels are an excellent foundation for an annular repair therapy, and can be used to deliver cells in order to enhance repair.

BIOGRAPHICAL SKETCH

Brandon Hayden Borde is the son of Jennifer and Hayden Borde, both medical professionals based in New York. He entered college at the University of Maryland, Baltimore County as a Meyerhoff and MARC U*STAR Scholar, with a focus in biology and intent on medical school after graduation. After learning about the engineering methodology and coursework offered in the College of Engineering and Information Technology, Brandon switched official majors to mechanical engineering, in which he completed is Bachelors of Science Degree in May 2010. The Meyerhoff and MARC programs introduced Brandon to various research opportunities during this undergraduate tenure, all of which helped inform his decision to join the Biomedical Engineering program at Cornell University in pursuit of a doctoral degree with Dr. Lawrence Bonassar. While studying at Cornell, Brandon completed a master's degree in biomedical engineering as well as certification to be a personal trainer through the National Strength and Conditioning Association. He hopes to use knowledge on spine and cartilage injury gained during his doctoral journey to help aid the general public and more specifically those recovering from orthopedic injury.

This dissertation is dedicated to my Mom, Dad, sister Jillian,
and big brother Bobby Mozia.

ACKNOWLEDGEMENTS

First and foremost, I would like to that Lawrence Bonassar for guiding me through my journey from B.S., to M.S., to P.h.D. Larry is an excellent advisor who stuck with me through the great times and the many rough patches.

To Mom, Dad and Jillian: thanks for putting up with me being a student for so long and for all of your support.

Also, Dr. Roger Härtl at Weill Cornell Medical College has been a great guide and influence on me, especially when developing a technology with the ultimate goal of being in the operating room.

I would also like to thank Belinda Floyd, Amy Layton and Jason Millspaugh. Each of them, in their own special way, helped accommodate my some times crazy requests while being there to talk almost every morning.

None of this work would be possible without the Veterinary staff the Hospital for Special Surgery. They supported every surgery as well as looked after the animals for us.

Thanks to the amazing owners and staff members at Sheldrake Point Winery, The Cellar D'or, Corks and More/Red's Place and Hector Wine Company for providing community outside of the academic setting.

TABLE OF CONTENTS

CHAPTER 1

Introduction:

1.1 The Annulus Fibrosus

Vertebrate animals are allowed central motion and flexibility through the spinal column, which consists of an alternating series of vertebral bones and cartilaginous intervertebral discs (IVDs). Each IVD is comprised of two distinct main regions, an inner nucleus pulposus (NP) and outer annulus fibrosus (AF). The NP is gelatinous, glycosaminoglycan (GAG) rich, and as such very hydrated when normal and healthy. It comprises the core of the IVD, encased between the adjacent vertebral bodies and inside of the AF[1,2].

Unlike the NP, the AF has a more rigid fibrous structure comprised of concentric lamellae. Each lamella contains type I collagen fibers angularly aligned at 30-45 degrees from the transverse anatomical plane[3]. In the outermost lamellae these fibers, called Sharpey's fibers, run into the adjacent vertebral bodies creating anchors within the bone[1]. Fibers in the inner AF run parallel to the vertebral endplates, creating an envelope around the gelatinous NP. When the IVD is healthy, the NP is pressurized between the vertebral bodies and within the annulus, creating tensile forces transferred through the annulus via the collagen network. This interplay between the NP and AF makes the IVD a strong but flexible structure, able to facilitate motion, such as bending and twisting, as well as the transfer of force through the body[4–7].

The IVD exhibits gradual cellular changes from the outer AF to the center of the NP[3]. The outermost lamella is the most fibrous, with cells that have large

processes and interconnected networks like fibroblasts. Cells in the inter-lamellar septae are flat and also have large processes. Towards the inner AF, the length of the cellular processes decreases, with lower interconnectivity between cells. The nucleus contains rounded cells, reminiscent of articular chondrocytes, embedded in a network of glycosaminoglycans and type II collagen[8].

1.2 Annulus Damage and Disc Disease

IVD damage spans a range from relatively benign focal lesions in the outer AF to full blown degenerative disc disease (DDD). Along this spectrum, is the case of a bulging, or herniated disc. This condition occurs when the AF is weakened by age or trauma, and pressure in the NP causes the disc to bulge at the damaged site into the surrounding disc space[9]. Complete loss of AF integrity leads to the displacement of NP tissue through a full-thickness AF defect (Figure 1.1) , putting pressure on the surrounding nerves and causing pain. The architecture of the posterolateral AF makes it especially prone to herniation since studies have shown that this region of the IVD often possesses more irregularities, creating stress concentrations in transition zones that often coincide with the location of disc hernations[10–12]. Disc damage at these transition zones directly contribute to back pain since the spinal cord and nerve roots are located directly adjacent to the posterolateral annulus. Furthermore, NP tissue has been shown to be an irritant to surrounding nerve tissue[6,13], often resulting in

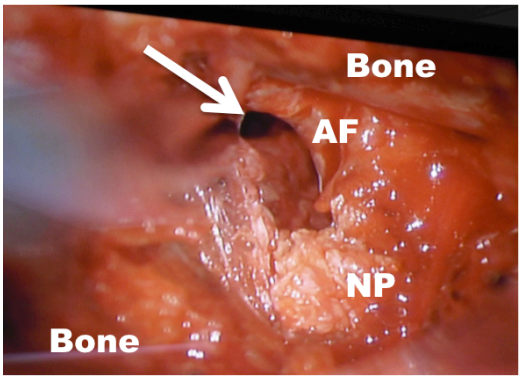

Figure 1.1: Photo of an intra-operation AF defect. Photo courtesy of Dr. Roger Härtl

inflammation to the associated nerve roots. If left untreated, the injury will progress to full degeneration.

DDD is a complicated condition, with many causes and manifestations. Generally, the afflicted disc exhibits a loss of height, damage to the endplates, osteophyte formation close to the endplates as well as changes in both the NP and the AF[2,11,14]. Major changes in the NP include loss of hydration and GAG content[8], with normal tissue being replaced with disorganized fibrous tissue. As the disease progresses, the AF begins to undergo phenotypic changes such as the fusing of lamellae and eventual ingrowth of nerves and vascular fibrous tissue[8,15,16].

While the physical changes in damaged IVDs play a major role in loss of function and diagnosis, researchers have also observed biological and chemical changes in animal models of disc degeneration that coincide with the physical transformations[13,14]. With knowledge of both the physical and biochemical manifestations of IVD damage and degeneration, a slew of treatment options have become available, ranging from conservative all the way to surgical. Spine and intervertebral disc research efforts have also intensified to continue foster understanding of degeneration and new treatment directions.

1.3 Current Treatment Options

Much like IVD disease conditions, treatment options cover a range depending on type and severity of the damage. Very severe cases consist of a degenerated disc that is no longer able to facilitate motion without pain, and has begun to fuse between the adjacent vertebral bones. In this case, medical personnel would often choose to remove the remaining disc and accelerate fusion already occurring within the disc

space[17,18]. While this creates a stable motion segment, there is often a dramatic loss of motion for the patient, even more so if the fusion is done in the cervical or thoracic region of the spine. If the diseased disc space shows little signs of osteophyte formation (fusion), or if the patient is young, total disc replacement becomes a more appealing option[18].

The majority of total disc replacements are low profile ball-socket joints made of synthetic materials. While they allow for a wider range of motion than a fusion, the use of synthetic materials do not allow for biological healing at the disc space[19]. Tissue engineered IVD replacements are currently being developed that look to provide the mechanical support necessary to the disc space while allowing for cell infiltration and regeneration of the IVD[19–24]. This research shows great promise, however due to drawbacks in mechanical performance, biomaterial choice and regenerative potential, it is favorable to treat disc damage earlier in the degenerative spectrum in order to preserve as much native tissue and function as possible.

The focus on specific NP and AF repair methods has increased recently in attempts to treat early degenerative damage. These repair methods range from solely mechanical structures to biological therapeutics meant to induce regeneration of the damaged tissue[17,25–30]. Nucleus replacements are being developed that have been shown to return mechanical function to a damaged IVD once the native NP is removed. Replacements developed with biological materials such as collagen sponges have been implanted to return mechanical function while providing a scaffold material for tissue ingrowth[24]. While results from these studies have been promising, their

efficacy is limited due to the lack of integrity in the AF[31]. As such, AF regeneration and repair strategies have become more prevalent (Table 1.1).

A slew of surgical treatment options for AF are available for current use in the OR, with many more working through the research and development pipeline. Suture methods for small AF defects have been tested on cadaver models as well as in the clinic with encouraging results [32–34]. This method is limited by the defect size that can be addressed as well the introduction of additional defects to the AF with the sutures. Barbed plugs have also been developed that act as a physical barrier to NP displacement, however these plastic plugs have been shown to displace or wear and break in the disc space causing further damage[35]. An internationally available technology, called the Barricaid, is anchored into the adjacent vertebral bone and is a physical barrier to additional NP hernation[36,37]. While promising, these too have been displaced or damaged in the disc space. Furthermore, the anchoring of the implant imparts necessary damage the adjacent bone/endplate. These AF repair technologies all provide some mechanical support, but suffer physical failure and do not allow for biological healing at the defect.

1.4 Tissue Engineering For Annulus Repair

The natural characteristics of the annulus, such as the multi-lamellar structure, pose various challenges to research groups in development of AF-mimics and possible repair methods. Many of these characteristics have been recapitulated as part of tissue engineered total disc replacements (TE-IVDs). Nerurkar et al was able to recreate the lamellar and angular alignment of the natural AF in electrospun sheets[38]. Nesti also employed electrospinning to recreate the AF using PLLA sheets[19]. Bowles et al

recreated the natural circumferential alignment of the AF using primary ovine AF cells suspended in a collagen gel allowed to contract around an inner mandrel[21,39]. A handful of other TE-IVDs exist that attempt to recreate the characteristics of the natural AF, with varying degrees of success[40–45]. These technologies show potential for total disc replacement and possibly large AF region repair, however they would be difficult to implement in focal defect repair through modern surgical methods. As such, tissue engineered AF repair methods are developing to address these difficulties.

When considering AF repair methods, Bron et al. published a set of criteria that an effective treatment should satisfy to encourage both mechanical and biological healing[9]. Since the disc provides both mechanical function in support of stability and movement, and biological function as a living tissue, a successful repair method should satisfy these criteria[9]:

1. Restore mechanical function
2. Fill gap in the AF
3. Affix to surrounding tissue
4. Allow cells to survive, thrive
5. Do no further damage or cause irritation

The mechanical repair methods referenced in Section 1.3 have shown limited success, with many of the limitations linked to criteria 4 and 5 listed above. Tissue engineered AF structures, while aiming to recreate components of the native AF for replacement, often fall short in application to repair when preservation of much of the native AF is desirable.

Injectable AF repair methods are currently being developed that would allow for healing at the defect site while providing short-term mechanical support to prevent NP hernation. Some of these employ currently used surgical glues[34,46,47], while others have been developed specifically for AF repair[46,48–51]. Schek et al have developed at genipin-crosslinked fibrin glue that has been shown to meet the mechanical performance of native AF tissue, while allowing for high cell viability[48]. Further studies will help assess the ability of the glue to maintain its place in an actual annular defect. Chik et al. have developed a pre-formed annulus plug made of collagen made to keep NP therapeutics from leaking out of the AF once delivered[52]. They have shown limited success in a rabbit model, with some evidence of osteophyte formation even with the treatment. These studies, although limited, underscore the need to repair the annulus to encourage healing. Furthermore, they support the efficacy of an injectable method of AF repair in the treatment of early disc damage. In both of these cases, a "natural" biomaterial was used in order to encourage biological healing the defect site. Fibrin and collagen are found in the body, however fibrin is most closely associated with clotting.

1.5 Collagen: The Biomaterial

Collagen is one of the most abundant proteins in the human body, providing much of the structural integrity to organs and other structures. Multiple types of collagen have been characterized, but the fibrous type I is known for its contribution to tensile load bearing tissues such as the AF. Each type I collagen backbone is comprised of a repeating Glycine-X-Y primary structure in which proline and hydroxyproline are the most common side chains in the "X" or "Y" position[53,54].

These backbones are arranged in a triple helix with "unwound" ends to form the most fundamental building block of the collagen fiber, procollagen. Once procollagen is secreted into the extra cellular space, the unwound ends are enzymatically cleaved resulting in tropocollagen. These tropocollagen molecules then assemble into fibrils, and then eventually large fibers, such as those seen in the AF[53,55–57].

The molecular structure of collagen is highly conserved between species, making it an excellent candidate for biomedical applications. Collagen can be sourced from a variety of places such as animal skin[56], plant material[58], and rat tendon[59]. Once harvested, the collagen can be broken down, purified and reconstituted in many forms[56]. Perhaps the most widespread use of collagen, other than in food, is the application of collagen hydrogels in medicine and scientific research.

Collagen gels are most often made by harvesting large fibers from one of the previously sources, and solubilizing them in an acidic solution. The low pH disrupts the molecular interactions that keep the collagen as fibrils, while preserving the basic triple helical structure [59–61]. In preparation for use, the pH of the solution can be restored to neutral, allowing the collagen fibrils to polymerize and create a hydrogel. These gels have marked advantages for use in research applications such as high availability, biocompatibility, and relative ease of use[62].

While collagen gels have seen tenured use in biomedical research, their application is often limited in load-bearing settings. They are most often employed at low densities (<5 mg/ml), which have been known to exhibit weak bulk mechanical properties[63]. Furthermore, with the common reconstitution methods mentioned above,

the large fibrous formation and alignment is lost leading to reduced tensile performance compared to natural type 1 collagen tissues[64,65].

The use of crosslinking in collagen hydrogels has been shown to help enhance their mechanical performance[66–68]. Crosslinking can be achieved using chemical, photochemical and thermal means. The most common crosslinking agents, especially for collagen, include aldehydes, enzymes, carbodiimides and sugars[69–73]. The aldehydes are employed as tissue preservatives because of their ability to create relatively irreversible links within tissues, thus "freezing" them in their current state. While wildly effective, these aldehydes are toxic and are not normally used for biomedical purposes. Enzymatic and carbodiimide crosslinkers are studied for their role in development of tendon and ligaments[67,72,74], but have seen limited use is biomedical applications. Sugars have been shown to crosslink over time when in the presence of collagen through the Maillard Reaction[75,76]. This process, called glycation, is most associated with aging and in diabetic populations due to the increased presence on glucose in the blood stream[77–79]. However, glucose is not the only sugar capable of glycation. Ribose and riboflavin have been used as crosslinkers of collagen that also act through glycation[66,70,80–82].

1.6 Riboflavin Crosslinking of Collagen

Riboflavin is a relatively common molecule with a host of applications ranging from nutrition to clinical application. Its structure consists of a five-carbon ribose backbone with a three-ring flavin bonded to the end of the chain. While its most traditional usage is as vitamin B2 in supplements and food additives, it is employed in research as a fluorescent dye and crosslinker.

As a type-I photocrosslinker, riboflavin interacts directly with the collagen to create crosslinks [59,81]. It is currently used clinically in the treatment of the ocular condition keratoconus [68], in which structural stability in the cornea is lost causing it bow out. A riboflavin solution is introduced to abrasions made on the cornea and the eye is exposed to UVA light in order to initiate crosslinking of the existing corneal collagen fibers[68,83,84]. This strengthens the cornea, preventing further deformation and preserving eyesight.

In scientific research, riboflavin has been studied as a method for preventing fibrous collagen construct contraction[66]. When seeded with cells, type I collagen gels will contract over time, which is unfavorable in applications where size and shape fidelity are needed. Post-glycation with riboflavin has been shown to prevent the contraction of low density collagen gel constructs, while preserving high cell viability[66]. The use of UVA light in the initiation of crosslinking is not required, as blue wavelength light can initiate the crosslinking process as well[85], further enhancing the biocompatibility of riboflavin crosslinking.

1.7 Objective Statement

With this work, we endeavor to establish collagen hydrogels as an injectable repair for the damaged annulus fibrosus. Collagen is a versatile biomaterial that has been shown to be applicable to a wide variety or biomedical applications, including the intervertebral disc. Once crosslinked with riboflavin, the applicability of the gel as an injectable repair method increases due to the enhanced mechanical performance while maintaining the biological compatibility needed for long-term healing.

1.8 Specific Aims

This dissertation investigates the use of collagen hydrogels for injectable repair of the annulus fibrosus through three aims:

1) Establish the efficacy of collagen hydrogels in an in vitro model of AF repair through screening multiple gel formulations and evaluating the mechanical effects on an entire IVD.
2) Investigate the ability of crosslinked collagen gels to biologically repair the AF and observe the effects of repair on disc degeneration.
3) Evaluate the effect cell-seeding on the integration of crosslinked collagen gels with the remaining native AF

CHAPTER 2

Injectable, high-density collagen gels for annulus fibrosus repair: An *in vitro* rat tail model.

This chapter has been published:

Borde, B., Grunert, P., Härtl, R., & Bonassar, L. J. (2015). Injectable, high-density collagen gels for annulus fibrosus repair: An in vitro rat tail model. *Journal of Biomedical Materials Research - Part A*, 2571–2581. http://doi.org/10.1002/jbm.a.35388

2.1 Abstract

A herniated intervertebral disc often causes back pain when disc tissue is displaced through a damaged annulus fibrosus. Currently the only methods available for annulus fibrosus repair involve mechanical closure of defect, which does little to address biological healing in the damaged tissue. Collagen hydrogels are injectable and have been used to repair annulus defects *in vivo*. In this study, high-density collagen hydrogels at 5, 10 and 15 mg/ml were used to repair defects made to intact rat caudal intervertebral discs *in vitro*. A group of gels at 15 mg/ml were also crosslinked with riboflavin at 0.03 mM, 0.07 mM or 0.10 mM . These crosslinked, high-density collagen gels maintained presence in the defect under loading and contributed positively to the mechanical response of damaged discs. Discs exhibited increases to 95% of undamaged effective equilibrium and instantaneous moduli as well as up to four fold decreases in effective hydraulic permeability from the damaged discs. These data suggest that high density collagen gels may be effective at restoring mechanical function of injured discs as well as potential vehicles for delivery of biological agents such as cells or growth factors that may aid in the repair of the annulus fibrosus.

2.2 Introduction

A bulging or herniated intervertebral disc (IVD) can cause back pain, leg pain and neurological deficits when the nucleus pulposus (NP) is displaced through a damaged annulus fibrosus (AF). AF damage occurs in a variety ways including natural weakening over time, trauma, or as an unintentional result of medical treatment (e.g. discography, discectomy). In the United States, an estimated $90 billion per year is spent on assessment and treatment of lower back pain alone [86]. This damage also affects the motion segment mechanically, with loss of disc stiffness [12,87,88] and biologically, in subsequent degenerative effects [87,89–91].

In most cases, partial discectomies alleviate the pain of a bulging or herniated disc; however the resulting annular defect is often left untreated. This increases the likeliness of recurrent disc herniations through the open defect. Clinical studies have shown that the rate of recurrent herniation after partial discectomy lies between 5%-20% with many of the patients requiring additional procedures. Furthermore, the rate of reherniation has been shown to correlate with the size of the original surgical defect [9,92,93]. In order to improve recovery after treatment, it is highly desirable to address the remaining AF defect after discectomy.

Annulus repair strategies have been devised to address many different defects in damaged AF tissue [31,32,35,37,48,94,95]. These therapies aim to mechanically close lesions in the AF to prevent prolapse and perhaps slow or inhibit degeneration. The types of annulus closure treatments that are in development range from purely mechanical methods to tissue engineered strategies, all with varying degrees of success. Many mechanical strategies are already commercially available (i.e. suture,

barrier, plug). These mechanical treatments block the AF defect while inhibiting short term reherniation. Studies have shown that disc compressive mechanical properties are affected when the annulus fibrosus is subject to full thickness defects, leading to diminished time dependent mechanical behavior and eventual degeneration[16,96,97]. While these solutions address the load bearing requirements of the IVD, they do not encourage the long-term regeneration of tissue in the damaged area, which is intrinsically difficult to achieve due to the limited self-healing potential of the AF [98].

Tissue engineered strategies are being developed with the goal of achieving biological healing, along with satisfying the requirements for mechanical support. Various scaffolds such as fibrin and silk have been used to develop laminates or adhesives to address the damaged AF. Furthermore, a host of studies have examined the effectiveness of different cell/scaffold combinations in creating AF-mimicking structures [38,44], while others have created tissue engineered total disc replacements with a construct that mimics the native AF [5,19–21,99]. These approaches are promising but their effectiveness in repairing AF defects *in situ* has not been reported. A major obstacle for many tissue engineering approaches is delivery of the material or device to an irregularly shaped defect. For clinical use, an injectable formulation is desirable due to the potential delivery by minimally invasive approaches.

Collagen hydrogels have been used for a variety of tissue engineering applications, enabling delivery of many cell types including chondrocytes and IVD cells [66,100]. Collagen is injectable and highly biocompatible in the disc space as both an NP replacement material and AF repair material [101,102]. Typically, collagen gels are

weak and exhibit low stiffness at densities less than 5mg/ml. However, gel stiffness can be tuned by controlling concentration or crosslinking [69,70,82,103–105].

A variety of crosslinking agents have been used with collagen, including formaldehyde, and glutaraldehyde. Although their effectiveness has been proven, these aldehydes are also cytotoxic, thus limiting their application in biological systems[69,103]. To address these limitations, groups have used sugars and flavins to induce crosslinking in collagen-based structures[66,70]. Riboflavin is particularly attractive because it is used clinically to strengthen the collagen structure of the cornea in the treatment of keratoconus[68,106]. Further, riboflavin is photo activated and as such crosslinking is tunable by exposure to UVA-wavelength light. Riboflavin crosslinking of collagen gel constructs was shown to increase their mechanical stiffness while maintaining high cell viability[66]. These factors make riboflavin crosslinking a viable tool in the use of collagen hydrogels for tissue engineering.

We have successfully used high density, riboflavin-crosslinked collagen gels in an *in vivo* rat tail AF repair model. Crosslinked gels slowed or prevented the onset and progression of degeneration in rat caudal IVDs as evidenced by higher disc heights and NP hydration than untreated discs for up to 5 weeks after treatment[102]. Furthermore, discs treated with crosslinked collagen gels maintained healthy disc phenotype as seen in histological sections. Although these results were encouraging, the mechanical contribution of injectable repair with these gels is unknown. This study investigated the use of injectable, crosslinked high-density collagen gels to fill and mechanically repair focal defects in the annulus fibrosus of a rat caudal intervertebral disc. We report the effect of different defect sizes on effective disc

mechanical properties, as well as the effects of increasing gel collagen density and riboflavin concentration on effective disc stiffness and hydraulic permeability.

2.3 Materials and Methods

Mechanical testing was performed on intact, cadaveric rat caudal motion segments to assess the extent to which injectable collagen gels restored performance to damaged intervertebral discs. In parallel studies, the effect of two different sized defects were examined, with each motion segment tested prior to damage, after the introduction of a defect to the AF, and after this defect was filled with a high density collagen gel. In separate studies the effect of crosslinking was assessed using a range of concentrations of the photocrosslinking agent riboflavin.

Collagen gel preparation

Collagen fibers were harvested from rat tail tendons as described previously [39,104,107]. The resulting collagen mass was then weighed and digested in a 0.1% acetic acid at a concentration of 150 ml/g tendon for at least 48 hours. Digested collagen was then centrifuged at 9000 RPM for 90 minutes at 4°C and the supernatant collected and frozen at -80°C. After lyophilization for 48 hours, the dehydrated collagen was weighed and reconstituted in 0.1% acetic acid at the stock concentrations of 6, 12, and 20 mg/ml. Each collagen stock solution was stored at 4°C until use.

For high-density samples, final collagen gel solutions at 5, 10, and 15 mg/ml were made by mixing the acidic stock solutions with basic working solutions composed of 10x Dulbecco's Phosphate Buffered Saline (DPBS), 1N sodium hydroxide (NaOH) and 1x DPBS. Each working solution was dyed with trypan blue at a ratio of 10:1, respectively, to track the fate of the injected gel. Crosslinked collagen

gels were mixed at the highest density (15 mg/ml), with varying amounts of riboflavin. Each gel was prepared in the method above, however riboflavin was added to the 1X DPBS at concentrations of 0.25, 0.50, or 0.75 mM , resulting in gel concentrations of 0.03, 0.07, and 0.10 mM respectively. Upon delivery to the defect site, crosslinked gels were exposed to 468 nm blue light (~1400 mW/cm^2) for 40 seconds to initiate crosslinking.

Dissection and segment handling

Frozen tails from 34 7-8 week old Sprague-Dawley rats were thawed in room temperature DPBS. The skin was removed and the tissue was dissected from the most proximal three vertebrae. The most proximal complete motion segment (bone-disc-bone) was cut from the rest of the tail at the adjacent intervertebral disc. Remaining tail material was discarded and the dissected motion segments were kept in room temperature DPBS. After the first phase of mechanical testing, a defect was created at the midline of the intervertebral disc by either rotating a beveled 21-gauge needle (small), or by removing a ~1 mm^2 window of the AF using a #11 scalpel blade (large) (Figure 2.1). Each defect was limited to only the AF by using a depth stopper (small)[108] or using care to only remove the AF with the scalpel (large). The damaged motion segment was tested mechanically again before filling the defect with the desired final collagen gel solution. About 100µL of the collagen gel was delivered to each defect using a 27-gauge precision tip needle (Nordson EFD, Robbinsville, NJ). Allowing 30 minutes for collagen gel polymerization after delivery, the motion segment was mechanically tested again. Upon completion of testing, the segments were either stored at -20°C for gross examination, or processed for histology.

Mechanical testing

Dissected motion segments were loaded into an Enduratec ELF 3200 test frame (Bose, Eden Prairie, MN) using custom grips (McMaster-Carr, Aurora, OH)[21]. All manipulation of the motion segment was performed while mounted on the load frame so as to preserve the original undamaged height of the motion segment. Each motion segment was allowed to relax for 10 minutes to ensure all initial transient effects were gone before testing began. Stress-relaxation testing was performed on each motion segment in steps of 5% compressive strain to a total displacement of 20% initial disc height. Testing in this manner allowed us to observe compressive stiffness as well as the hydraulic permeability from relaxation. This loading scheme was performed on the undamaged motion segment and repeated for both damaged and treated phases.

Data Analysis and Statistics

Load data were recorded directly during mechanical testing at 1 Hz for 50 minutes. All data analysis was performed using Excel or MATLAB software. Load curves were generated for each test in order to qualitatively compare disc behavior before and after treatment with the collagen gels. Using a custom MATLAB script, a poroelastic model (Figure 2.2, Equ. 1) was fit to the raw load data to determine the effective equilibrium modulus (A+B), effective instantaneous modulus (B) and time constant of relaxation (τ) with time (t). Effective hydraulic permeability (k) was calculated using the equilibrium modulus (E), disc radius (r), and time constant from poroelastic model fit (Figure 2.2, Equ. 2)[21,104,109]. One-way ANOVA with repeated measures including Tukey's HSD test for *post hoc* analysis was conducted to examine

the general effect of injectable collagen gel treatment on all samples. Analysis of the separate effects of collagen gel density or crosslink concentration was carried out using separate one-way ANOVA with Tukey's HSD test for *post hoc* pairwise analysis. All statistical analyses were conducted using JMP.

Histology

Whole IVDs were dissected from the frozen motion segments and fixed in 10% formalin for at least 48 hours before transfer to 70% ethanol. Fixed discs were embedded in paraffin wax and sectioned parallel to the transverse plane and affixed to glass slides. Histological slides were stained with Safranin-O with a Fast Green counterstain for proteoglycan content and general tissue architecture. Stained slides were viewed under bright-field microscopy for NP content and general tissue organization.

2.4 Results

The ability of high density, crosslinked collagen gels to repair defects in the AF of rat caudal IVDs was assessed both visually and quantitatively though effective disc mechanical properties. Photographs of transverse cross-sections of discs treated with 10 and 15 mg/ml gels in smaller defects (Figure 2.3a and 2.3b) and 15 mg/ml gel in the larger defect (Figure 2.3c) demonstrated the presence of dyed collagen gels in all cases, after the completion of the loading studies. In all cases collagen was present in the AF defect, while in the larger defect, some gel was also observed in the NP space. Histological analysis showed a clear defect in the AF created with both the 21-gauge needle and scalpel blade, severing all lamella and exposing the NP (Figure 2.4). Figure 4 shows a small defect repaired with a crosslinked collagen gel, with a gel

patch adhered to the outer AF. Figure 2.4 also shows a large defect treated with a crosslinked collagen, however there is no evidence of the collagen gel after testing. These data indicate that injected high density collagen gels remained in place in AF defects either in whole or in part after IVDs had been compressed by up to 20%.

Based on temporal traces of the load, both defects had a profound effect on the compressive behavior of the motion segment. In particular, the instantaneous, peak stresses achieved directly after steps in compression were significantly diminished by the injury and were partially restored immediately after the injection of the collagen gel. Stress relaxation after steps in strain appeared to occur much more rapidly in damaged motion segments compared to either uninjured motion segments or those in which defects had been filled with collagen gels (Figure 2.5).

Using the temporal load data, the effective equilibrium and instantaneous moduli and effective hydraulic permeability were calculated for both defect types and for all collagen gel densities. The average effective equilibrium and instantaneous moduli of uninjured intervertebral discs were 170 ± 54 kPa and 272 ± 133 kPa, respectively, while the average effective hydraulic permeability was $2.07 \times 10^{-14} \pm 1.27 \times 10^{-14}$ $m^2/Pa \bullet s$. These values are similar to those reported previously for rat caudal intervertebral discs[20,21,110].

To specifically assess the effect of injury and treatment on the mechanical performance of the intervertebral discs, the mechanical properties after injury and treatment for each sample were normalized by the value of the uninjured disc. As such, all data displayed are unitless, with 1 being the value of the uninjured sample. The efficacy of each collagen gel formulation at restoring the effective equilibrium

and instantaneous moduli and effective hydraulic permeability were assessed separately, as well as pooled to assess the general effect of treatment.

Larger defects had profound effects on mechanical properties, resulting in 60% ($p<0.001$) decreases in effective equilibrium and instantaneous moduli, and a 400% ($p<0.05$) increase in hydraulic permeability, compared to smaller defects which produced 18% and 28% ($p<0.05$) decreases in moduli and a 114% ($p<0.01$) increase in permeability (Figure 2.4). Treating AF defects with collagen gel formulations increased the effective equilibrium modulus of samples with small defects to 85% of uninjured values. In contrast, filling large defects with collagen gels had little effect on the effective equilibrium modulus. Delivery of collagen gels nominally increased the effective instantaneous modulus by 6-8% of the undamaged values, but this change was not statistically different from the damaged case. The largest effect of delivering collagen gels to the defect was in restoring the hydraulic permeability of samples with small defects. Delivery of collagen gels decreased the effective hydraulic permeability from 215% of the undamaged value to 133% of the undamaged value ($p<0.05$ compared to damaged and $p>0.98$ compared to damaged). Treatment with collagen gels had a similar effect on the effective hydraulic permeability of intervertebral discs with large defects, which were 600% of control both before treatment and 400% after repair.

Collagen gel density showed no significant impact on AF repair in small defects. Collagen gels of 5 mg/ml increased effective equilibrium and instantaneous moduli slightly over the damaged value. All three tested gel densities decreased effective hydraulic permeability by 50% from damaged values. In samples with larger

defects, both 5 and 10 mg/ml samples did not improve effective equilibrium or instantaneous modulus. However, samples treated with 15mg/ml gels exhibited dramatic improvement in effective equilibrium modulus, with an increase to 70% of undamaged from the damaged mean of 50%. Effective instantaneous moduli in these samples exhibited a greater increase of 30%, which was statistically significant ($p<0.05$). All three tested collagen gel densities decreased effective permeability in large defect samples.

In small defects, riboflavin crosslinking of collagen did not statistically increase moduli; however the nominal increases in modulus were such that samples treated with crosslinked gels were not significantly different than uninjured samples. At the highest concentration of riboflavin, effective equilibrium modulus was 95% of undamaged. Crosslinked gels all decreased hydraulic permeability, with 0.10 mM group falling to within 5% of the undamaged mean. In large defect samples, none of the experimental groups exhibited increased effective equilibrium or instantaneous moduli significantly over damaged values. Non-crosslinked gels showed the most profound increase with effective equilibrium and instantaneous moduli rising to 75% and 70% of undamaged values, respectively. Although all three experimental groups decreased hydraulic permeability in large defect samples from 6-fold to 4-fold over undamaged, non-crosslinked controls exhibited the most profound decrease with a fall to 3-fold over undamaged discs.

2.5 Discussion

The goal of this study was to assess the effect of increased collagen density and riboflavin crosslinking on repair of AF defects with injectable collagen gels. This

was accomplished through gross visual evaluation and comparison of mechanical properties with undamaged discs. We report several metrics that captured the mechanical performance including effective moduli and hydraulic permeability. It is shown here that injectable high density type I collagen gels had a positive effect on the mechanical behavior of injured IVDs once delivered to focal defects in the annulus fibrosus. Both large and small defects in the AF decreased effective disc moduli and increased effective permeability, which collectively represent the diminished ability of the disc to bear load. Furthermore, we report that crosslinking with riboflavin had limited positive effects, but did not diminish the effectiveness of high-density collagen gels for AF repair.

This study addressed the performance of an annular repair technique directly in an *ex vivo* whole motion segment. IVD defect models in rat tails are often used to study degeneration and to assess possible therapies[87,111]. The decision to address two defect sizes, created differently, was motivated by the clinical need to address different damage types. Our beveled needle defect simulated standardized diagnostic procedures such as a discography, while our larger free-hand defect was meant to simulate a surgical intervention (e.g. annulotomy). Although defect variation adds to the variability in "damaged" data sets, it also enhances the rigorousness of our approach. An effective AF repair technique would be expected to comply with the irregularities of any AF defect. Our collagen hydrogel formulations were low viscosity upon delivery, allowing it to mold to the form of the defects.

Repaired IVDs were assessed based on effective equilibrium and instantaneous moduli for stiffness as well as effective hydraulic permeability for flow of water out of

the disc. Effective equilibrium modulus and hydraulic permeability values were within the range reported previously for rat caudal IVDs [5,110]. Diminished IVD performance from the smaller defect was not as profound as that seen with larger defect samples; however, in these samples collagen gels were more effective at repairing smaller defects. All three hydrogel densities improved IVD stiffness and hydraulic permeability in the small defects. IVDs with the larger defects also seemed to experience some benefit from treatment with collagen hydrogels, with the most profound increase in effective stiffness being delivered by 15 mg/ml collagen gels.

All collagen gel densities improved effective hydraulic permeability in large defect samples. The function of the IVD was highly dependent on the ability of the AF to keep the NP hydrated and enabling maintenance of large hydrostatic pressure in the disc space. Improvements in IVD stiffness were evident with repair using our collagen hydrogel; however the profound decreases in hydraulic permeability underscored the ability of high-density collagen gels to contain water within the IVD. Tested samples exhibited dramatic increases in permeability when damaged, and decreases in permeability of over 2 fold when repaired. When compared to slight changes in both effective equilibrium and instantaneous moduli, it seems that effective hydraulic permeability is better suited to evaluate disc mechanical function after AF repair in this model. The hydrostatic pressures and total stresses imposed on repaired samples during testing were as high as 83kPa and 150kPa respectively. These were about 20% of those seen in the human lumbar spine while standing [112] and over 80% of that seen by the human cervical spine under static loading or bending [18,113]. While this result was encouraging, the pressures were only 4% of that seen in lumbar spine

while lifting a 45lb weight[112], which supports our plan to continue testing these gels in a large animal model.

The improved mechanical responses in repaired IVDs discussed above strongly suggest that high-density collagen gels remained in AF defects. In order to help support the mechanical data, gross visual examination was conducted on repaired IVDs after mechanical testing. Gel formulations were dyed with trypan blue to allow tracking of the collagen throughout the testing process. After testing, motion segments were frozen and bisected transversely through the repaired disc (Figure 4). Blue gels were seen localized to the AF after testing in both the small and large defects. Some evidence of gel in the NP was seen, however it is unclear whether this happened during delivery, testing or bisection. The visual presence of gels after mechanical testing confirms that these high-density gel formulations were able to be delivered to the defect and maintained presence after compression and processing for visual analysis. Histology shows clear evidence of a patch in small defect samples, while there is evidence of material in large defects.

There studies were motivated in part by previous work demonstrating the efficacy of injected collagen gels for repair of AF defects *in vivo*[102]. While promising, these previous studies did not address the extent to which these gels restored mechanical function immediately after injury. In both *in vivo* and in the current study, we tested 15 mg/ml collagen gels containing varying amounts of the crosslinker riboflavin. Riboflavin crosslinked collagen gels were best in needle puncture defects in either study. Histology from both studies showed that collagen gel formulations work as a patch, with the majority of the injected gel localized to the outer AF. This

patch type repair was successful in keeping the NP intact and in place. According to our study, we would move forward with higher concentrations of riboflavin. The highest concentration (0.1 mM) was observed to have the greatest impact on the damaged AF, however the other tested concentrations also had positive effects. As we move forward with larger animal models, we will use larger (0.07+ mM) concentrations of riboflavin and maintain a 15 mg/ml collagen gel unless a different formulation is needed for increased loading observed in larger animals.

Our previous *in vivo* study on AF repair in the rat model supports our observation that punctured discs treated with these crosslinked gel formulations retained healthy phenotype and NP hydration [102], especially over the long term. Our *in vivo* samples treated with crosslinked collagen exhibited a brief dip in both dish height and NP hydration after surgery, but recovered and maintained higher properties by five weeks post-operation[102]. Therefore, the crosslinking of the gels may be more successful at promoting biological healing as opposed to a purely mechanical repair.

Until recently, the major focus for annular repair has been mechanical closure of the native AF with little attention to biological healing. Proposed criteria for effective AF repair[9] include: filling the AF gap; mechanically augmenting injured disc function; maintaining or promoting cell survival and/or differentiation; integrating with surrounding tissues; and exhibiting biocompatibility. Our study showed that collagen hydrogels can be injected into a gap in the AF and remain in the defect under load. Furthermore, once delivered the gels contributed to the mechanical function of the damaged IVDs. Stiffness of the discs, as assessed by effective modulus values, showed increases towards undamaged discs. Our collagen hydrogel formulations have

proven to directly satisfy two of the criteria set forth by Bron et al. in an *ex vivo* AF defect model[9].

Remaining factors considered in the literature and criteria above address the regenerative nature of AF repair treatments. An effective repair method must support cell survival, cannot be harmful to the surrounding native tissue and must have the potential for integration with surrounding tissue. Research groups have showed that collagen gels crosslinked with riboflavin are capable of supporting various cell types[66]. Furthermore, our *in vivo* studies show that these gel formulations are not only harmless to surrounding tissue, but allow for cell migration into the repaired area with accompanied native tissue ingrowth[102]. Thus, according to the criteria above, our type I collagen hydrogel is an ideal candidate for AF repair.

While the rat caudal motion segment model is widely used in disc degeneration and repair studies, there were limitations to the model in this study that cannot be overlooked. The reported work only addressed the short term, mechanical contribution of both crosslinked and non-crosslinked high-density collagen gels.

While it is known that the IVD experiences six degrees of motion *in vivo*[114], we only studied axial compression in this model. Compressive stress-relaxation allowed us to observe the dramatic changes in IVD effective permeability with puncture. Our studies have shown that once damaged, the hydraulic permeability increases dramatically (up to 6 fold with large defects) over undamaged values. Furthermore, other groups have seen changes in time-dependent compressive mechanical properties of IVDs with AF damage[96,115]. Other testing modalities, such as torsion, do not allow us to study the effects on fluid flow out of the disc. As such,

this model represented an important screening tool for assessing AF repair, but must be followed with assessment of efficacy in larger animal models, where loading better approximates that in humans.

The method of mechanical testing and analysis used in the current study reported effective material properties (i.e. moduli and hydraulic permeability) that assume material homogeneity. Although this did not allow us to address the mechanical integrity of the AF or NP directly, it did enable assessment of the effects of AF repair on function of the whole IVD as part of a motion segment. It may be beneficial to test the AF directly with the collagen hydrogel repair method once we expand the formulation to facilitate repair in larger IVDs, however the effective mechanical effects were suitable for establishing the feasibility of a crosslinked, high-density collagen hydrogel for AF repair. Such an approach could involve directly measuring local AF strains[116] or analytic finite element models that account for differing properties between the AF and NP[117].

Another limitation was that AF defects in the reported work were made while maintaining the motion segment at constant height, preventing immediate collapse of the IVD upon puncture. Without immediate collapse, NP tissue was only displaced during testing instead of upon puncture, which we experienced during *in vivo* puncture. NP tissue is known to be lost with puncture or aspiration, which has profound effects on mechanical behavior[12,87,98]. Although keeping the motion segment in displacement control was a concern, histological sections show that we lost a considerable amount of NP, especially in large defects (Figure 3). Furthermore, loss

of mechanical stiffness and corresponding increase in hydraulic permeability support our observation that we still do lose NP tissue.

This study demonstrated that crosslinked, high-density collagen gels mechanically enhanced the effective properties of damaged IVDs after injection into AF defects. Although the current study used gels alone, multiple studies have used type I collagen gels with various additions such as cells, growth factors, and other therapeutics to support tissue growth and development [21,62,101]. As we move forward, we will also look to seed the collagen gels with ovine AF cells, as has been shown previously with tissue engineered total disc replacements, which exhibited enhanced integration with surrounding native AF tissue[21,39].

2.6 Acknowledgments

This work was funded by NIH F31AR064695-02, the AO Foundation, AO Spine International, NFL Medical Charities, and the Howard Hughes Medical Institute. The authors would like to thank Robert Mozia, Drs. Robby Bowles, Andrew James, and Harry Gebhard for their thoughtful suggestions.

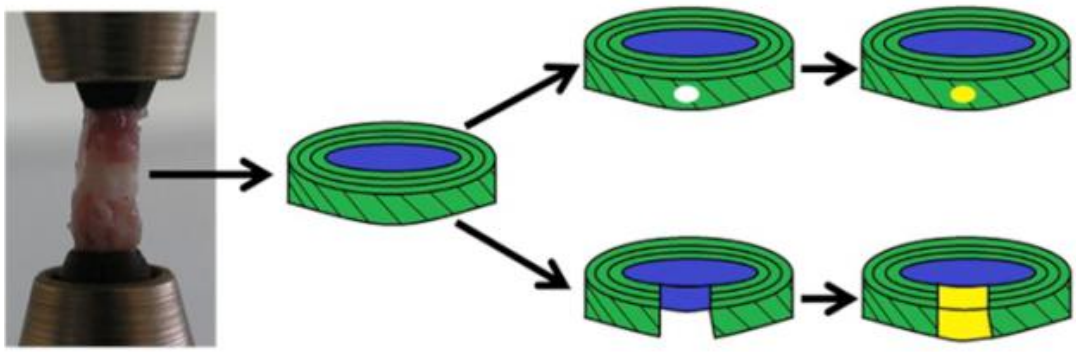

Figure 2.1: Schematic of experimental design showing mounted, undamaged caudal motion segment, small and large defects as well as treated drawings.

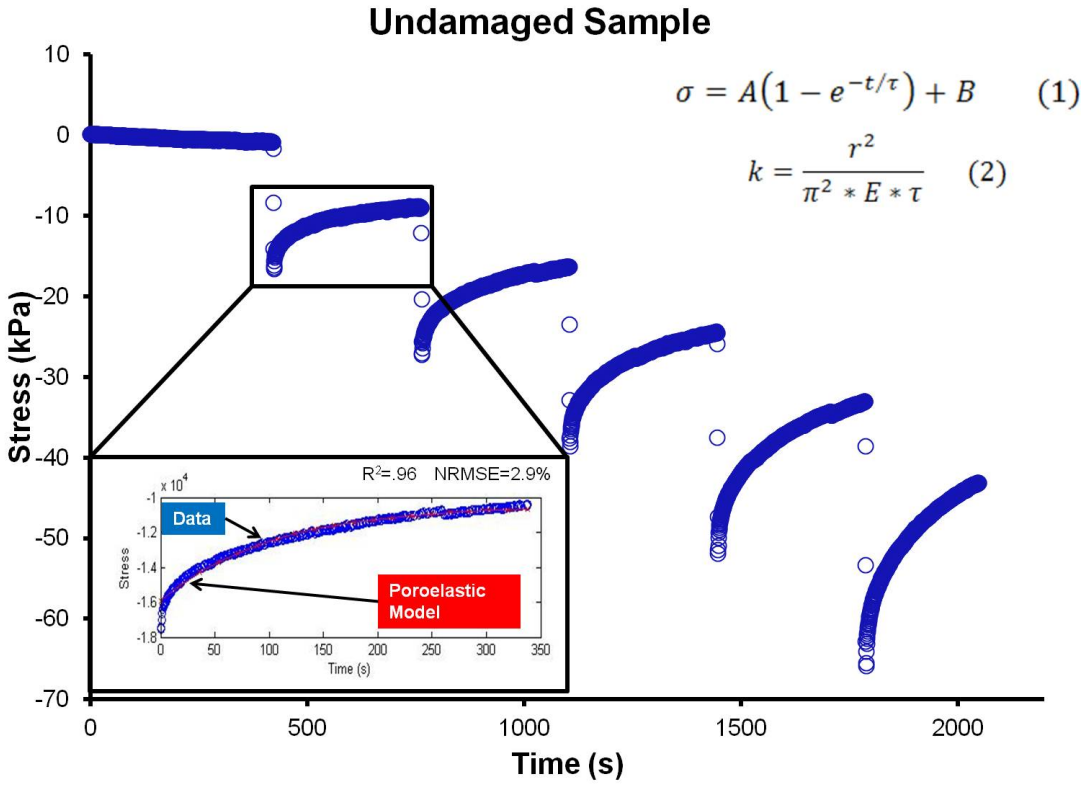

Figure 2.2: Representative temporal data set of an undamaged segment. Inlay shows custom MATLAB fit of poroelastic model to single step of stress relaxation data.

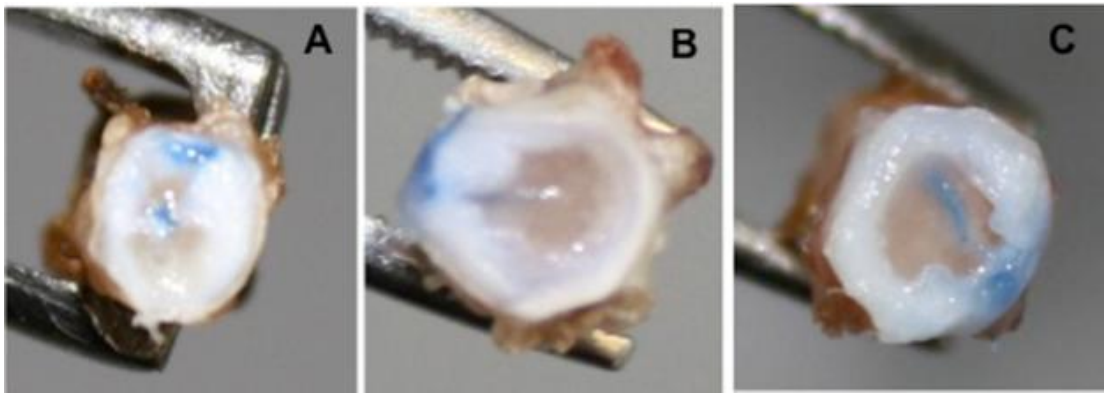

Figure 2.3: Gross transverse cross-sections of treated IVDs after mechanical testing. High density, non-crosslinked collagen gels were dyed with trypan blue to track presence in the disc. Pictures show the presence of gel after loading small defect (A&B) as well as large defect (C) samples.

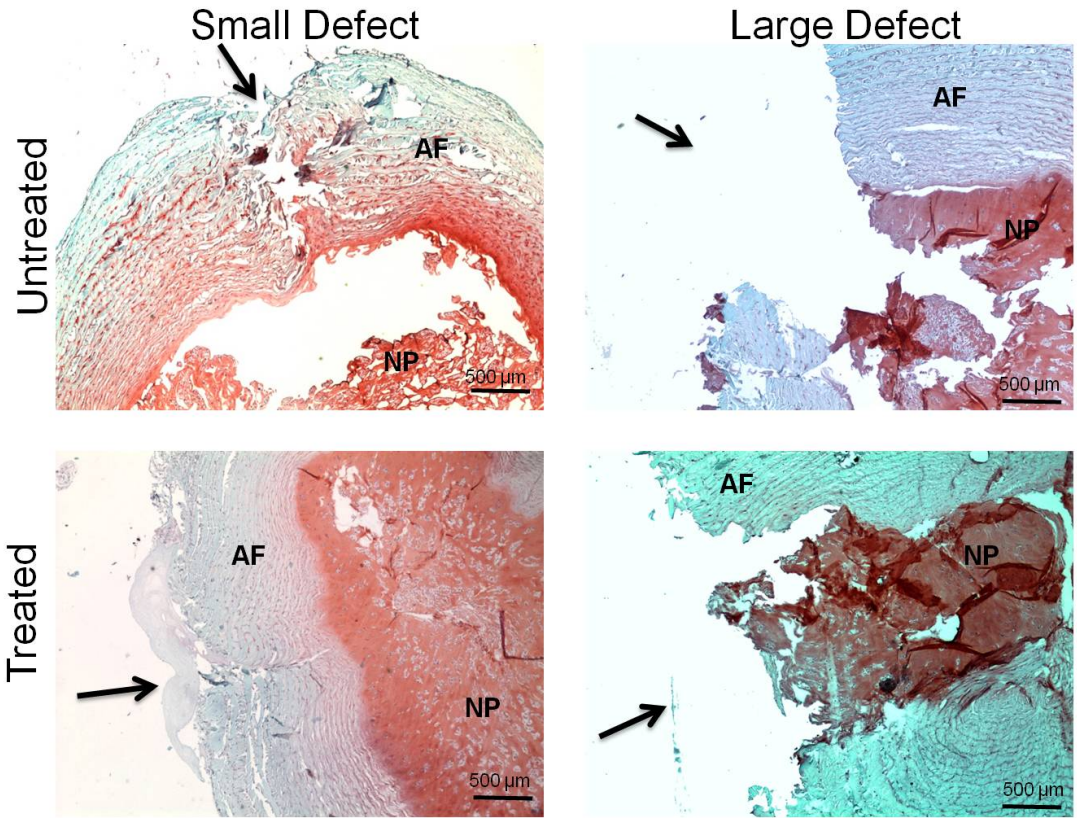

Figure 2.4: Safranin-O stained transverse sections of damaged and treated IVDs. Histology shows clear defects made with both 21ga. and scalpel blades. Arrows highlight defect sites. Collagen patch can be seen in treated small defect sample.

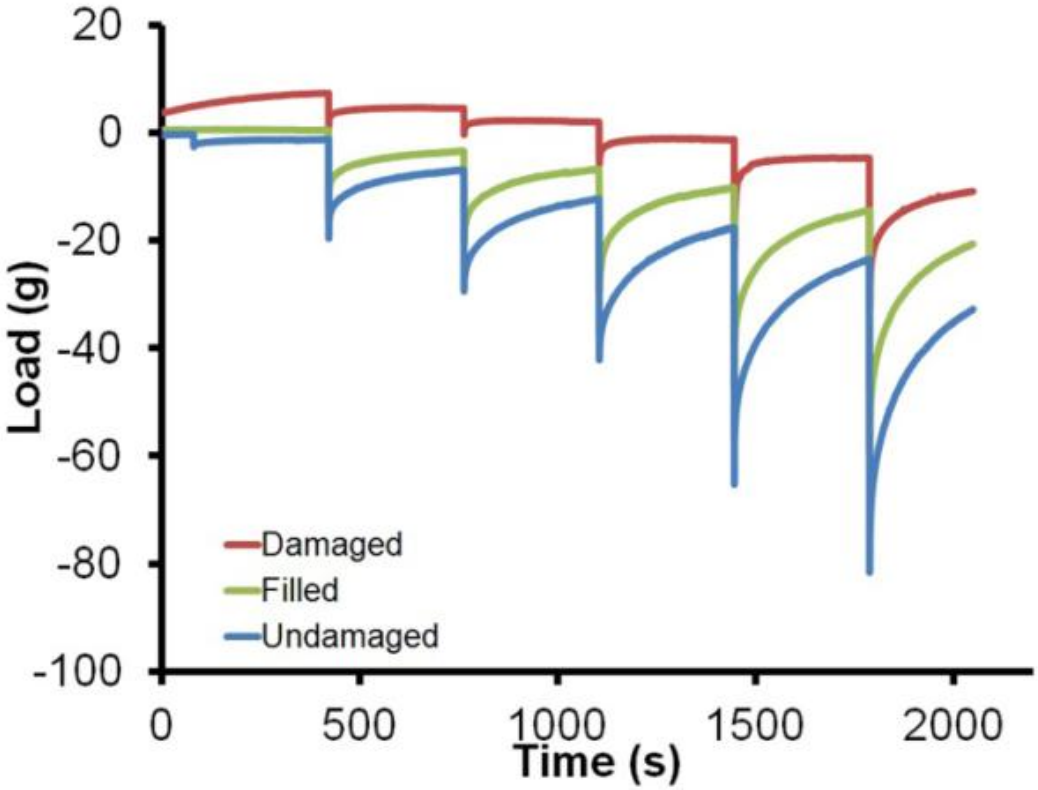

Figure 2.5: Representative temporal data set of load during a series of stress relaxation tests. As shown here, each sample was tested prior to imposition of a defect (blue), after damage (red), and after the defect was filled with a collagen gel (green). The sample shown here was a small defect filled with a 15 mg/ml collagen gel.

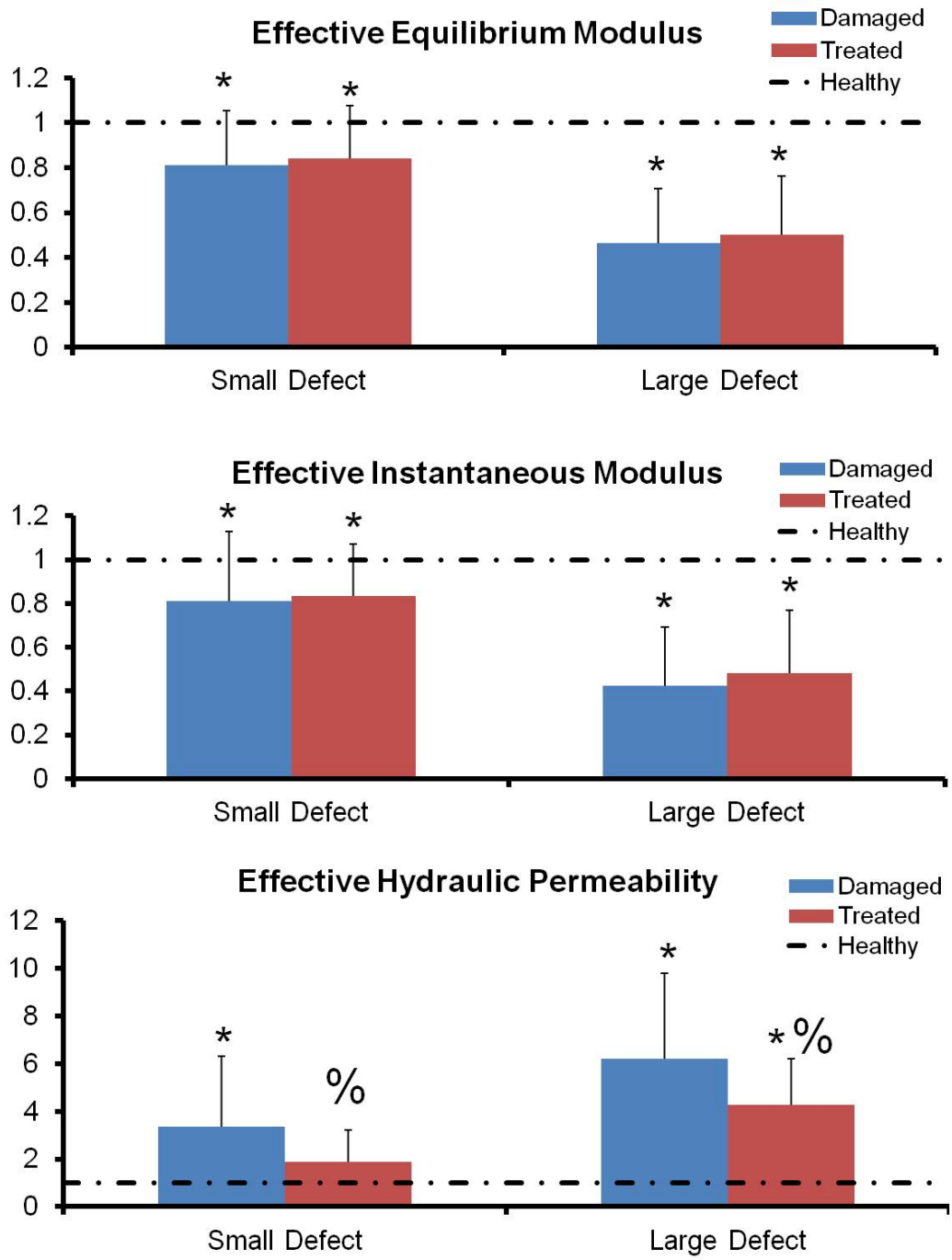

Figure 2.6: Normalized effective mechanical properties (pooled) of intervertebral discs after injury and after treatment with collagen gel formulations. The values of effective equilibrium modulus, effective instantaneous modulus, and effective hydraulic permeability were normalized to those of the undamaged disc (dashed line) on a sample by sample basis. % indicates that the noted conditions were significantly ($p<0.05$) different from damaged. * indicates that the noted conditions were significantly ($p<0.05$) different from undamaged condition. Error bars represent standard deviation. n=34

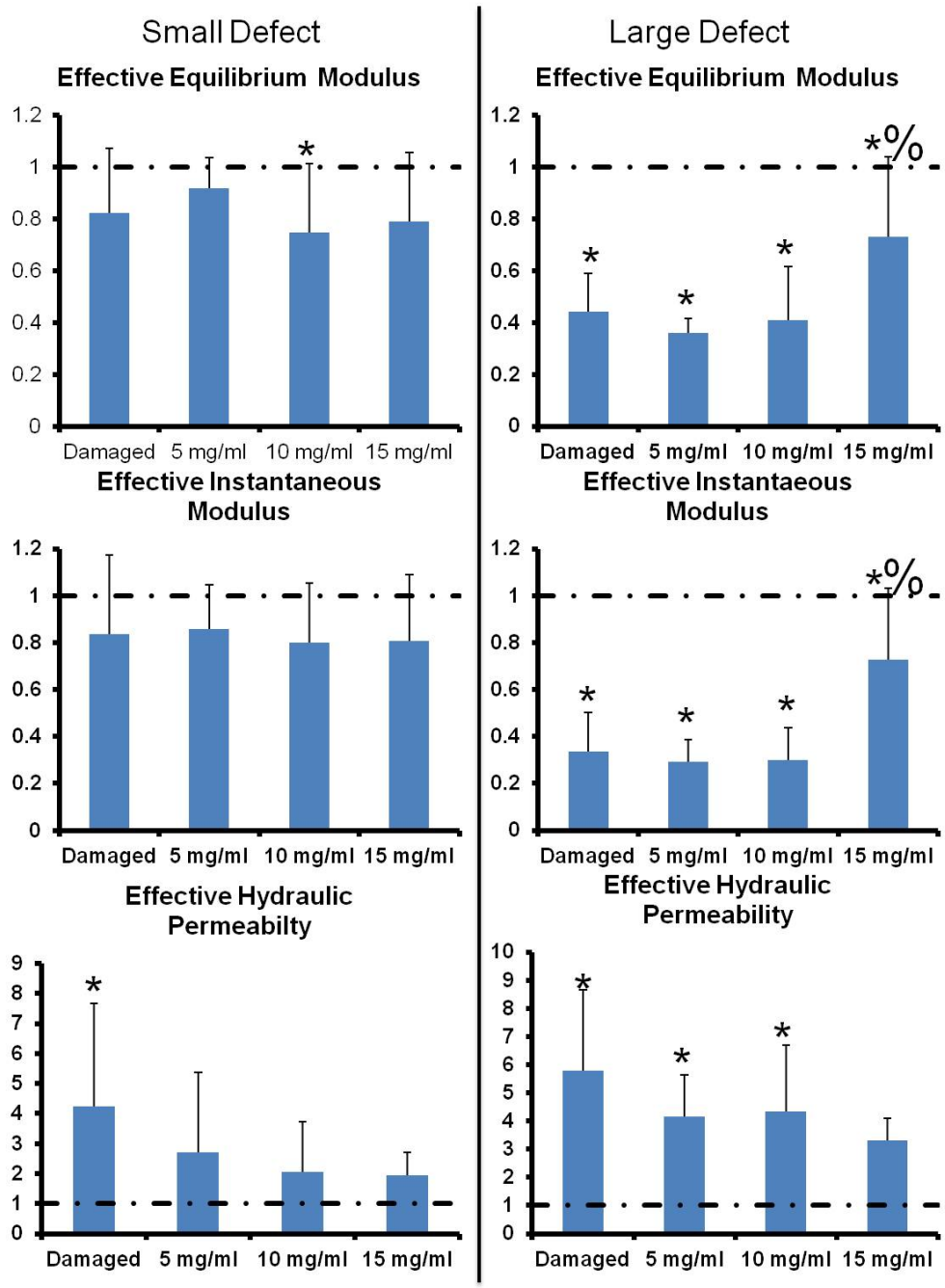

Figure 2.7: Normalized effective mechanical properties of intervertebral discs after injury and after treatment with high density collagen gels. % indicates that the noted conditions were significantly ($p<0.05$) different from damaged. * indicates that noted conditions were significantly different from undamaged ($p<0.05$). Error bars represent standard deviation. n=10±3

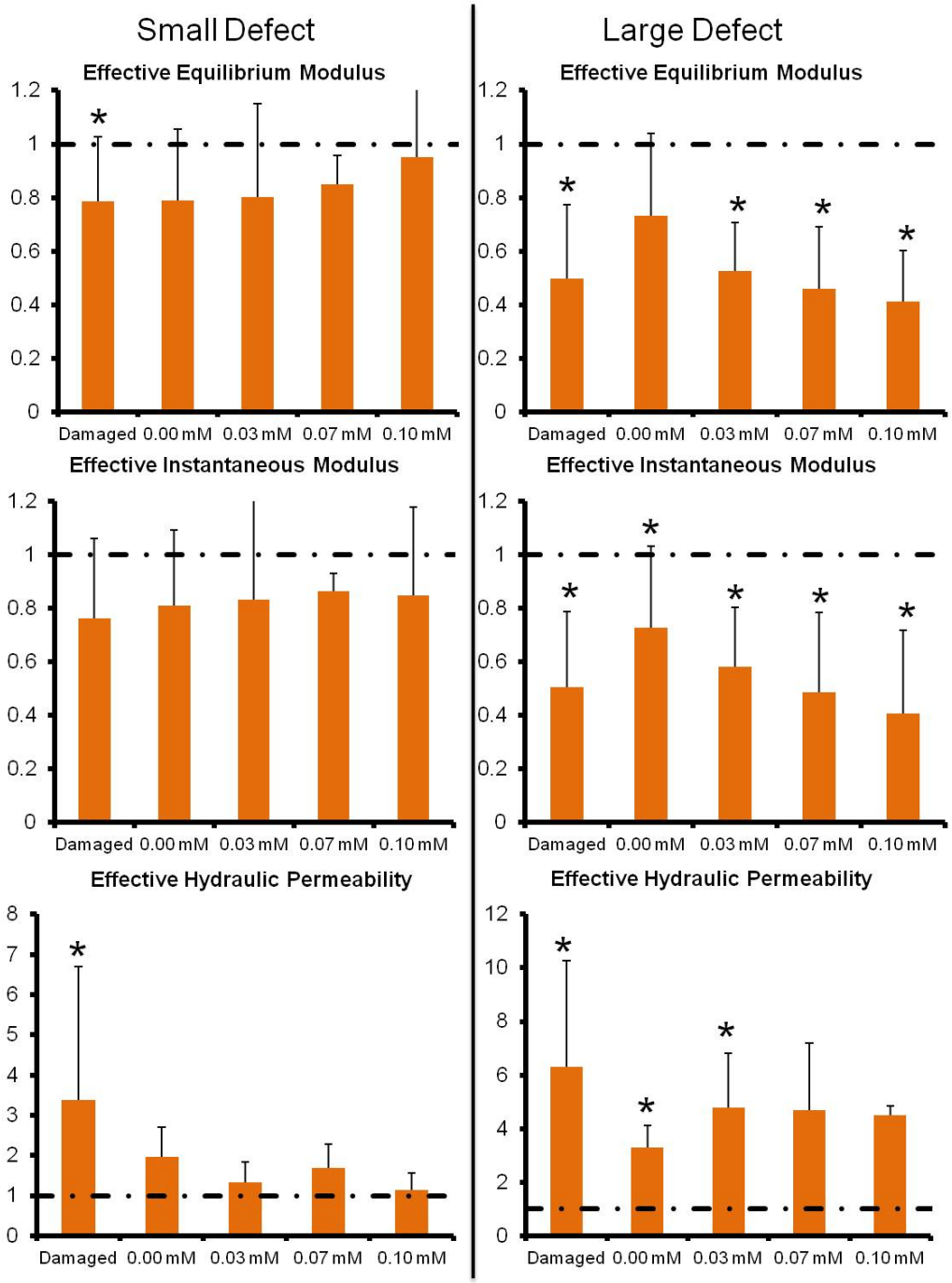

Figure 2.8: Normalized effective mechanical properties of intervertebral discs after injury and after filling with riboflavin-crosslinked collagen gels. * indicates that noted conditions were significantly different from undamaged ($p<0.05$). Error bars represent standard deviation. n=10±3.

CHAPTER 3

Annular repair using high-density collagen gel; a rat-tail in vivo Model.

This chapter has been published:

*Grunert, P., *Borde, B. H., Hudson, K. D., Macielak, M. R., Bonassar, L. J., & Härtl, R. (2014). Annular repair using high-density collagen gel: a rat-tail in vivo model. *Spine*, *39*(3), 198–206. http://doi.org/10.1097/BRS.0000000000000103

**Borde and Grunert are listed in publication as co-first authors on this manuscript*

3.1 Abstract

Study design: Animal in vivo study.

Objective: Test the capability of high-density collagen gel to repair annular defects.

Summary of background data: Annular defects are related to the occurrence of disc reherniations following discectomies and disc degeneration after intradiscal diagnostic procedures. Therefore, several biological materials have been developed for annular repair and tested in vitro. This is the first study to test a biomaterial in vivo.

Methods: We punctured the IVD of 42 athymic rats using an 18-gauge needle to create an annular defect that leads to extrusion of the nuclear tissue with consecutive degenerative changes. Subsequently high-density collagen (HDC) gel was injected to seal the defect. Riboflavin (RF) was added to increase the stiffness of the collagen gel by inducing cross-link formation. The animals were subdivided into four groups. The first group was injected with uncross-linked HDC gel, the second with collagen cross-linked using 0.25mM RF, the third using 0.50mM RF, and the fourth control group was punctured and left untreated. The animals were followed for five weeks with X-ray measurements to assess the disc heights and MR imaging to evaluate degenerative changes of the IVD. We developed an algorithm based on T2-relaxation time measurements to assess the size of the nucleus. Tails were collected for histological analysis to assess disc degeneration and the cross-sectional area of the NP.

Results: After five weeks, the 0.50mM RF cross-linked group showed only minimal decrease of nuclear tissue when compared to healthy discs, with no obvious signs of IVD degeneration. The AF appeared partially repaired by a fibrous cap bridging the defect. The 0.25mM RF group showed signs of moderate degeneration with extrusion

of nuclear tissue. After five weeks, the uncross-linked group was not significantly different from the control group that showed signs of progressive degenerative changes and no residual NP tissue in the disc space.

Conclusion: HDC is capable of repairing annular defects induced by needle puncture. The stiffness of HDC appears to influence the repair mechanism.

3.2 Introduction

Repair of annular defects could significantly improve treatment of degenerative spinal diseases.[1] Open defects compromise the ability of the annulus fibrosus (AF) to contain nuclear tissue in the disc space, thereby increasing the likelihood of reherniation and progressive degeneration after discectomies.[2–6] Furthermore, there has been concern that annular puncture for therapeutic or diagnostic procedures accelerates the progression of degenerative disc disease and promotes nuclear tissue extrusion.[7] Successful treatment of puncture defects could inhibit these degenerative changes.

Annular defects persist because of the very limited intrinsic healing capability of the AF, which does not significantly improve upon simple mechanical closure.[1,8–11] As a result, several research groups have investigated using biological materials for annular repair.

Rigid implants have been studied by Vadala et al. using tissue-engineered AF constructs in vitro[12] and by Ledet EH using small intestinal submucosa in vivo.[13] Implanted submucosa tissue reduced degenerative changes after annulotomy in sheep spine.

Schek et al. have studied injectable biomaterials with genipin cross-linked fibrin hydrogels. Fibrin integrated with sections of human AF tissue, showing promising biomechanical and cell seeding properties in vitro.[14] Our group tested injectable high-density collagen (HDC) gels and found that HDC can partially restore mechanical function to a needle-punctured rattail AF in vitro.15 However, no studies reported use of injectable biomaterials to treat annular defects in vivo.

Annular defects induced by needle puncture lead to predictable patterns of disc degeneration in the rat-tail spine.[16,17] In such models, degeneration is initiated by extrusion of nucleus pulposus (NP) tissue through the puncture defect. Although the needle puncture model has been frequently used to test biological materials for IVD regeneration,[18–21] no study yet has used this model to investigate repair of induced defects to prevent disc degeneration.

The goal of our study was to evaluate the ability of HDC to repair a needle-puncture AF defect in the rat-tail spine. Specifically, we wanted to test whether injected HDC gel can prevent nuclear tissue extrusion and consequent IVD degeneration, as determined by histological and radiological outcomes. In addition, we assessed whether cross-linking of injected collagen influences the repair process. For that purpose, riboflavin (RF), a photoactive initiator of collagen cross-linking, was added in different concentrations. In the presented study, the rat-tail model was used to screen these various compositions of collagen gels.

3.3 Methods

Study groups

We used 42 male, 10–12 week-old, inbred, nude, athymic rats for this study. Animals were divided into four groups. The first group of 14 was needle-punctured and injected with HDC of 15mg/ml concentration. The second group of 16 was punctured and injected with RF cross-linked HDC (15mg/ml): nine with 0.25mM RF, and six with 0.5mM. A third group of six was punctured and left untreated to serve as control. All the animals in these three groups were sacrificed after five weeks. Tails were collected and used for histological analysis. A fourth group of six animals was sacrificed; tails were collected and subsequently needle punctured and injected with HDC. This group was used to study the morphology and distribution of the collagen directly after injection.

All animals were euthanatized with carbon dioxide following standard protocol from the American Veterinary Medical Association. The study was approved by and undertaken in accordance with guidelines outlined by the Hospital of Special Surgery Institutional Animal Care and Use Committee (IACUC) and New York State.

Collagen gel preparation

Collagen was harvested and reconstituted from rat-tail tendon as previously described.[22,23] Fibers were digested in 0.1% acetic acid, frozen for 48 hours, lyophilized and reconstituted at 20mg/ml in 0.1% acetic acid. Immediately before delivery, acidic collagen solutions were mixed with working solutions consisting of 10X Dulbecco's Phosphate Buffered Saline (DPBS), 1N NaOH and 1X DPBS to initiate polymerization of final collagen gels at 15mg/ml. For RF groups, riboflavin was added to 1X DPBS at the desired concentration. Gels with RF were exposed to blue light with a 480nm wavelength for 40 sec after injection to initiate cross-linking.

Open needle puncture and collagen injection

The target level between the 3rd and 4th vertebra of the tail was localized under X-ray control. The animals were anesthetized and placed in the prone position. A 2cm longitudinal skin incision was made over the marked level. The AF was then exposed, and great care was taken to preserve it without damage. Subsequently the AF was punctured using an 18-gauge needle attached to a syringe containing the collagen gel. Approximately 0.5 ml of the gel was injected around the defect immediately after puncture. When RF was added to the collagen, the gel was cured in situ. The control group was punctured and left untreated. In order to standardize the puncture technique the needle was always inserted in the same orientation (with the needle bevel up) and to the same depth (until the bevel completely penetrated the AF).

Quantitative MR Imaging

Quantitative imaging was utilized to assess the size of the NP according to the number of MRI voxels that composed it, here labeled NP voxel count. MR imaging was obtained on a 7T MRI (Bruker 7T USR Preclinical MRI System) at one, two and five weeks post puncture (Fig. 3.1A).

We used a sagittal multi-slice multi-echo (MSME) pulse sequence (TR=2000ms, TE=12ms, NEX=2, number of echoes=12, echo spacing=12ms, slice thickness=1mm and matrix size=320 × 320, resolution: 125μm × 125μm × 1mm) to create a T2 map based upon fitting semi-log plots of T2 signal intensity versus relaxation time for the twelve acquired echoes. Bruker's proprietary program TopSpin™ was used for the fitting process. A color map was assigned to the resulting T2 map (Fig 3.1B). Next, a standard region of interest (ROI) measuring ~1mm^2 was

drawn within the center of NP of the healthy disc proximal to the punctured IVD. The average T2-RT of that ROI was measured, and this value minus two standard deviations was used to set a subtraction threshold for all voxels in that slice (Fig. 3.1B). Voxels with T2 values lower than the threshold were subsequently subtracted (Fig. 3.1C). As a result, only voxels with T2 values representing NP tissue remained in the disc space and were then counted. At each time point, the mean voxel count of punctured discs was compared to the mean voxel count of proximal adjacent healthy IVDs.

Qualitative MRI analysis

A sagittal TurboRare sequence (TR=2017, ms, TE=60ms, NEX=6, echo train length=12, slice thickness=1mm and matrix size=320 × 320, resolution: 125μm × 125μm × 1mm) was utilized for qualitative assessments. We used a modified Pfirrmann scale[24] that outlines four grades of degeneration as defined by NP signal intensity, homogeneity and loss of disc height.

Disc height measurements

Disc heights were obtained in a digital radiographic cabinet. Great care was taken to achieve true lateral X-rays of the index segment. The IVD height was expressed as a disc height index (DHI), calculated by dividing disc height by adjacent vertebral body height based on the modified method of Lu et al.[25] The disc height was measured preoperatively and postoperatively at one, two and five week time points.

Histology

After appropriate fixation, tails were decalcified, cut mid-sagittally and transferred to 75% ethanol. Segments were embedded in paraffin, then cut to 5μm

thickness and stained with Alcian Blue and Safranin-O. We measured the size of the NP by drawing a ROI around the nucleus and subsequently measured the cross-sectional area of that ROI using the Bioquant image program (Fig. 3.2). The average cross-sectional area measurements of punctured discs were compared to those of healthy proximal adjacent IVDs. The Han grading system was used to describe the degenerative stage of the punctured IVDs. This system is based on AF/NP cellularity, morphology and border.[17] The grading system ranges from 5, a healthy disc, to 15, a terminally degenerated disc.

Statistics

The NP voxel count and disc height data were evaluated using nested multilevel ANOVA modeling with nesting in punctured and healthy adjacent levels, untreated puncture versus collagen injection, and riboflavin concentrations. Analysis was done in JMP 9.0 (SAS Institute Inc.). We considered $p \leq 0.05$ indicated a statistically significant correlation between the variables and measured outcomes.

3.4 Results

Qualitative MRI

Five out of six animals in the 0.5mM riboflavin group showed no obvious signs of degenerative changes at the five week MRI (Fig. 3.2). The modified Pfirrmann Grade of that group ranged from I to III (avg. 1.3). At the same time point, all animals in the 0.25mM riboflavin group displayed decreased NP size, yet the nucleus remained homogenous and hyperintense (Fig. 3.2). The Pfirrmann grade ranged from II to III (avg. 2.6). The uncrosslinked collagen group showed a more heterogeneous, smaller NP with a significantly increased AF/NP ratio (Fig. 3.2). The

AF bulged into the nucleus giving it an hourglass shape. All animals had a Pfirrmann grade of III. Five out of six specimens in the untreated group showed black IVDs, indicating terminal disc degeneration (Fig. 3.2). The Pfirrmann grade ranged from III to IV (avg. 3.8).

NP voxel count

The control IVDs had an average NP voxel count ranging from 140 to 153 voxels at 1, 2 and 5 weeks; the voxel count for the 0.5mM RF group was between 129 (SD±16.3) and 140 (SD±22.5). The 0.25mM RF group exhibited lower values: 71 voxels (SD±59.14) at week one and 57 (SD±56.40) at the second and fifth weeks. The NP voxel counts of both RF groups remained constant between weeks two and five.

The uncross-linked collagen group showed 46 (SD±25) voxels at week one which continuously dropped to 14 (SD±15.6) at week five. The untreated group showed the lowest voxel counts values at each time point, decreasing to 5 (SD±4.17) after five weeks (Fig. 3.3A). Overall, HDC gel injection significantly increased voxel count values ($p<0.0001$) as compared to untreated discs. Increasing RF concentration (0mM, 0.25mM, 0.5mM) proved to significantly increase NP voxel count values ($p<0.0001$).

Disc height measurements

All punctured IVDs dropped in disc height after needle puncture but remained constant between weeks two and five (Fig. 3.3B). The 0.5mM group maintained an average of 84% (SD±8.77) of its initial disc height, the 0.25mM riboflavin group 77% (SD±8.72). The uncross-linked collagen group maintained 67% (SD±16.86) and the untreated group 53% (SD±13.82) of disc height. Overall, HDC treatment gel

significantly improved the DHI ($p<0.0001$) of punctured discs. Increasing RF concentration (0mM, 0.25mM, 0.5mM) significantly increased the DHI ($p = 0.0264$).

Histology

The annular defect—The needle puncture defect pierced through all AF lamella layers (Fig. 3.4A–B, 3.5A–C) and was still visible after five weeks in all animals. In the control and uncross-linked groups, the AF fibers remained separated, and infiltrated the surrounding scar tissue (Fig. 3.4D). No granulation tissue, increased cellularity or vascularity was visible to indicate an annular repair process. The 0.5mM RF group showed formation of a fibrous cap at the outer third of the AF that infiltrated annular fibers, bridging both disrupted ends (Fig. 3.5). This fibrous cap was composed of fibroblasts embedded in a dense collagen matrix that stained more intensely with Safranin-O and Alcian blue than surrounding AF and scar tissue. The 0.25mM RF group showed formation of either a similar cap (Fig. 3.4A–B) or a thin fibrous string repairing the outer part of the AF (Fig. 3.4C). In both cross-linked groups, the inner two thirds of the AF showed no signs of tissue repair.

Disc degeneration—There were no obvious signs of degeneration in the 0.5mM RF group. IVDs showed an average Han degeneration grade of 6.8. IVDs in the 0.25mM RF group showed a decline in NP cells with clusters formation, and reached an average Han grade of 9.3. All IVDs in the uncross-linked collage group showed signs of progressed degenerative changes with only residual NP tissue visible in the disc space (Fig. 3.2). The puncture defect branched into the AF, creating multiple fissures. NP tissue herniated through the open defect (Fig. 3.4E). Discs a showed a Han grade of 12.8.

All animals in the untreated group showed severe signs of degeneration; the NP was completely replaced with connective tissue. The AF appeared ruptured and disorganized (Fig. 3.4F). Several specimens showed significant endplate damage (Fig. 3.2). The average Han grade was 14.3.

Histological cross-sectional area—After five weeks, healthy NP proximal to punctured IVDs had an average NP cross-sectional area of 1.59mm^2. Means of 0.5mM RF, 0.25mM RF, and uncross-linked collagen groups were 1.29mm^2, 0.78mm^2, and 0.78mm2 respectively. No measurable NP tissue remained in the disc space of untreated IVDs.

Fate of the injected collagen

Immediately after injection, the collagen distributed into the paravertebral space covering the outer part of the annular defect but did not migrate into the defect (Fig. 3.6). HDC appeared as homogenous amorphous tissue that stained weakly with Alcian Blue or Safranin-O. After five weeks residual collagen still appeared homogenous and amorphous and was infiltrated with host fibroblasts to varying degrees. Resorptive zones were visible, indicating reorganization of the injected material by the host cells (Fig. 3.7). No sign of inflammatory or foreign body reaction was visible.

3.5 Discussion

Summary of our results

The first objective of this study was to test the ability of HDC to repair annular defects in a needle-punctured rat-tail model. We found that collagen can preserve the ability of the AF to retain nuclear tissue in the disc space and thereby prevent

degenerative changes to the IVD. We also observed the potential of collagen gel to induce formation of fibrous tissue that partially restores annular integrity. The second objective was to evaluate whether adding RF affects the quality of AF repair. We found that RF improved retention of NP size and disc height for up to five weeks after needle puncture.

The beneficial effect of RF was dose-dependent. In its absence, collagen gels yielded only a nominal increase in NP size and disc height compared to untreated IVDs. The 0.5mM RF group retained most of its nuclear tissue according to NP voxel counts and histological cross-sectional area measurements. An average disc height of 84% was maintained. Neither MRI analysis nor histological assessment revealed significant degenerative changes.

There are several potential mechanisms by which cross-linking may have positively influenced AF repair. Chemical cross-linking is known to increase the stiffness and decrease the hydraulic permeability of collagen gels.[26–28] Increased stiffness may help form a more robust barrier for sealing the defect. Decreased hydraulic permeability limits the loss of highly hydrated NP material through the defect.[15] In addition, cross-linking may enhance collagen adhesion to the AF tissue as has been shown with other biopolymer gels.[14] This prevents detachment of the implanted material from the annulus and subsequent loss of NP tissue.

A notable histological finding was the formation of a fibrous cap bridging the outer portion of the annular defect in both cross-linked groups. Collagen gel showed varying degrees of host fibroblast infiltration with signs of tissue reorganization, which could explain the formation of this fibrous tissue. The mechanism of host cell

invasion with subsequent tissue remodeling of collagen gels has already been described in the literature.[29,30] Staskowski et al. injected type I collagen gel in a canine model and described that secondary fibroblast invasion led to deposition of new host collagen within the gel. According to his study, cellular infiltration progressed more rapidly in a cross-linked collagen preparation, which could explain why fibrous cap formation occurred only in cross-linked groups of the presented study. Further, cross-linking is known to delay degradation and increase persistence time of collagen scaffolds, which would also support cell migration and remodeling.[31,32]

RF cross-linking and injectable biomaterials

RF is already used clinically to cross-link collagen fibers of the cornea to treat keratoconus,[33] but has never been applied to repair IVD tissue. RF serves as a photosensitizer to induce production of oxygen radicals, which then induce chemical bonds between collagen fibrils, thereby cross-linking them.[28] Several different substances have been used to cross-link biopolymer gels.[14,31,32] Using RF is advantageous because it cross-links fibers only after activation by blue light in situ, allowing collagen gel to remain liquid prior to injection. Injectable biomaterials may prove more technically feasible for use in spinal procedures than rigid biological implants, as they do not require anchoring to the AF or vertebral body. Moreover, only injectable substances can be applied percutaneously.

The rat-tail model

The rat-tail model proved to be suitable for testing various compositions of collagen gels. An 18-gauge needle creates a large defect comprising almost the entire posterior wall of the AF in the rat-tail disc. This defect is proportionally much larger

than defects induced by annulotomy during discectomies or punctures for discographies. High intradiscal pressure combined with the liquid consistency of the NP leads to rapid extrusion of nuclear tissue if left untreated. Untreated IVDs degenerated more rapidly than described in other studies that used the same model with a percutaneous approach.[16] We believe this is due to the open approach used in our study, in which the paravertebral muscles are dissected off the AF, creating a large tissue defect.

Limitations

We consider the small size of the specimen to be the main limitation of this study. The relatively small IVDs did not allow us to inject collagen gel into deeper layers of the AF against the intradiscal pressure. As a result, the potential of collagen gel to repair deeper layers of the AF could not be studied. It is unclear if the described fibrous cap at the outer part of the annulus could mechanically compensate for defects in larger animals or humans, whose IVDs are exposed to much higher mechanical forces. In addition, the instantaneous sealing of the defect by the injected collagen could be less effective under higher axial loads in humans. One other limitation of this model is that the AF is not degenerated at the time of collagen injection. A degenerated AF, as often seen in discectomy procedures, might respond differently to the collagen gel. However, the potential of collagen gel to induce tissue repair is very promising and should be explored in degenerated discs and larger animals.

3.6 Conclusions

High-density type I collagen is able to repair annular defects for up to five weeks after induction of a needle-puncture defect in the AF of the rat-tail spine. This

capability correlates positively with RF cross-linking. The needle-punctured rat-tail has been shown to be a suitable in vivo model for studying biomaterials for annular repair. Testing different concentrations of RF in longer-term studies will be an important next step. Additionally, future experiments may look to increase the size of the animal model or to incorporate cell-loading of the collagen gel.

3.7 Acknowledgements

We express our gratitude to AOSpine North America for their support with fellowship funding for Peter Grunert. We thank Stephen Doty PhD, for his work on the histology. We would also like to thank Sara Towne for her tremendous help with writing and reviewing this paper.

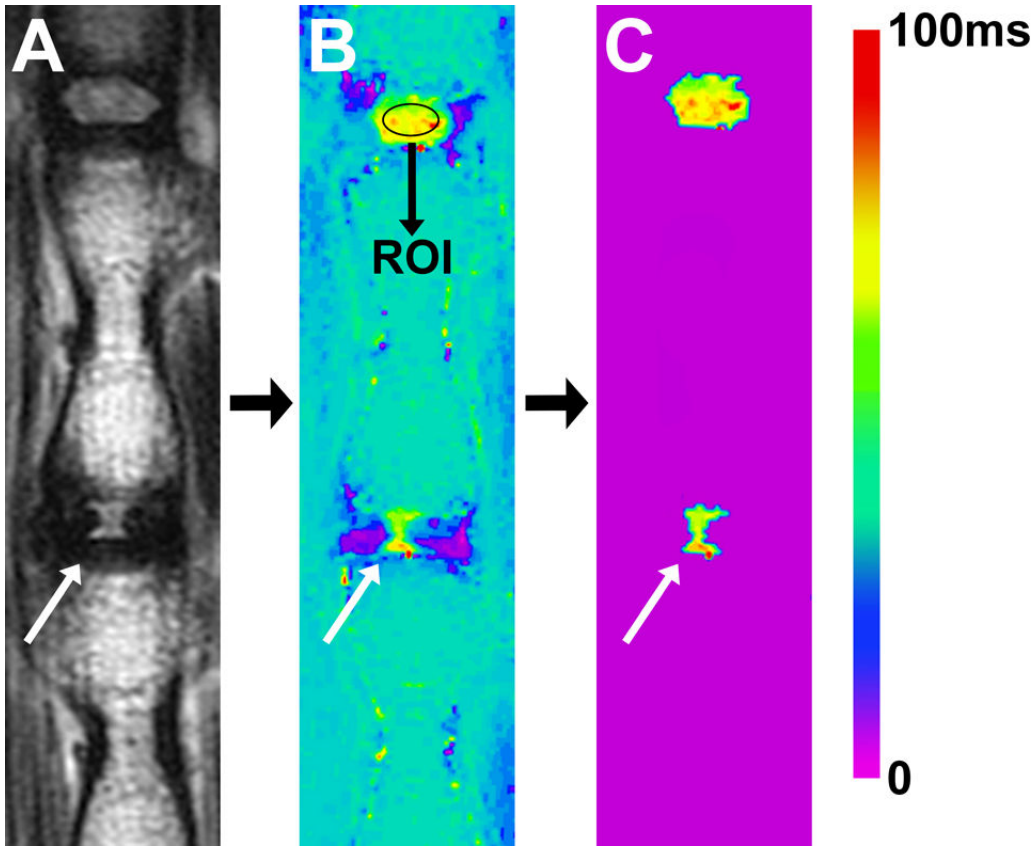

Figure 3.1: Illustrating the method used to determine NP size according to T2-RT. (A) T2-weighted MRI of a rat-tail with a needle-punctured disc (white arrow). (B) Matching image with T2- RT measurements displayed as a color map. A ROI was drawn within the NP of the proximal healthy adjacent disc. A subtraction threshold was set at two standard deviations below the T2-RT mean of the ROI. (C) All voxels below the threshold were subtracted. Subsequently, the remaining voxels in the disc space were counted.

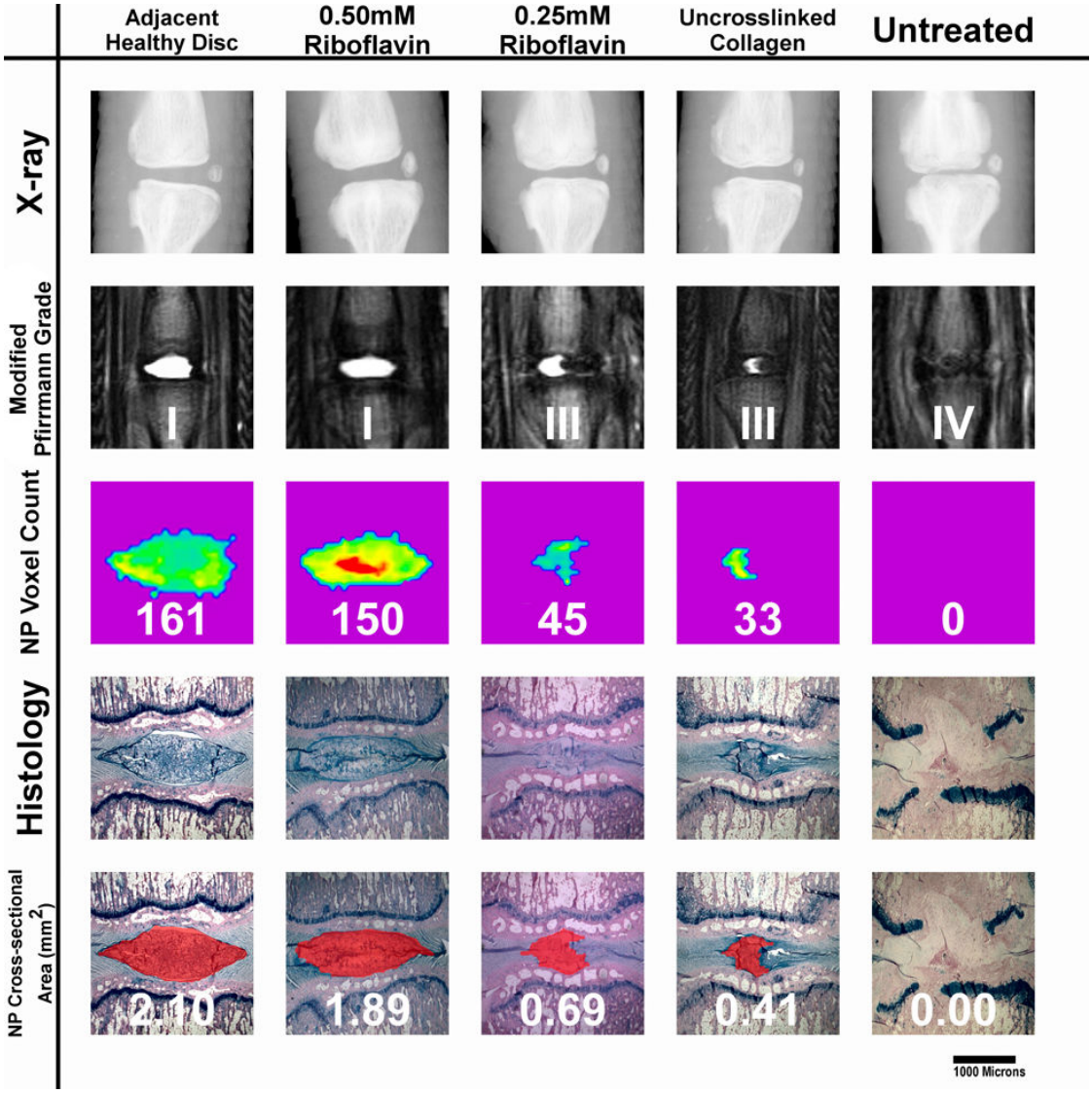

Figure 3.2. Five-week outcome examples of all punctured groups. The displayed specimen from the 0.5mM RF group shows only a slight reduction in NP size when compared to healthy discs, according to the NP voxel count and histological cross-section measurements. The IVD from the 0.25RF group shows a reduced nuclear size. The NP appears still homogeneous and hyperintense but has lost its oval shape. The decreased disc height, which is also seen on X-Ray, results in a Pfirrmann grade of III. The uncross-linked collagen injected IVD shows a greater reduction in NP size. The NP is still hyperintense but appears more heterogeneous. The untreated disc shows terminal degenerative changes: a black disc on MRI combined with collapsed disc space. The NP tissue has been completely replaced with connective tissue. Endplate damage is visible.

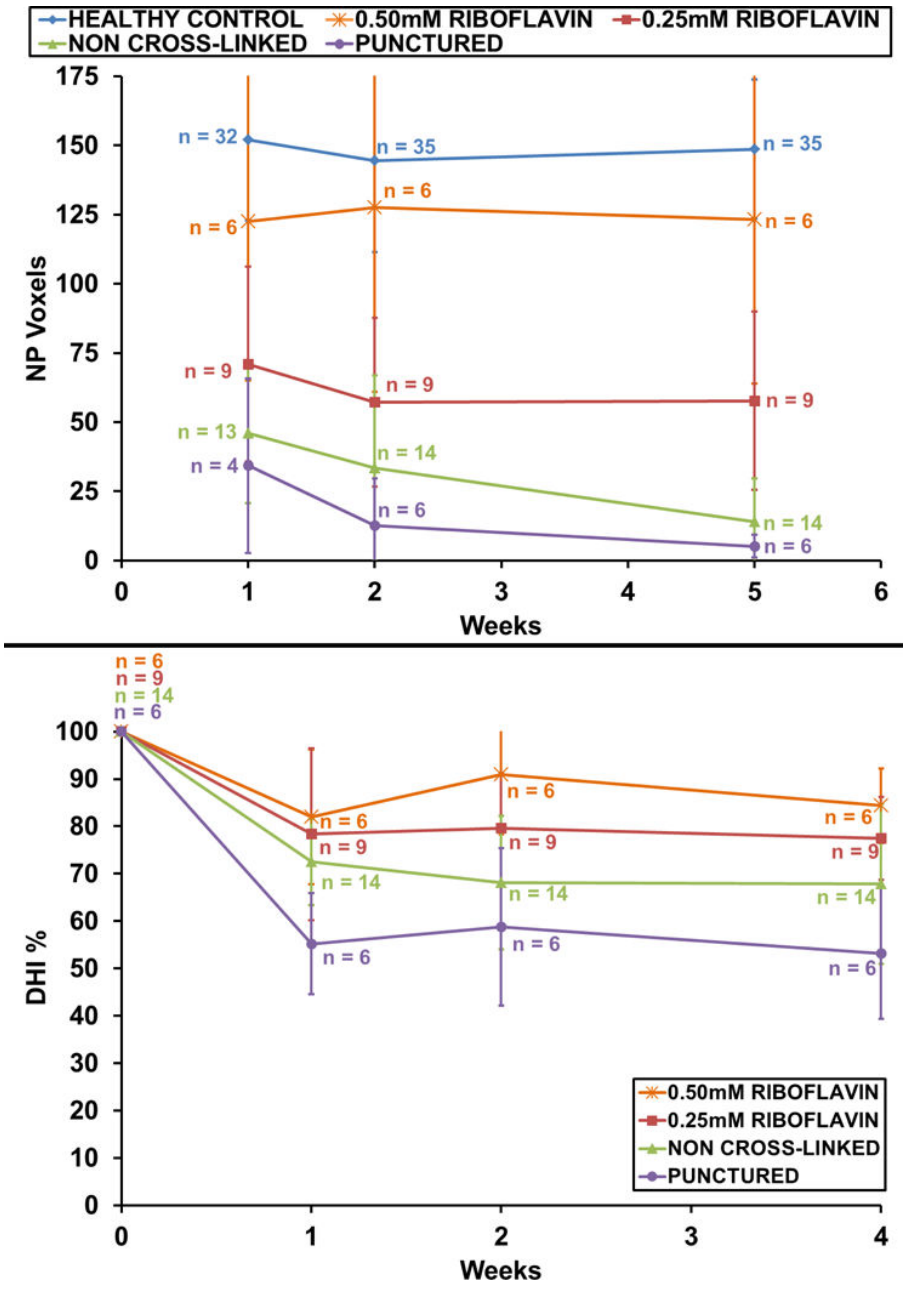

Figure 3.3: (A) Nuclear size according to NP voxel count measurements. The 0.5mM group showed slightly fewer NP voxels than did healthy discs over 5 weeks. Voxel counts of both crosslinked groups remained constant between the 2nd and 5th weeks. Animals injected with uncross-linked collagen gel showed a continuous drop in NP voxels over 5 weeks. The untreated group showed the lowest voxel count numbers at all time points. (B) Disc height initial disc height; the untreated group dropped to 55%. Variations in n within groups resulted from MRI scheduling constraints. measurements correlated with NP voxel count results. The 0.5mM group retained 88% of its initial disc height; the untreated group dropped to 55%. Variations in n within groups resulted from MRI scheduling constraints.

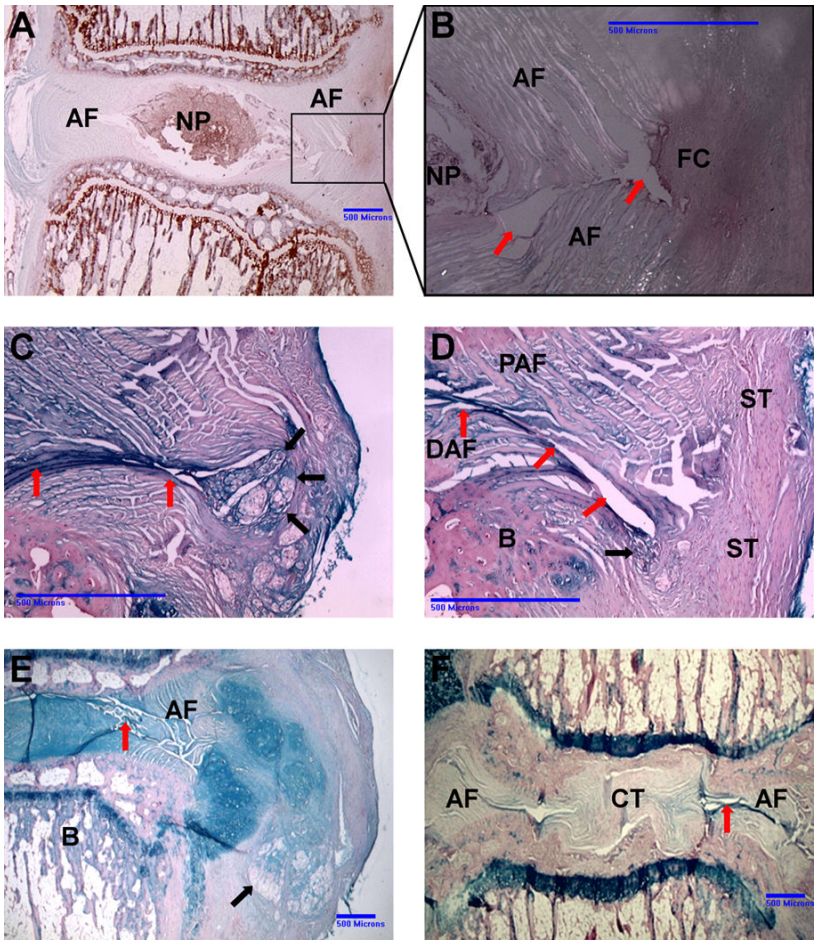

Figure 3.4: Different histological outcomes of punctured IVDs after five weeks. (A) Safranin O stain, 0.25mM RF group. The disc displays an ovular NP of standard size. The needle-puncture defect and fibrous cap are outlined by the box. (B) Higher magnification under polarized light. The needle-puncture defect is clearly visible (red arrows). The inner 2/3 of the AF lamellae remain separated; there is no sign of tissue repair. The outer 1/3 of the defect is bridged by a fibrous cap (FC). The non-birefringent FC matrix appears to infiltrate the bright, birefringent AF fibers. (C) Alcian blue stain. 0.25mM RF group. Only a thin fibrous string (black arrows) bridges the annular defect (red arrows). **(D)** Alcian blue stain. **Uncross-linked group** . No fibrous tissue visible repairing the defect (red arrows). Distal annular fibers (DAF) and proximal annular fibers (PAF) remain separated and infiltrate the surrounding scar tissue (ST). The black arrow points to sequestered NP material. B indicates endplate bone. **(E)** Alcian blue stain. **Uncross-linked group** . NP tissue (black arrow) extrudes through the annular defect into the paravertebral space. The AF shows multiple fissures (red arrow). **(F) Untreated control IVD** . Needle-puncture defect (red arrow) induced severe degenerative changes. There is no organized AF tissue visible; the NP has been replaced with connective tissue.

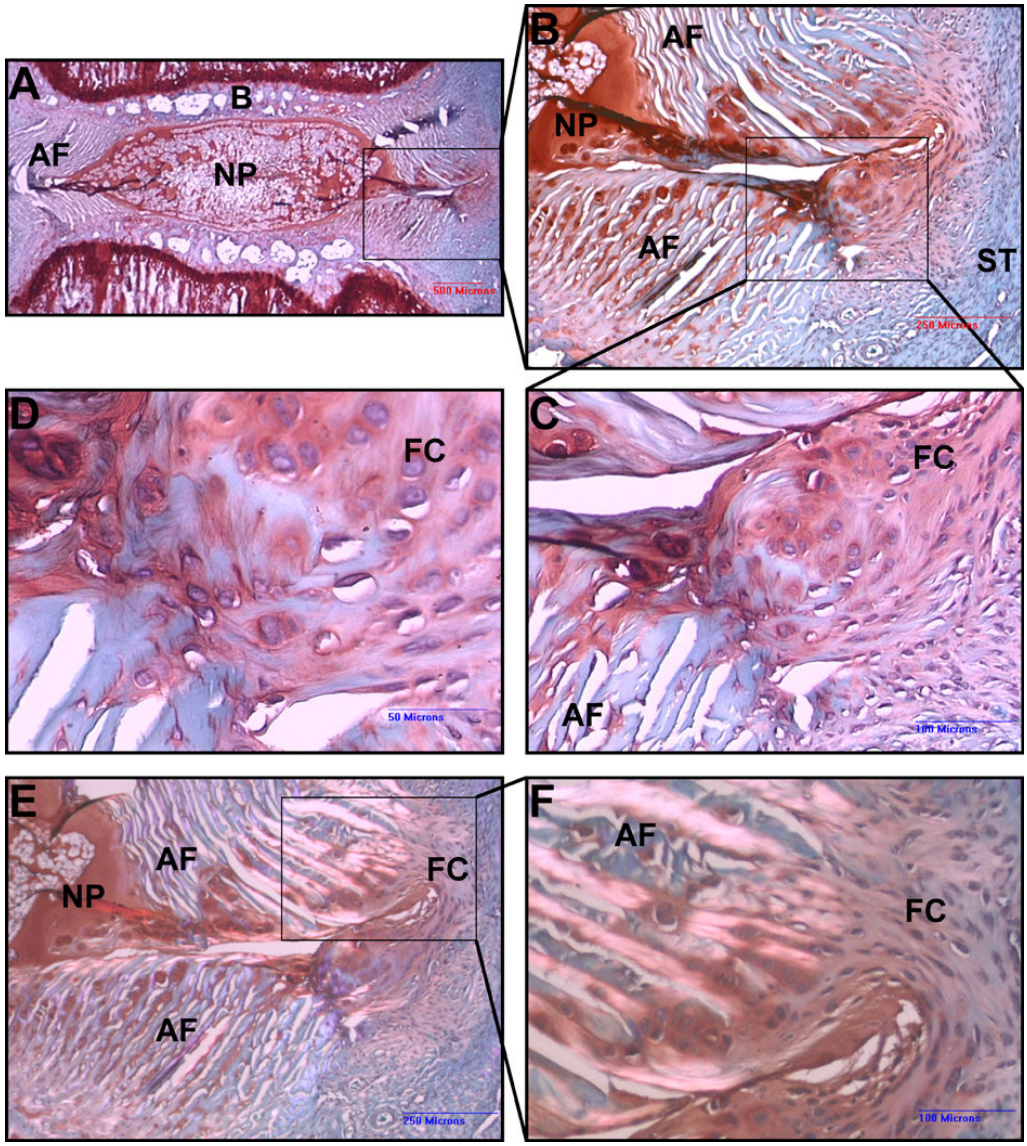

Figure 3.5: Safranin O stain. Punctured IVD, 0.5mM RF group after 5 weeks. (A) Low magnification. The NP displays standard size and ovular shape. A clear border separates the NP from the AF and endplate bone B. The box marks the needle puncture defect. (B) Higher magnification shows the needle puncture defect piercing through every layer of the AF. A fibrous cap, marked by the box, bridges the annular defect at the outer portion of the AF. The matrix of this fibrous tissue stains more intensely with Safranin O than does the surrounding scar tissue (ST). (C), (D) Higher magnification of the fibrous cap, which appears to be infiltrating AF fibers. **(E), (F)** Same specimen as in A–C, viewed under polarized light. The bright birefringent AF fibers mesh with the non birefringent tissue of the fibrous cap.

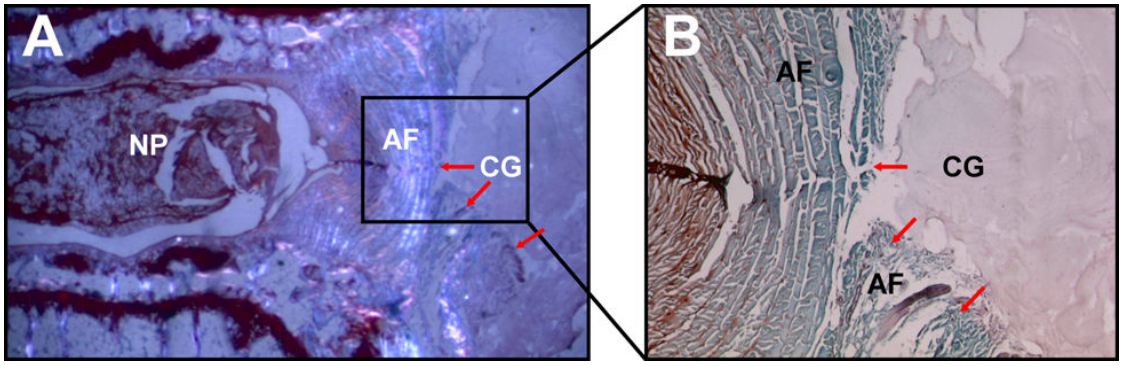

Figure. 3.6: Fate of the collagen gel. (A) Safranin O stain, polarized light immediately after collagen gel (CG) injection. HDC distributes in the paravertebral space, covering the AF defect. In contrast to the AF, HDC is non birefringent under polarized light, indicating a lower tissue organization. (B) Higher magnification. The puncture defect is visible (red arrows). CG appears as an amorphous homogenous tissue, which stains slightly positive for Safranin O. It does not migrate into the AF defect.

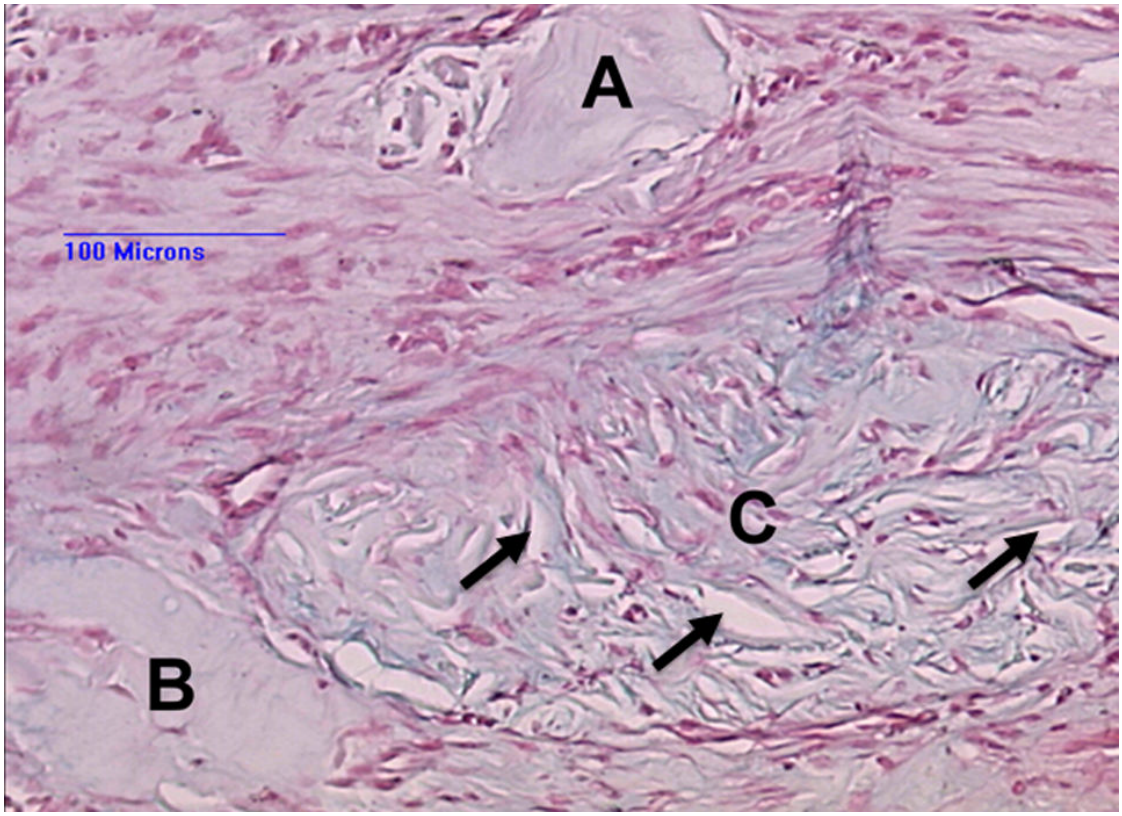

Figure. 3.7: Fate of the collagen. Alcian blue stain. Paravertebral space 5 weeks after collagen injection. Three islets of amorphous homogenous collagen surrounded by scar tissue. Islet A shows no cell infiltration, islet B very limited. Islet C shows a high degree of fibroblast infiltration. The cells appear to reorganize the tissue, as indicated by resorbtive zones (black arrows) within the collagen tissue. There is no sign of an inflammatory response.

CHAPTER 4:

In Vivo Annular Repair using High-Density Collagen Gel Seeded with Annulus Fibrosus Cells

This chapter has been submitted for publication:

*Moriguchi, Y., *Borde, B., Pennicooke, B., Berlin, C., Kahir, T., Grunert, P., Navarro-Ramirez, R., Bonassar, L. J., & Härtl, R. (2016). Annular repair using high-density collagen gel: a rat-tail in vivo model. *Spine*, *Submitted*

**Borde and Moriguchi are listed in publication as co-first authors on this manuscript*

4.1 Abstract

To assess the *in vivo* efficacy of annulus fibrosus (AF) cells seeded into collagen at enhancing the reparative process around annular defects and preventing further degenerative changes in a post-puncture rat-tail model.

Despite alleviating associated neurological symptoms, discectomy of herniated intervertebral discs fails to repair the underlying degenerative process. Persistent annular defect post discectomy is associated with increased risk of reherniation, progressive degeneration, and chronic low back pain. We recently demonstrated that riboflavin cross-linked high-density collagen gels (HDC) can facilitate annular repair *in vivo*.

Forty-two athymic rats, tail disc punctured with an 18-gauge needle, were divided into 3 groups: untreated (n=6), injected with crosslinked HDC (n=18), and injected with AF cell-laden crosslinked HDC (n=18). Ovine AF cells were mixed with HDC gels prior to injection at a concentration of 10^6 cells/ml. A series of *in vivo* imaging with X-ray and 7T MRI were conducted over 5 weeks to determine disc height index, NP size, and hydration. Histological assessments evaluated the viability of implanted cells, degree of annular repair, and secondary disc degeneration.

Both HDC gel groups, AF cell-laden and acellular, had significant retention of disc height, NP size, and NP hydration at five weeks when compared to puncture controls. Average NP voxel count of cellular gels were higher than those of acellular gels at all time points, and statistical significance was demonstrated at 1 and 5 weeks. Further histological assessments indicate that while HDC gels influence reparative

sealing of the defect, the addition of cells accelerates this process by as early as 2 weeks.

AF cell-laden HDC gels have the ability to better repair annular defects than acellular gels after needle puncture, thereby suggesting their potential feasibility in a cell-based therapy for annular defects.

4.2 Introduction

Occurring in 40% of individuals younger than 30 and in more than 90% of those older than 50 years of age[1], degenerative disc disease (DDD) is a prevalent clinical condition that can lead to nerve compression and chronic back pain. Disc herniation with radiculopathy is one of the most common DDD-linked clinical diagnoses that effects the lumbar spine [2]. When pharmacological and physiotherapeutic treatments fail to relieve patient symptoms in lumbar disc herniation (LDH), a discectomy procedure is often performed, with an estimated 300,000 cases per year in the United States[3]. Although discectomies decompress neural tissue, they leave the annular defect or tear untreated. This increases the risk of recurrent disc herniation through the open defect, which occurs in 6%-23% of all patients following discectomy[4-6], and is associated with compromised patient outcomes and increased health care costs[7,8]. A persistent annular defect is also associated with progressive degenerative changes of the intervertebral disc (IVD)[9-11], and may be the primary cause of chronic low back pain following discectomy[12]. To date, there is no established method for repairing annular defects in order to reduce the re-herniation rate and limit the progression of disc degeneration[13].

A fundamental problem is the low intrinsic healing capability of the annulus fibrosus, as demonstrated in animal experiments[14,15]. To address this issue, several attempts have been made to repair annular defects either mechanically or biologically. However, mechanical solutions such as suturing or annuloplasty devices do not significantly alter annular healing strength in animal models[16] or demonstrate long-term benefits in clinical trials[17]. Clinical and experimental biological treatment approaches for degenerative disc disease have recently been reviewed [Yu Moriguchi, Marjan Alimi, Thamina Khair, George Manolarakis, Connor Berlin, Lawrence J. Bonassar, Roger Härtl. Biological Treatment Approaches for Degenerative Disk Disease: A Literature Review of In Vivo Animal and Clinical Data. Global Spine J DOI: 10.1055/s-0036-1571955]; biological, rigid implants using tissue-engineered AF constructs have been tested *in vitro*[18-22]. Implants made from small intestinal submucosa reduced degenerative changes after annulotomy in the sheep spine[23], but in order to improve clinical applicability, injectable biomaterials have recently been developed. Injectable genipin cross-linked fibrin hydrogels were shown to integrate with sections of human AF tissue and showed promising biomechanical and cell-seeding properties in vitro[21].

A similar solution involves the use of collagen gels, which have been used extensively in regenerative therapies due to accumulating evidence supporting their biocompatibility and safety[24,25]. We recently demonstrated that injectable high-density collagen gels (HDC) cross-linked *in situ* by blue light exposure, can effectively seal annular defects, facilitate annular repair, prevent further NP herniation and subsequent degeneration, and restore disc functionality in an *in vivo* rat-tail model[26,27]. In addition,

previous studies have shown that fibrochondrocytes, component cells of the AF, seeded into collagen, are able to produce a matrix which is similar to the native AF and remodel the composite into a more biocompatible and mechanically-stable material[28,29]. Accordingly, the addition of AF cells can enhance the ability of collagen gels to repair annular defects in early to mid-stage disc degeneration. These cell-laden gels can potentially reduce the rate of re-herniation and limit further degeneration, yielding a favorable clinical outcome.

In the present study, we assessed the *in vivo* efficacy of AF fibrochondrocytes seeded into riboflavin crosslinked HDC gels for enhancing the reparative process at the site of annular defects, and preventing further degenerative changes, in a post-puncture rat-tail model.

4.3 Materials & Methods

High-density Collagen Gel Preparation.

Collagen type I was extracted from rat-tail tendons[26,27]. The tendons were dissected and digested in a dilute solution of acetic acid (0.1% 80 mL/g, at 4 ° C for 2 d). The resulting solution was centrifuged and the collagen concentrated to 20 mg/mL by lyophilization and resuspension in acetic acid.

AF cell isolation and preparation of cellular collagen gels

Cell preparation was based on previously described techniques[28]. Lumbar spines of skeletally mature sheep were purchased and IVDs were dissected out of the segments. Tissue was washed in PBS (Dulbecco's PBS; Gibco BRL) and then separated into AF and NP regions. To isolate AF cells, the AF was dissected into small pieces and digested in 200 mL of 0.3% wt/vol collagenase type II at 37 °C for 9

hours. Digested tissue was filtered through 100 μm nylon mesh (BD Biosciences) and centrifuged at 936 g for 7 min. Cells were counted and seeded at 2,500 cells⁄cm^2 in culture flasks with Ham's F-12 media (Corning Mediatech) that contained 10% fetal bovine serum, penicillin (Gemini Bio Products), (100 units⁄mL), streptomycin (100 μg⁄mL), amphotericin B (250 ng⁄mL), and ascorbic acid (25 μg⁄mL). Cells were cultured at 37 °C, 5% CO2, and normoxia to confluence with media changes every 3 days. At confluence, cells were removed from flasks with 0.05% trypsin (Corning Mediatech) and counted with a hemocytometer. Cells were then seeded into high density collagen gels at a concentration of 10^6 cells/ml prior to injection.

Needle puncture-induced degeneration model and collagen injection.

Forty-two skeletally mature male athymic rats (Hsd: RH-Foxn1^{rnu}) were utilized. The animals were 10 to 12 weeks old at time of surgery, with weight of 200-300 g. All surgical procedures were performed in accordance with the RARC guidelines for large animal surgery, including sterilization of surgical supplies, aseptic techniques, preoperative care, monitoring and supportive care, surgical procedures, and postoperative care. A needle puncture-induced degeneration model was employed as previously described[26,27] to determine the efficacy of the gel-based treatment in comparison with solely punctured control specimens. A total of 42 rats, punctured with an 18-gauge needle in the tail disc, were divided into three groups: 1) untreated (n=6); 2) injected with crosslinked HDC (n=18); 3) injected with AF cell-laden crosslinked HDC (n=18). In brief, a dorsal, 2-cm longitudinal skin incision was made and the AF was exposed and punctured. The 18-gage needle penetrated the AF until the bevel was completely inserted. In the collagen-injected groups, the IVD was

punctured and simultaneously injected with either AF-cell laden or acellular collagen gels around the annular defect. In the control group, discs were punctured and left untreated. The wound was closed cutaneously with 3-0 polyamide-nylon sutures. Postoperative care was provided by Veterinary Services personnel, as per RARC guidelines. Sutures was removed 10-14 days postoperatively.

Qualitative MRI Analysis

A sagittal TurboRare sequence (TR = 2017 ms, TE = 60 ms, NEX = 6, echo train length = 12, slice thickness = 1 mm and matrix size = 320 × 320, and resolution: 125 μ m × 125 μ m × 1 mm) was utilized for qualitative assessments. We used a modified Pfirrmann scale 24 that outlines 4 grades of degeneration as defined by NP signal intensity, homogeneity, and loss of disc height[30].

Quantitative Magnetic Resonance Imaging

All 32 animals underwent 7 Tesla MRI (Bruker 7T UST preclinical MRI System, BRUKER AXS Inc., Madison, WI) imaging at 1 week, 28 animals at 2 weeks, and 24 animals at 5 weeks, postoperatively. For quantitative assessment, the voxel count and average T2 relaxation time in NP were measured according to an algorism we previously developed[31]. We used a sagittal multislice multiecho pulse sequence (TR = 2000 ms, TE = 12 ms, NEX = 2, number of echoes = 12, echo spacing = 12 ms, slice thickness = 1 mm, and matrix size = 320 × 320, resolution: 125 μ m × 125 μ m × 1 mm) to create a T2 map on the basis of fitting semilog plots of T2 signal intensity *versus* relaxation time for the 12 acquired echoes. Bruker's proprietary program TopSpin was used for this fitting process. A color map was assigned to the resulting T2 map. Next, a standard region of interest (ROI) measuring approximately 1

mm^2 (comprising 90 voxels) was drawn within the center of NP of the healthy disc proximal to the experimental segments. The average T2-relaxation time (T2-RT) of that ROI was measured, and this value minus 2 standard deviations was used to set a subtraction threshold for all voxels in that slice. Voxels with T2 values lower than the threshold were subsequently subtracted. As a result, only voxels with T2 values representing NP tissue remained in the disc space and were then counted. At each time point, the mean voxel count of experimental segments was compared with the mean voxel count of proximal adjacent healthy discs. The mean T2-RT of aforementioned NP voxels was also calculated and compared with that of the healthy control.

Disc Height Measurements

X ray imaging was performed at one, two and five weeks to measure the disc height of treated segments. Great care was taken to achieve true lateral radiographs of the index segment. The IVD height was expressed as a disc height index, calculated by dividing disc height by adjacent vertebral body height on the basis of the modified method of Lu et al.[32].

Histology

Animals were sacrificed at one, two, or five weeks postoperatively. Tail spines were collected and processed for further ex vivo histological assessments as previously described[27]. After fixed with 10% neutralized formalin supplemented with 1 % cetylpyridinium chloride (CPC), specimens were decalcified, cut in the mid-sagittal plane, and transferred to 75% ethanol. Segments were embedded in paraffin, then cut to 5-μm thickness, and stained with Alcian Blue and Safranin-O.

Statistics

All the quantitative values from X-rays and MRIs represent the proportion of experimental to adjacent healthy control measurements, and were expressed as mean ± SD. For the analyses for continuous outcomes in disc height index, NP size, and NP hydration, we employed linear regression models with a generalized estimating equation and robust standard errors to estimate differences in mean changes from baseline controls (discectomy) across stable and displaced implantation groups for the 1, 2 and 5-week time points. Statistical analyses were performed with IBM SPSS Statistics 22 (SPSS, Chicago, IL, USA). P values <0.05 were considered statistically significant.

4.4 Results

Qualitative MRI

On 5-week MR images, all the punctured IVDs, whether treated or not, displayed decreased NP size (Figure 4.1). The cellular gel-injected IVD showed hyperintense, but slightly heterogeneous NP. The Pfirrmann grade (a semi-quantitative measurement of degeneration) of the cellular group ranged from II (moderate) to IV (severe), while the punctured and untreated segments had grade IV, indicating potentially milder degeneration in the cellular group than the untreated group based. The acellular group showed more heterogeneous, smaller NP, with a black fissure in the middle as well as a detectable decrease in disc height. The Pfirrmann grade of this acellular group ranged from III to IV. The punctured and untreated groups showed black IVDs with collapsed disc spaces.

Disc height Index (DHI)

Quantitative analyses based on X rays showed that the cellular (but not the acellular) gel had significant retention of disc height at 5 weeks ($p=0.020$ in cellular vs puncture and $p=0.102$ in acellular vs puncture, Fig 4.2). Although the cellular group had a higher mean DHI at all time points compared to the acellular group, this difference between the two groups was not statistically significant. Both cellular and acellular groups showed arrest of deterioration at 2 weeks in terms of mean DHI (the disc height did not decrease), while only the puncture group demonstrated a consistent downward trend over time with a statistical significance between 2 and 5 weeks ($p=0.02$).

NP Voxel Count and T2-Relaxation Time (T2-RT)

Quantitative MRI analysis demonstrated that the gel-treated groups, whether cellular or acellular, had a higher average NP voxel count following needle puncture when compared to the puncture group at all time points, with the cellular group having the highest mean NP voxel counts. The cellular gels significantly retained NP tissues compared to the untreated puncture group at 1 and 5 weeks ($p<0.001$ and $p=0.012$, respectively), and the acellular group at 5 weeks ($p=0.046$). Both puncture and acellular groups showed a downward trend over time after 2 weeks, while the cellular group demonstrated resurgence at 2 weeks in terms of average NP size. However, these time-dependent changes failed to demonstrate statistical significance ($p>0.05$).

Likewise, both cellular and acellular groups showed significantly higher NP T2 relaxation time, an indicator of NP physiological hydration, at all time points ($p<0.001$ / <0.001 / <0.001 in acellular vs untreated and $p<0.001$ / <0.001 / <0.001 in cellular vs puncture at 1, 2, and 5 weeks, respectively). In addition, the cellular group

significantly maintained NP hydration compared to the acellular group. There was a significant time-dependent decrease of NP T2 relaxation time from 1 and 2 to 5 weeks in the puncture and acellular group (p=0.004/ 0.021 in puncture and p=0.001/0.002 in acellular, between 1 and 5 weeks, and 2 and 5 weeks respectively). The cellular group maintained over 90 % of adjacent native disc T2 relaxation over 5 weeks, displaying a much greater retention of hydration than the other groups.

Likewise, both cellular and acellular groups showed significantly higher NP T2 relaxation time, an indicator of NP physiological hydration, at all time points (p=0.003 / 0.004 / 0.001 in acellular vs untreated and p=0.002 / 0.01 / 0.001 in cellular vs puncture at 1, 2, and 5 weeks, respectively). Despite the lack of statistical significance in intergroup differences, the cellular group had a higher mean value of NP T2 relaxation (around 90%) at 5 weeks, although there was a significant overall time-dependent decrease in NP T2 relaxation time in this cellular group (p=0.005). In contrast, the segment treated with acellular gels lost more than 35% of NP hydration at 5 weeks after needle puncture (p=0.025 in 1 week vs 5 weeks and p= 0.021 in 2 weeks vs 5 weeks), suggesting there was a more significant decrease after 2 weeks in this group compared to the cellular group. The untreated control group also had a downward trend over time, resulting in a significant decrease in T2 relaxation time between 1 and 5 weeks (p=0.014).

Histology

Histological images stained with Safranin-O demonstrated abundant proteoglycan-rich matrices of NP, which is stained in red, in the center of an adjacent healthy disc segment (Fig 4.1). The cellular group retained NP tissues in the core but

lost more at the peripheral region, which is well corroborated by MRI T2 map images (Fig 4.1). Acellular gels, although still retaining some NP tissue, showed an AF bulge into the NP, giving the NP an hourglass shape. The NP tissue in the punctured and untreated segment has been completely replaced with fibrous tissue at 5 weeks. As a proof of terminal disc degeneration, disruption of the endplate was also observed.

Close-up images at an earlier time point such as 2 weeks demonstrated some remnant NP even in the untreated group, although the core of NP was already replaced with fibrous tissue in this group. There was no reparative tissue observed that bridged the gap between both ends of disrupted annulus tissue at the site of the needle puncture. Therefore, the annular defects were persistent (Fig 4.4A, a). In the acellular gel-treated segments, there was more tissue at the outer part of the annular defects, but this did not display good integration with the host AF; these defects were not physically closed either (Fig 4.4B, b). In the cellular gel-treated segments, there was a fibrous patch that integrated outer ends of the disrupted annular fiber and thereby physically closed the annular defect, although no substantial tissue was observed inside the annular defect (Fig 4.4C, c). At 5 weeks, this fibrous cap accompanied with scattered fibrochondrocytes grew thicker and robustly closed the gap at the outer edge of annular defect (Fig 4.4D, d).

In order to assess the fate of injected collagen gels, histological sections stained with Alcian blue were utilized at 2-week time point. Our previous study demonstrated that Alcian blue stains the collagen gels mildly/moderately blue[26]. In the present study, both cellular and acellular group demonstrated several islets of amorphous matrix, which is consistent with remnant collagen gels, in the paravertebral

space (Fig 4.5). These islets in the cellular group, even at 2 weeks, were intensively reorganized by infiltration of fibroblastic host cells, and the implanted fibrochondrocytes with lacuna structure are also observed in the gel domain (Fig 4.5A-C). In contrast, the acellular gels demonstrated a lower degree of host cell infiltration and no chondrocytic cells inside. No sign of inflammatory or foreign body reaction was visible in both groups (Fig 4.5D).

4.5 Discussion

The present study demonstrates the feasibility of disc component AF fibrochondrocytes to facilitate annular repair in a needle puncture model. Discs treated with AF cell-laden collagen gels had more significant retention of disc height, prevented further NP herniation as well as subsequent degeneration, and maintained physiological hydration of NP.

Biological approaches to DDD have reached remarkable feats over the past decade. Although cell-therapy focusing on NP regeneration has been well studied, whether at a clinical or preclinical stage, cell-based strategies are much less frequently employed to repair annular defects[33,34]. Sato et al. demonstrated that allografted cultured AF cells produced hyaline-like cartilage in the AF and NP region, and that segments receiving AF cells seeded in an atelocollagen honeycomb-shaped scaffold better maintained disc height compared to segments receiving scaffolds alone or untreated segments. Our results support Sato et al.'s existing data on disc height restoration as well as the conclusion that addition of AF cells can prevent or slowdown disc degeneration after annular injury. One conflicting finding is that reparative processes observed in the present study's cellular group after 2 weeks yielded more

fibrous tissues with fibrochondrocytic cells scattered throughout, in contrast to the hyaline-like cartilaginous tissues observed in Sat et al.'s study. However, as our previous study demonstrated the presence of similar tissues induced by collagen gels in the same in vivo settings[26,27], these differences in phenotypic features of reparative tissues may be caused by a discrepancy in animal species, mode of annular injury, utilization of rigid scaffolds, or mode of cell administration.

In the present study and our previous study, fibrous caps integrating with the host annulus fibrosis were detected at 5 weeks (but not 2 weeks) after injection of acellular gels[26]. Of note, the cellular group demonstrated fibrous caps beginning at 2 weeks. This cellular fibrous cap, which became thicker at 5 weeks, approximated the gap between ruptured inner annular fibers and thereby physically closed the annular defect, preventing further loss of NP. The early formation of reparative tissues in the present study can account for the intergroup difference in the time course of NP retention. Only the cellular group had a trend of improvement, halting deteriorations in NP size from 2 to 5 week and resulting in significant retention at 5 weeks compared to those of the puncture and acellular groups (Fig 4.3A). In addition, the puncture and acellular groups demonstrated significant loss of hydration from 2 to 5 weeks while the cellular group did not show this downward trend and maintained over 90 % of adjacent healthy NP (Fig 4.3B). Accordingly, these findings suggest that the addition of AF cells can accelerate gel-induced formation of a reparative, fibrous cap at an earlier phase, and can play an inhibitory role in the loss of hydrated tissues as well as the progression of disc degeneration after annular injury.

Successful annular repair can play an important role in primarily reducing the risk of reherniation and progressive disc degeneration after discectomy, but also in providing a solution to a common issue in biological NP treatments, employing transannular approaches. Annular defect can emerge not only from discectomy or discography, but also from regenerative treatments for the NP that proceed transannularly[35]. Given the sensitivity of the AF, lesions from NP treatment can provoke further degeneration, inducing leakage of the delivered material and eventual failure of the regenerative treatment. In fact, a previous study demonstrated that injecting mesenchymal stem cells (MSCs) through the AF into the NP led to cell leakage and augmented osteophyte formation[36]. An injectable biomaterial that seals the defect and delivers the cells of tissue-repairing capability can offer a platform for biological annular repair and may significantly improve patient outcomes, when combined with emerging biological treatments for NP.

That being said, there are limitations related to our rat-tail puncture model. Firstly, the relatively small size of discs inhibits the injection of the gels into annular defects, in opposition to the intradiscal pressure. Therefore, the injected gels were placed at a superficial layer of AF sealing the entrance of the annular defect. Eventually, the potential for collagen gels to repair deeper layers of AF was not possible to study. Secondly, an 18G needle might be too big to induce clinically relevant annular defects in a tiny rat-tail IVD model, which is likely the reason we observed a substantial loss of NP even at earlier time points. Thirdly, it is unclear whether the described fibrous cap can mechanically compensate for the motion in human IVDs, which are exposed to much higher mechanical forces and different axial

loads. Another limitation is the brevity of the experimental follow-up period. Although significant intergroup differences were observed at a 5-week time point with the cellular group having the best outcomes, a further follow-up is needed to elucidate longer-term durability of the cell-based treatment. Nonetheless, these limitations do not critically affect the major conclusion of our study.

Finally, there are two main limitations associated with a decision to use young, athymic rats: (1) these rats cannot offer insight into how these gels will integrate into immuno-competent animals (although a current pilot study we are performing in healthy sheep suggests no presence of immune inflammatory response), and (2) the rat IVD segments are young and healthy, and thus have none of the deficits in endplate nutrition, proteoglycan and collagen type II content, hydration, etc., that we observe in clinically relevant forms of human DDD and disc herniation—which limits any far reaching conclusions about gel performance in a degenerated disc segment. However, in terms of the overall objective of this study, which was to compare cellular vs. acellular gel performance *in vivo*, our experimental conclusions remain valid, and the rat-tail is still a useful and cost effective screening model.

Overall, the present study demonstrates the feasibility of AF cell-laden collagen gels to facilitate annular repair in a needle puncture rat-tail model. The cellular gels outperformed the acellular gels, having significantly greater retention of disc height, preventing further NP herniation as well as subsequent degeneration, and maintaining physiological hydration of remnant NP. A long-term follow up with sufficient sample size is needed to confirm these results and the *in vivo* durability of cell-based annular treatments.

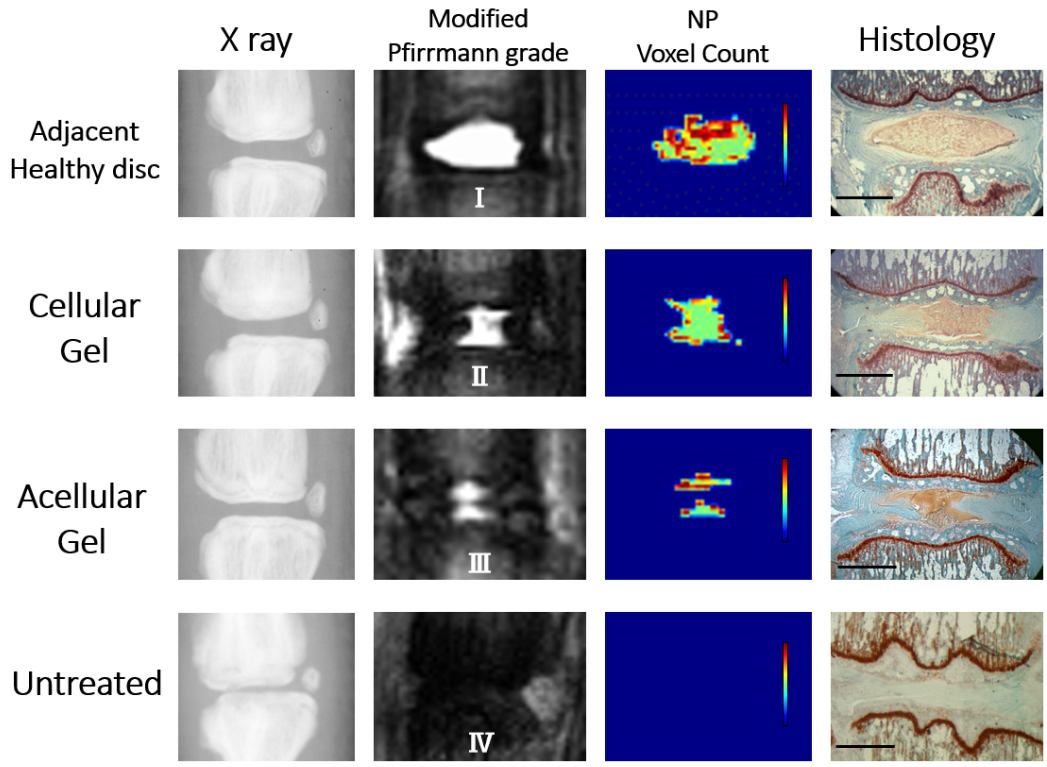

Figure 4.1: Five-week outcome examples. Adjacent healthy discs and punctured but untreated segments served as a positive and negative control, respectively. The cellular gel outperformed the acellular gel and maintained disc height on X rays as well as signal intensity on MRI T2 mapping, which was corroborated by retention of NP tissues on histology. Disruption of the endplate was observed in the puncture group, but not in the treated segments.

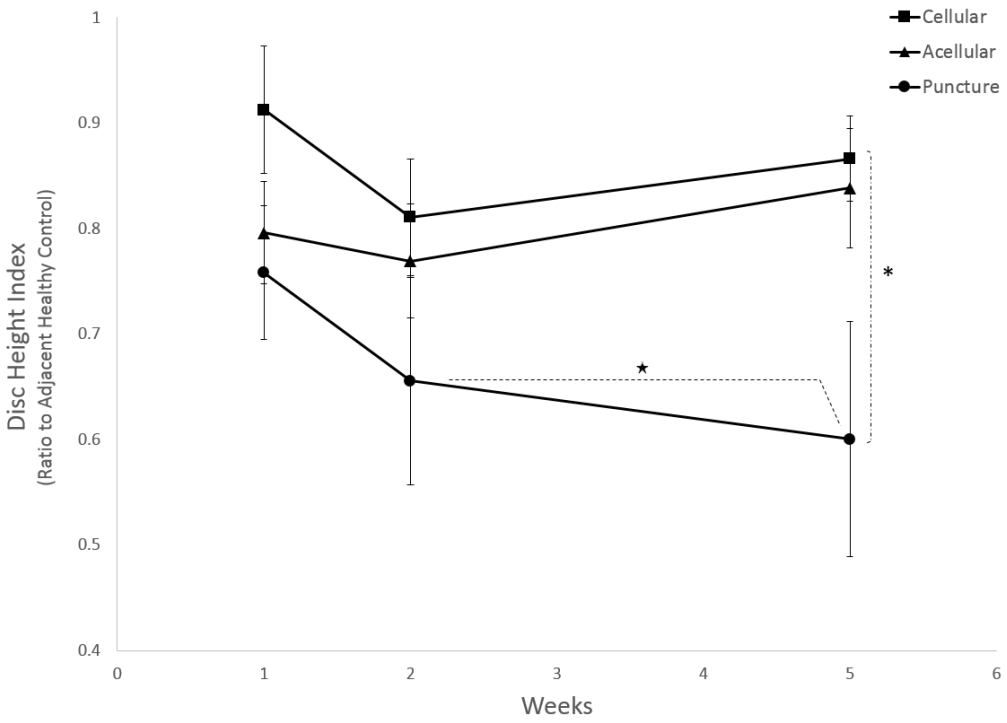

Figure 4.2: Quantitative assessment of disc height. Only the cellular gels maintained significantly greater disc height than the punctured segment. Asterisks and stars denote significant intergroup difference (puncture vs AF cell-laden, $p<0.05$) and intragroup time-dependent difference (2 week vs 5 week in the puncture group, $p<0.05$), respectively.

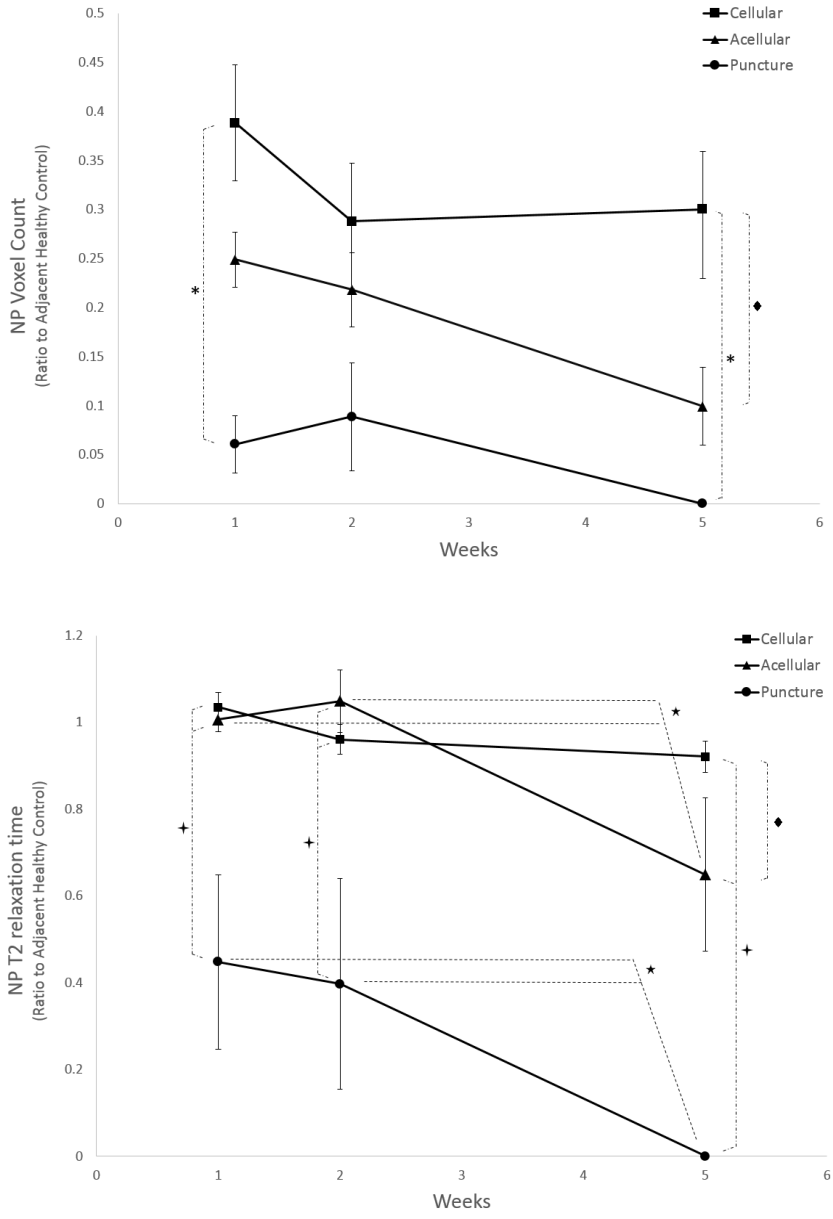

Figure 4.3: NP voxel count (*top*), and NP T2 relaxation time (*bottom*). Average NP voxel counts of cellular gels were higher than those of acellular gels at all time points and statistical significance was achieved at 1 and 5 weeks. There was a significant difference in NP retention between the cellular and acellular groups at 5 weeks. Both cellular and acellular groups had significant retention of T2 relaxation time compared to the puncture only group. The cellular group had significantly higher NP hydration than the acellular group. The puncture and acellular groups demonstrated significant loss of hydration at 5 weeks, while the cellular group maintained over 90 % of adjacent healthy NP hydration. Asterisk: untreated vs cellular, $p<0.05$; Cross: puncture and vs cellular and acellular, $p<0.05$; Star: intragroup time-dependent difference.

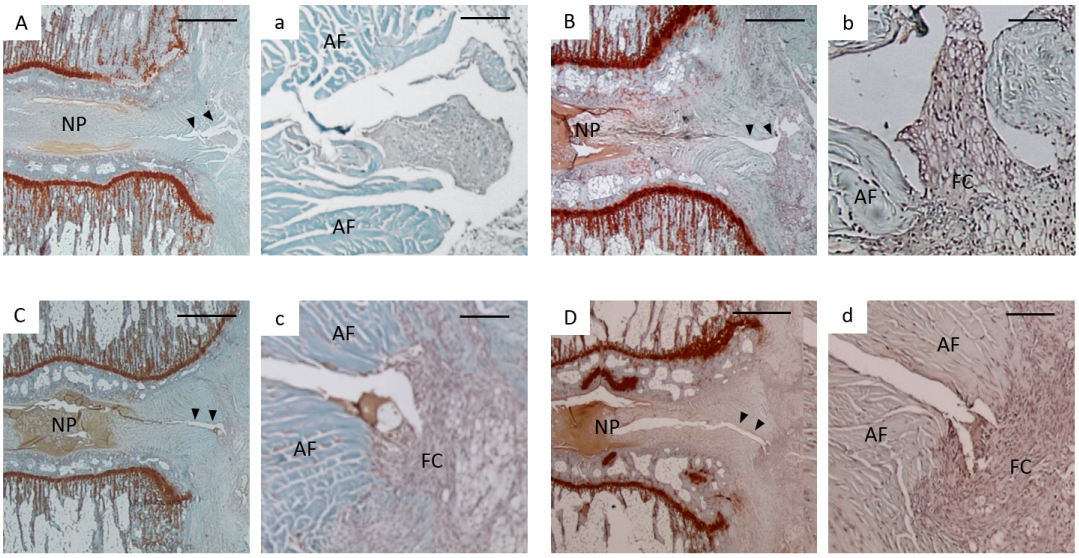

Figure 4.4: Histological images stained with Safranin O demonstrated retention of NP as well as reparative tissue at the site of annular defect. The punctured and untreated group demonstrated persistent annular defects without any sealing tissues, and thereby lost most of NP as early as 2 weeks (A, a). The segment treated with acellular gels demonstrated some reparative tissue that attached to the disrupted annulus fibers at the outer part of the defect (B, b). Unlike the other groups, the cellular group revealed reparative tissue closing the gap between disrupted fibers at 2 weeks (C, c) and more at 5 weeks (D, d). Bars = 500 / 50 μm (A-D, a-d). AF: annulus fibrosus; NP: nucleus pulposus; FC: fibrous cap. Black triangles denote the annular defect.

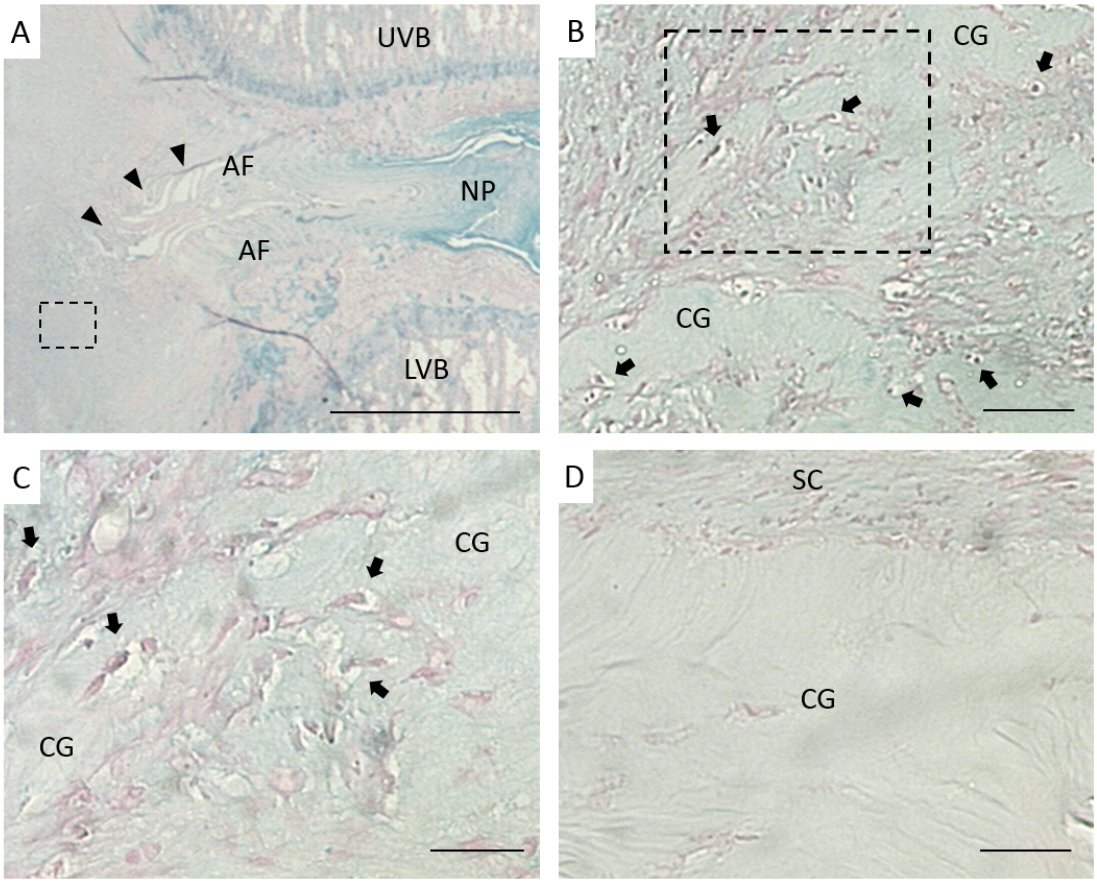

Figure 4.5: 2 weeks after injection, remnant gels were shown as amorphous matrices mildly stained by Alcian blue in the paravertebral space of AF cell-laden and acellular groups. AF cell-laden gels (A-C) showed the cells accompanied with lacunae in the gel domain, suggesting that the implanted AF fibrochondrocytes survived (black arrows), while acellular gels (D) have similar gel-like matrices but no substantial cells within. The gel reorganization process is more advanced in the AF cell-laden gels than the acellular gels, which may be attributed to the presence of implanted AF cells and/or host cell infiltration (this is observed with direct comparison between B and D at the same magnification). No sign of inflammatory or foreign body reaction was visible in either group. The squares in A and B are image B and C, respectively. Bar = 1000 / 50 / 25 / 50 μm (A / B / C / D). AF: annulus fibrosus; NP: nucleus pulposus; UVB: upper vertebral body; LVB: lower vertebral body; CG: collagen gels; SC: scar tissue. Black triangles denote the annular defect.

CHAPTER 5:

Conclusions

This dissertation establishes riboflavin crosslinked collagen as a novel, injectable method for the repair of annulus fibrosus defects in the IVD. Use of collagen hydrogels in research applications is wide spread, but its use in orthopedic applications is limited. Here, we have seen that collagen can be delivered to the AF for mechanical repair of a composite fibrous tissue (Chapter 2), while allowing for biological healing to begin at the defect site (Chapters 3 and 4). While only one application is addressed in this dissertation, it sets the groundwork for the expansion of riboflavin crosslinked collagen to other application where injectablilty is required for delivery.

5.1 From the In Vitro Studies

Chapter 2 explored the effect of AF repair with various collagen gel formulations and crosslinker concentrations on the effective mechanical properties of rat caudal IVDs. Small and large defects were tested, with the motivation being diagnostic and surgical procedures, respectively. All collagen gel formulations in small defects outperformed their counterparts in larger defects. Gross examination as well as histology confirmed gels at the defect site post-mechanical testing in both small and large defect samples.

Changing collagen density or riboflavin concentration had positive effects on the repair of AF defects, with density having the most profound impacts on performance. Small defects treated with the highest density, 15 mg/ml, showed significant differences from the untreated values for modulus and permeability. All

riboflavin concentrations tested showed similar results for small AF defects, with profound improvements in effective disc permeability. However, repair of larger defects gave mixed results, with many of the riboflavin concentrations having little effect on modulus and permeability.

While the mechanical tests preformed in this study allowed us to quickly and effectively evaluate different formulations for collagen gel-based AF repair, what we observed in the data have greater implications for the mechanical evaluation of repair of the intervertebral disc. As we touched on in the introduction, the correct mechanical function of the IVD is contingent upon having both AF and NP structures healthy. With loss of or injury to one, we can expect this mechanical function of the full IVD to be diminished. The most intuitive metric for assessing the mechanical integrity of a structure is often its stiffness, or modulus. Indeed, there have been many instances of reporting stiffness of the AF, NP or whole IVD when assessing a treatment option or replacement[23,30,116,118–120]. Assessing two types of moduli with small focal disc damage yielded little difference between the undamaged and damaged cases, which was unexpected. After introducing even a small defect to a structure that is under pressure, like a balloon, one would expect a significant change in the compressive resistance. However changes in moduli between undamaged, damaged and filled cases were insignificant. Once a large, full disc height defect was introduced, we observed dramatic decreases in moduli. Changes in stiffness of the IVD seemed to be insensitive to small defects, even though small defects (~40% disc height) have been shown to eventually lead to full disc degeneration.

While the modulus does yield vital information about the mechanical behavior of the IVD, the composite, interdependent nature of the disc lead us to wonder if other mechanical metrics would be best suited to gauge AF repair. We observed that perhaps the hydraulic permeability is more pertinent to effective IVD function and assessing AF repair. In the case of small defects, wherein moduli did not change significantly, hydraulic permeability increased almost 4-fold over undamaged values. According to these data, even minimal damage to the AF has a profound effect on its ability to impede the flow of water out of the NP. Mechanically, this effects the ability of the NP to pressurize against the AF, and may weaken the disc over the long term leading to a collapsed disc space. Even more than the mechanical effects are the biological implications coupled with fluid flow and diffusion, which we will discuss in the coming sections.

5.2 From the In Vivo Studies

Through the *in vitro* studies, we were able to identify effective collagen formulations to be tested in an *in vivo* rat tail model of degeneration. High-density collagen gels were injected into AF needle puncture defects in anesthetized athymic rats. As common markers of degeneration, disc height and NP hydration were assessed over time. In Chapter 3, the effect of riboflavin was tested, while in Chapter 4 the use of primary AF cells was assessed.

In either case, the needle puncture model successfully induced degeneration in untreated rats. Creation of a defect prompted an almost immediate loss of disc height, and loss of NP tissue as evidenced by a black disc space on MRIs. We found that using a riboflavin-crosslinked collagen gel greatly improved both disc height and

nucleus hydration over uncrosslinked counterparts at five weeks post-injection. Radiological and histological findings supported the qualitative data, since crosslinked samples exhibited a nearly indistinguishable phenotype compared to a healthy IVD (Figure 3.2), including a well-hydrated NP.

A similar trend was observed in the cell-seeded collagen gels. While both cell-seeded and acellular gels maintained disc height and hydrated NP tissue as expected, samples treated with the cell-seeded gels exhibited higher DHI and NP hydration. Histological examination of the AF defect sites revealed a continuous fibrous cap between severed ends of the outer AF in samples treated with cell-seeded collagen gels at 5 weeks. These data confirm that adding primary AF cells to the riboflavin crosslinked collagen gels enhanced repair of needle puncture AF defects.

The overall aim of the *in vivo* studies was to assess repair of the full disc by assessing the progression of disc degeneration. Specifically, we were interested in the biological repair of the IVD since we addressed mechanical repair in the *in vitro* studies. Like most biological tissues, AF repair is a multifaceted issue with interplay between structure, function and mechanism. In assessing degeneration in a live animal, we endeavored to study an overall manifestation of these facets. Perhaps the most telling data in these studies were the histological stains. We observed a normal disc phenotype in treated samples in both *in vivo* studies, with quantitative data supporting the histology. Upon further inspection, the site of treatment showed an unorganized fibrous cab that did not exactly match the alignment of native AF tissue (Figures 3.6 and 4.4). Although this fibrous cap is connected to the surrounding native tissue, its dissimilar phenotype prompted us to question the nature of our repair.

From the *in vitro* studies we observed that the most affected mechanical metric was effective hydraulic permeability, which is indicative of improved water retention with collagen gel repair. Due to the avascular nature of the disc, osmotic and convective flows are responsible for nutrient transport, waste removal, cell signaling and a host of other mechanisms[121]. Therefore, controlling the flow of water both to and from the NP would be essential to regaining full IVD function. Histology from the in vivo studies shows an irregular fibrous cap on the outer AF defect, but lesions toward the inner AF. Although the damage to the inner AF is still present, treated discs retained a healthier phenotype than untreated samples. From these data, we can infer that having the cap on the outside may have had a more profound effect on fluid flow to and from the NP, which in turn helped prevent NP loss and maintained proper fluid movement.

Since fluid flow is so critical to proper IVD function, it makes sense that an effective AF repair strategy should focus on not only stiffness and strength of the AF and IVD as a whole, but also allowing for communication between IVD cells and the para-vertebral space. Other studies have implicated IVD cell dysfunction, NP cells in particular, in playing a major role in the degenerative cascade[2,30]. Many of the signaling pathways used in normal IVD function and degeneration are dependent on flow of soluble factors for cell signaling. As we've shown, by restoring proper effective hydraulic permeability within the IVD we were able to retain a healthy disc even without full depth AF repair.

5.3 Next Steps

While the results the rat-tail studies outlined above are very encouraging, it only serves as a beginning. One of the major limitations of these studies is the size of the rat AF. The average disc height of the rat caudal IVD is 1.2 mm with a radial depth of less than 0.5 mm. This only leaves a small contact area for the delivered gel to contact and integrate. Furthermore, the disc space in live animals tends to collapse upon puncture, making delivery of the collagen gel more difficult, especially to the inner AF, which is apparent in histology (Figures 3.5 and 4.4). Moving to a larger animal model will allow for more precise delivery, more definitive gross examination, and higher degree of relation to human activity. Other AF repair studies report changes with ovine and porcine AF repair models and our own preliminary experiments in ovine lumbar IVDs have confirmed larger defect creation and more definitive gel delivery.

The collagen gel used in these studies is highly tunable and can be changed to better fit the needs of larger IVDs. Our studies in Chapter 2 explored a range of gel densities and riboflavin concentrations in the AF repair model. While 15 mg/ml is considered high when dealing with this injectable gel, groups have shown that it is possible to increase the collagen density even more without jeopardizing injectability[122]. Riboflavin is an effective i*n situ* crosslinker, which was shown to most notably enhance the *in vivo* repair of damaged intervertebral discs. However, greater concentrations can be used to further enhance the mechanical properties of these high-density collagen gels (Appendix A).

Additionally, more should be done to enhance integration with surrounding tissue. Incorporation of cells to the injectable gel increased fibrous cap tissue density and cell density in the affected area, as expected, but we still observed a different phenotype at the repair site. The use of growth factors, such as those already being studied for disc regeneration (e.g.TGF-β, OP-1, BMP-2)[30,123], with younger cells or perhaps stem cells may encourage remodeling of the damaged site to a more native architecture. The current studies on this are still young, but should be explored with an injectable therapeutic such as our collagen gel formulations.

With regards to annulus fibrosus repair, tissue engineered methods look to be the next wave of therapies to work through the research and development pathway. A gel, such as the one discussed in this thesis, would be the ideal option for repairing a wide range of AF defects, and may help open to door for delivering regenerative disc therapies. With some further optimization, *in situ*-crosslinkable collagen gels could succeed in human AF repair, and be applied to a wider range of surgical applications in which such a solution is desperately needed.

APPENDIX A

Effects of Riboflavin Crosslinking on High Density Collagen gels

A.1 Introduction

The previously discussed aims revolved around the use of riboflavin as a crosslinker in high-density collagen hydrogels for annulus fibrosus repair. While riboflavin has been shown to be an effective crosslinker, documentation of its structural and mechanical effects on high-density collagen hydrogels is wanting. Existing studies report only indirect evidence of enhanced mechanical properties through gel contraction assays while observing the behavior of cells in a low-density (<6 mg/ml) collagen environment. In an effort to specialize our injectable collagen, and develop a standardized method of formation, we investigated the effects of riboflavin crosslinking on the structural and mechanical properties of high-density collagen hydrogels.

A.2 Methods for Collagen Gel Fabrication and Analysis

Collagen Gels

Rat tail tendon fibers were harvested from young Sprague Dawley rat tails (BioReclamation IVT, Long Island, NY) and suspended in a 0.1% acetic acid at 150 ml/g. After 48 hours, the soluble collagen was suspended in the acetic acid solution creating a semi-translucent tendon mix. This mix was then centrifuged at 300xg for 90 minutes, kept at 4°C during the entire process. The resulting supernatant was collected, frozen and lyophilized for at least 48 hours. Once all water was removed, the pure collagen was then resuspended in 0.1% acetic acid at the desired stock solution concentration, which should be higher than the intended testing concentration.

To ensure a fully dissolved mixture, the collagen was shaken by hand for at least 30 seconds, twice per day. The reconstituted stock collagen was stored at 4°C.

In order to re-polymerize the collagen for use, it must be mixed with a working solution to neutralize the pH and normalize the osmolarity. Working solutions containing 10x Dulbecco's Phosphate Buffered Saline (DPBS), 1N NaOH and 1x DPBS were then mixed with stock collagen to create final collagen gels. The incorporation of riboflavin into these gels is done during this mixing stage. Before mixing the working solution components together, riboflavin was be added to the 1x DPBS at the desired concentration. This ensured that the riboflavin is mixed directly into the collagen, with the intent of maximizing crosslinks within the gel. With the stock and working solutions ready, they were mixed together using a two-syringe/stopcock setup making sure a well-mixed homogenous solution was the result. The final collagen mix can was then injected onto a surface for testing or into the defect site for animal studies.

For the purposes of crosslinking, riboflavin is sensitive to UVA/B light as well as blue wavelength visible light. Blue wavelength light is an attractive option for biological applications, as it is not cytotoxic at the levels needed to induce crosslinking. After injecting the mixed collagen into the desired location, the gel was exposed to blue light to accelerate crosslinking. Our studies employed a dental curing light for tooth whitening, which is a diode that emits between 450 and 500nm wavelengths. Each gel was exposed to a blue curing light (Spring Health Products, Norristown, PA) at 465nm and ~1200 mW/cm^2 for 40 seconds. The gels were then allowed to polymerize at room temperature for 30 minutes.

FITC-Labeling of Collagen

To investigate microstructure via confocal microscope, rat tail tendon collagen can be labeled with fluorescein isothiocyanate (FITC) following a modified labeling protocol for protein labeling. After lyophilizing collagen, the mass was resuspended in 1 N sodium bicarbonate at 2mg/ml and stirred at 4°C. FITC (Sigma Aldrich, St. Louis, MO) was dissolved in dimethyl sulfoxide (DMSO) (Sigma Aldrich, St. Louis, MO) at 1 mg/ml and added to the stirring collagen mixture at a ratio of 3:1 (FITC:collagen dry weight). The resulting mixture was allowed to react for 48 hours before dialysis against 0.1% acetic acid for another 48 hours.

A.3 Methods for testing and analysis

Confocal Microscopy

Biopsy punches (6 mm diameter) were taken from FITC labeled collagen sheet gels for microscopy on a Zeiss 710 inverted confocal microscope (Zeiss, Germany). All gels were imaged at various locations in the sample over a 63x oil-immersion objective lens. Excitation was achieved using a 488 laser with emission recorded between 500-540 nm.

Mechanical Testing

Dogbone punches were taken from polymerized collagen sheet gels for tensile testing (gauge LxW at 5x5 mm). Each sample was loaded into a uniaxial load fame (Bose Enduratec ELF3200, Eden Prarie, MN) using custom grips, and tested at 3% strain/s until failure. Load data was analyzed in excel for tensile modulus and ultimate tensile stress (UTS).

Cylindrical biopsy punches (6mm diameter) were used for confined compression testing. Each sample was loaded into a custom pot and hydrated with DPBS. Stress-relaxation testing was done to 30% strain in steps of 5% of initial height. Using a custom MATLAB program, poroelastic model was fit to the resulting load data for the calculation of equilibrium/instantaneous moduli as well as hydraulic permeability.

A.4 Expected Experimental Results

High-density collagen gels were crosslinked with various concentrations of riboflavin, and the structural and mechanical effects were analyzed. Confocal fluorescence microscopy revealed larger fibril formation with increased riboflavin concentration (Figure A.1). In 10 mg/ml gels, we observed larger fibrils embedded in a matrix of smaller fibrils much like those seen at the uncrosslinked, 0.0mM concentration. However in the higher density, 15 mg/ml gels exhibited more pronounced networks of interconnected fibrils (Figure A.2).

Tensile testing revealed peaks in modulus and UTS of crosslinked collagen gels, with a shift in maxima observed between collagen densities (Figure A.3a&b). In 10 mg/ml collagen gels, tensile modulus reached a peak of 12 kPa at 0.03 mM riboflavin, while a similar peak of 14.5 kPa was observed at 0.3 mM in 15 mg/ml collagen. Trends in UTS between collagen gel densities were the same as those observed in modulus, with peak values being 13 and 16 kPa in 10 and 15 mg/ml gels respectively.

Equilibrium modulus reached 12 kPa at 0.03mM riboflavin in 10 mg/ml collagen, a significant 6 fold increase from uncrosslinked gels ($p<0.05$). At higher

concentrations of riboflavin, the equilibrium modulus remained unchanged. In 15 mg/ml gels, equilibrium modulus significantly increased almost 10 fold over uncrosslinked counterparts to 22.5 kPa when crosslinked with 0.6 mM riboflavin (Figure A.4). Instantaneous modulus in 10 mg/ml collagen exhibited an immediate rise to 100 kPa when crosslinked at 0.03mM riboflavin, but maintained this level at increasing levels of riboflavin. However, 15 mg/ml collagen gels exhibited a more steady rise in instantaneous modulus, reaching 500 kPa when crosslinked at 1.0 mM riboflavin ($p<0.05$) (Figure A.5). Hydraulic permeability decreased dramatically, by over an order of magnitude, once the gels were crosslinked with riboflavin. This decrease was independent of riboflavin concentration, and significant in the 10 mg/ml collagen gels ($p<0.05$).

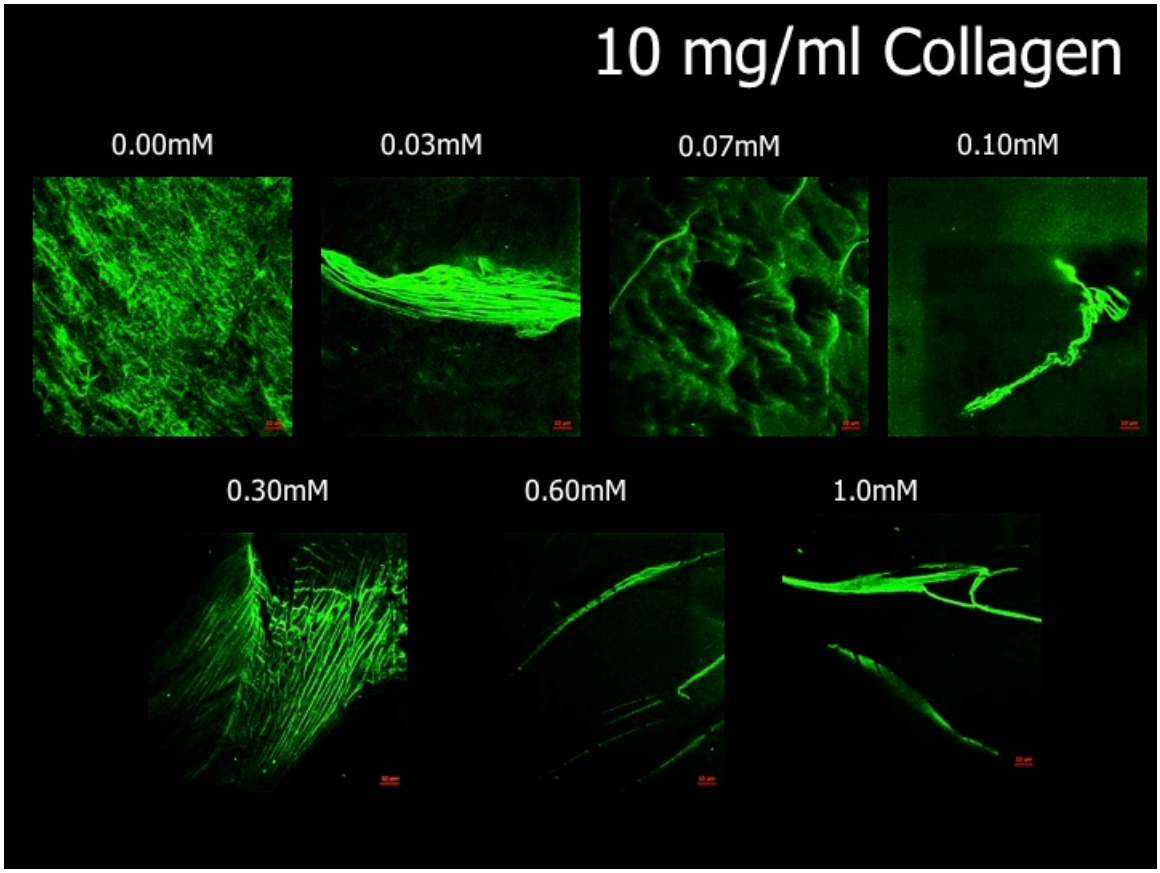

Figure A.1 Confocal fluorescence images of 10 mg/ml FITC-labeled collagen gel crosslinked with riboflavin.

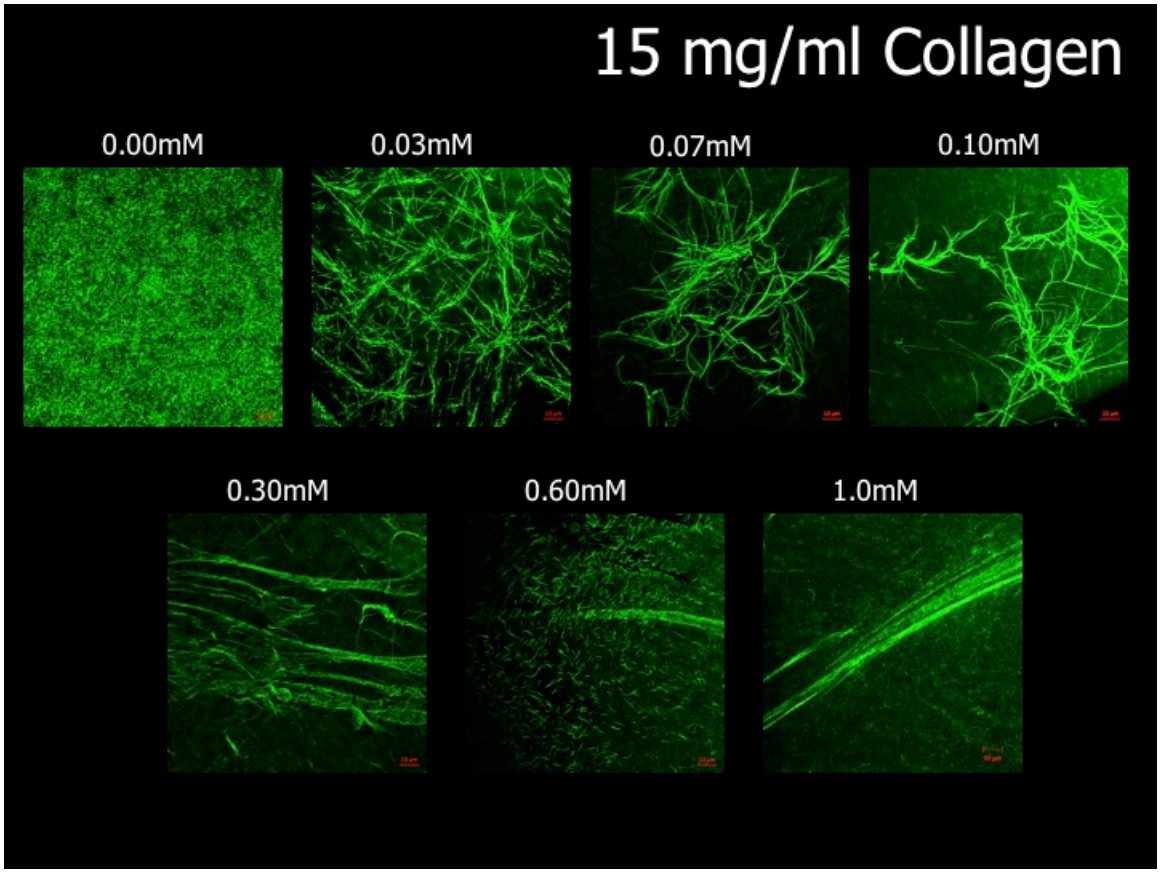

Figure A.2 Confocal fluorescence images of 15 mg/ml FITC-labeled collagen gel crosslinked with riboflavin.

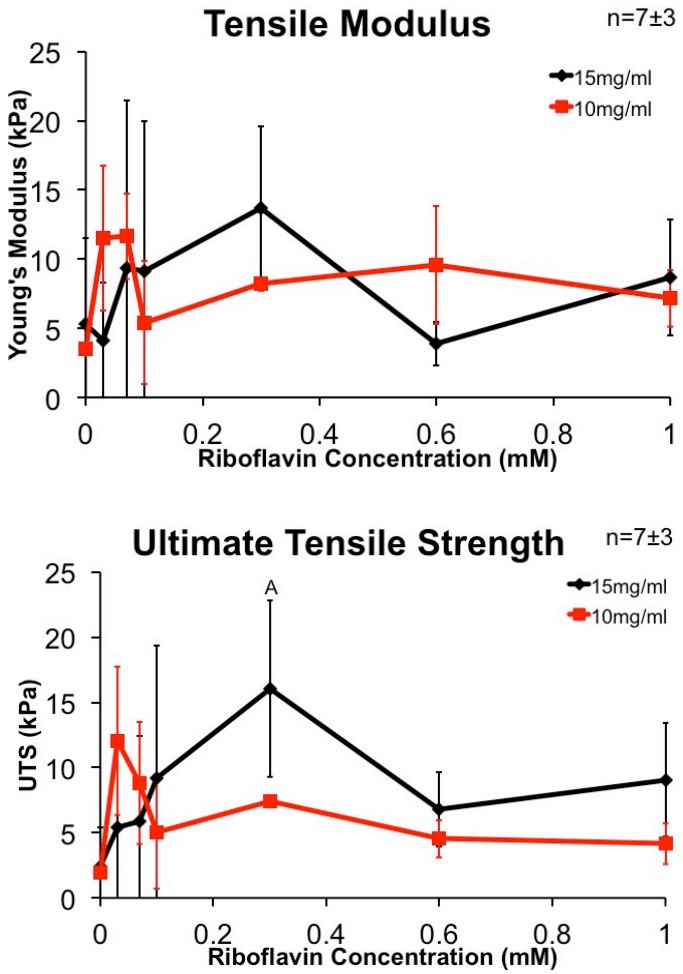

Figure A.3: Results of tensile data analysis showing (a) Young's Modulus and (b) ultimate tensile strength (UTS). Points not joined by letter are significantly different ($p<0.05$).

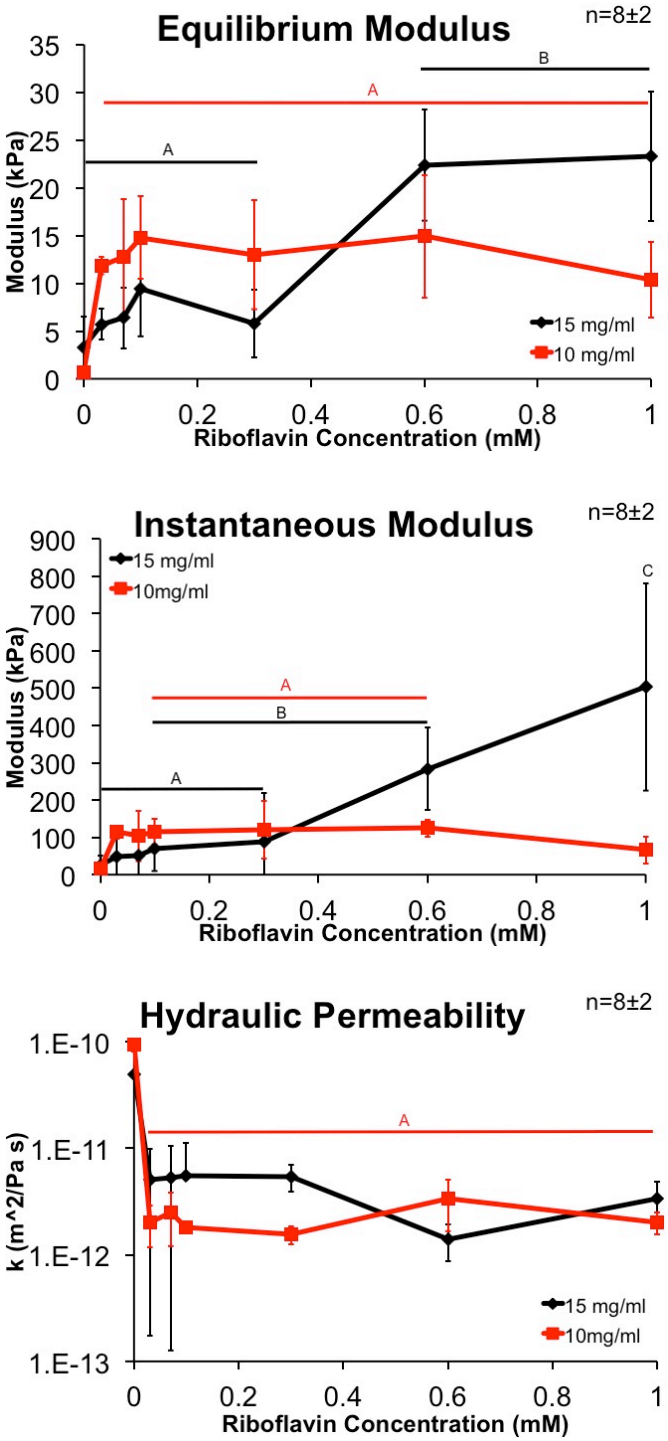

Figure A.4: Results of poroelastic fit for compressive data. (a) Equilibrium modulus, (b) instantaneous modulus and (c) hydraulic permeability of crosslinked collagen gels. Points not joined by letter are significantly different ($p<0.05$).

APPENDIX B

Statistical Methods and Considerations

B.1 In Vitro Studies (Chapter 2)

Objective

Our goals with these studies were to establish a mechanical model for *in vitro* AF repair that would allow us to quickly and effectively test multiple repair formulations, and report the effects of multiple different collagen formulations on AF repair though whole-IVD mechanics. Collagen gel density as well as riboflavin crosslinker concentrations were varied during the studies. The reported properties were effective equilibrium and instantaneous moduli, as well as hydraulic permeability, which were measured for each stage of mechanical testing.

Study Design

This study was a multi-level hierarchal design, with repeated measures on a single sample, and different variables being tested (Figure B.1).

Each caudal rat tail motion segment contained one IVD with both of the adjacent vertebral bones. The bones were secured in the load frame, allowing us to actuate only the IVD. Each disc was tested in compression, first undamaged, then damaged, and finally treated. Each undamaged case was physically the same, with the IVD unchanged from dissection. The damaged case consisted of two possible scenarios, one small defect or one large defect. Within each of these damaged cases, three different collagen densities (5, 10 and 15 mg/ml) were tested. Once the performance of different collagen gel densities was recorded and analyzed, the riboflavin based studies were conducted using 15 mg/ml collagen gels containing various

concentrations of riboflavin (0.0, 0.03, 0.07, 0.10 mM). The control (0.0mM) group was the same data as the 15 mg/ml collagen gel group in the previous study, shown on the same level in Figure B.1. Due to variability in the healthy values between each individual sample, we chose to normalize mechanical measurements of each individual sample before statistical comparison, and report standard deviation. As such, the reported data is shown as fractions of unity, which represents the healthy condition.

Statistical Analyses

The hierarchal nature of the experimental design called for multiple different statistical analyses to answer questions at each stage of testing, and then comparison of different stages to draw conclusions about repair with varying formulations. With some initial guidance from the Cornell Statistical Consulting Unit, we chose to address three areas of interest with our data. The first question was of overall repair; was there a significant difference between damaged cases and treated cases? Did treating the segments with high-density collagen positively affect IVD mechanical behavior? To assess this, we first tested pooled experimental data sets, with the variables being damage vs treatment using any collagen gel formulation. This was carried out using the JMP (mixed model/two-way ANOVA) and Sigmaplot (two-way-ANOVA) statistical software packages. With all samples listed, the two factors were presence of treatment (healthy/damaged/treated) and treatment type (all collagen densities and riboflavin concentrations). No significant differences were observed among the treatment type groups, however the pooled data shoed significant differences between the presence of treatments.

After evaluating overall treatment, the second and third questions were of specific formulation factors; collagen density and riboflavin concentration respectively. We addressed each study separately, with a one-way ANOVA analysis on collagen densities: 0, 5, 10 and 15 mg/ml, and a separate one-way ANOVA for the riboflavin densities: 0, 0.03, 0.07, and 0.10 mM. These analyses were on repeated measures with preliminary tests for normality and equal variance. After, finding initial significance, Tukey-HSD was used for direct comparison between treatment groups with statistical significance at $p<0.05$.

B.2 In Vivo Studies (Chapter 3 and 4)

Purpose

Both *in vivo* studies looked to assess the extent of biological repair of the AF through established markers of IVD degeneration. Caudal IVDs in live athymic rats were either punctured and left untreated, or punctured and immediately treated with one of many different treatments. In the first *in vivo* studies, we were interested in the performance of uncrosslinked versus crosslinked collagen, with multiple different concentrations of the crosslinker riboflavin. In the second *in vivo* study, we shifted the focus to the incorporation of cells. The analyzed and reported quantitative metrics were disc height index (DHI), T2 relaxation time (Chapter 4) and Voxel counts.

Study Design

To accurately evaluate the extent of repair, it was necessary to track the IVDs for a period of time via radiological assessments. Thus, all of the reported results time-dependent, with final radiological (non-lethal) measures taken at different time points. Regardless of treatment time point "zero" was the initial operation. With the

exception of histological samples, all rats were allowed to roam within cages under care of veterinary staff for up to 5 weeks, with additional time points taken at weeks 1 and 2.

Statistical Analyses

Due to the nature of the studies, comparisons occurred at between multiple treatments, at different timepoints and within a single timepoint. For example, DHI at two weeks were compared between all different treatment groups, but the two week time points for the puncture control was also compared to the five week timepoint of the same treatment group. The chapter 3 studies were analyzed in JMP using mixed model ANOVA, with nesting for the adjacent healthy controls for each sample. Chapter 4 studies were analyzed in the SPSS statistical software package using a generalized linear regression model, comparing normalized values for DHI, voxel count and T2 relaxation time.

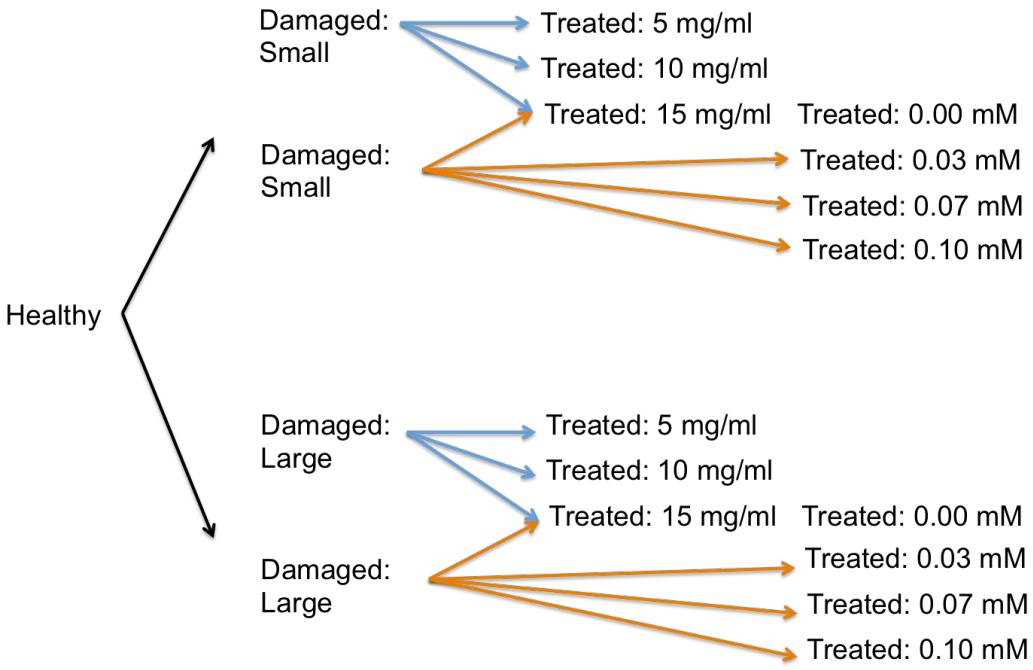

Figure B.1: Schematic of hierarchal study design for the study described in Chapter 2. Each IVD was tested three times: once healthy, once damaged and then again treated. Two different types of damage were administered (small or large) and one of six different treatments (shown from damage levels with colored arrows).

REFERENCES

Chapters 1,2, and 5

1. Humzah MD, Soames RW. Human intervertebral disc: structure and function. *Anat Rec*. 1988;220(4):337-356. doi:10.1002/ar.1092200402.
2. Whatley BR, Wen X. Intervertebral disc (IVD): Structure, degeneration, repair and regeneration. *Mater Sci Eng C*. 2012;32(2):61-77. doi:10.1016/j.msec.2011.10.011.
3. Bruehlmann SB, Rattner JB, Matyas JR, Duncan NA. Regional variations in the cellular matrix of the annulus fibrosus of the intervertebral disc. *Society*. 2002:159-171.
4. Alini M, Roughley PJ, Antoniou J, Stoll T, Aebi M. A biological approach to treating disc degeneration: not for today, but maybe for tomorrow. *Eur Spine J*. 2002;11 Suppl 2:S215-20. doi:10.1007/s00586-002-0485-8.
5. Nerurkar NL, Elliott DM, Mauck RL. Mechanical design criteria for intervertebral disc tissue engineering. *J Biomech*. 2010;43(6):1017-1030. doi:10.1016/j.jbiomech.2009.12.001.
6. Shapiro IM, Risbud M V. *The Intervertebral Disc: Molecular and Structural Studies of the Disc in Health and Disease*. First. Springer; 2014.
7. Smith LJ, Fazzalari NL. Regional variations in the density and arrangement of elastic fibres in the anulus fibrosus of the human lumbar disc. *Society*. 2006:359-367. doi:10.1111/j.1469-7580.2006.00610.x.
8. Colombier P, Clouet J, Hamel O, Lescaudron L, Guicheux J. The lumbar

intervertebral disc: From embryonic development to degeneration. *Joint Bone Spine*. 2014;81(2):125-129. doi:10.1016/j.jbspin.2013.07.012.

9. Bron JL, Helder MN, Meisel H-J, Van Royen BJ, Smit TH. Repair, regenerative and supportive therapies of the annulus fibrosus: achievements and challenges. *Eur Spine J*. 2009;18(3):301-313. doi:10.1007/s00586-008-0856-x.
10. Osti OL, Vernon-Roberts B, Moore R, Fraser RD. Annular tears and disc degeneration in the lumbar spine. A post-mortem study of 135 discs. *J Bone Joint Surg Br*. 1992;74(5):678-682.
11. Galbusera F, van Rijsbergen M, Ito K, Huyghe JM, Brayda-Bruno M, Wilke H-J. Ageing and degenerative changes of the intervertebral disc and their impact on spinal flexibility. *Eur Spine J*. January 2014. doi:10.1007/s00586-014-3203-4.
12. Latham JM, Pearcy MJ, Costi JJ, Moore R, Fraser RD, Vernon-Roberts B. Mechanical consequences of annular tears and subsequent intervertebral disc degeneration. *Clin Biomech*. 1994;9(4):211-219. doi:10.1016/0268-0033(94)90001-9.
13. Risbud M V, Shapiro IM. Role of cytokines in intervertebral disc degeneration: pain and disc content. *Nat Rev Rheumatol*. 2014;10(1):44-56. doi:10.1038/nrrheum.2013.160.
14. Vergroesen PPA, Kingma I, Emanuel KS, et al. Mechanics and biology in intervertebral disc degeneration: A vicious circle. *Osteoarthr Cartil*. 2014:1-14. doi:10.1016/j.joca.2015.03.028.
15. Gregory DE, Bae WC, Sah RL, Masuda K. Disc degeneration reduces the

delamination strength of the anulus fibrosis in the rabbit anular disc puncture model. *Spine J*. March 2014. doi:10.1016/j.spinee.2013.07.489.

16. Iatridis JC, Setton L a, Foster RJ, Rawlins B a, Weidenbaum M, Mow VC. Degeneration affects the anisotropic and nonlinear behaviors of human anulus fibrosus in compression. *J Biomech*. 1998;31(6):535-544. http://www.ncbi.nlm.nih.gov/pubmed/9755038.

17. Lewis G. Nucleus pulposus replacement and regeneration/repair technologies: Present status and future prospects. *J Biomed Mater Res B Appl Biomater*. May 2012:1-19. doi:10.1002/jbm.b.32712.

18. Connor DE, Shamieh KS, Ogden AL, Mukherjee DP, Sin A, Nanda A. Biomechanical performance of rigid compared to dynamic anterior cervical plating: analysis of adjacent upper and lower level compressive forces. *J Clin Neurosci*. 2012;19(12):1706-1710. doi:10.1016/j.jocn.2012.03.026.

19. Nesti LJ, Li W-J, Shanti RM, et al. Intervertebral disc tissue engineering using a novel hyaluronic acid-nanofibrous scaffold (HANFS) amalgam. *Tissue Eng Part A*. 2008;14(9):1527-1537. doi:10.1089/ten.tea.2008.0215.

20. Mizuno H, Roy AK, Zaporojan V, Vacanti C a, Ueda M, Bonassar LJ. Biomechanical and biochemical characterization of composite tissue-engineered intervertebral discs. *Biomaterials*. 2006;27(3):362-370. doi:10.1016/j.biomaterials.2005.06.042.

21. Bowles RD, Gebhard HH, Hartl R, Bonassar LJ. Tissue-engineered intervertebral discs produce new matrix, maintain disc height, and restore biomechanical function to the rodent spine. *Proc Natl Acad Sci*. 2011;108(32).

doi:10.1073/pnas.1107094108.

22. Nerurkar N, Sen S, Huang A, Elliott DM, Mauck RL. Engineered Disc-Like Angle-Ply Structures for Intervertebral Disc Replacement. *Spine (Phila Pa 1976)*. 2012;35(8):867-873. doi:10.1097/BRS.0b013e3181d74414.ENGINEERED.

23. Martin JT, Milby AH, Chiaro J a, et al. Translation of an engineered nanofibrous disc-like angle-ply structure for intervertebral disc replacement in a small animal model. *Acta Biomater*. February 2014. doi:10.1016/j.actbio.2014.02.024.

24. Bron JL, Mulder HW, Vonk L a, Doulabi BZ, Oudhoff MJ, Smit TH. Migration of intervertebral disc cells into dense collagen scaffolds intended for functional replacement. *J Mater Sci Mater Med*. January 2012. doi:10.1007/s10856-011-4545-7.

25. Bron JL, Koenderink GH, Everts V, Smit TH. Rheological characterization of the nucleus pulposus and dense collagen scaffolds intended for functional replacement. *J Orthop Res*. 2009;27(5):620-626. doi:10.1002/jor.20789.

26. Sivan SS, Roberts S, Urban JPG, et al. Acta Biomaterialia Injectable hydrogels with high fixed charge density and swelling pressure for nucleus pulposus repair : Biomimetic glycosaminoglycan analogues. *Acta Biomater*. 2014;10(3):1124-1133. doi:10.1016/j.actbio.2013.11.010.

27. Vernengo J, Fussell GW, Smith NG, Lowman a M. Synthesis and characterization of injectable bioadhesive hydrogels for nucleus pulposus replacement and repair of the damaged intervertebral disc. *J Biomed Mater Res*

B Appl Biomater. 2010;93(2):309-317. doi:10.1002/jbm.b.31547.

28. Takegami K, An HS, Kumano F, et al. Osteogenic protein-1 is most effective in stimulating nucleus pulposus and annulus fibrosus cells to repair their matrix after chondroitinase ABC-induced in vitro chemonucleolysis. *Spine J*. 2005;5(3):231-238. doi:10.1016/j.spinee.2004.11.001.
29. Hu J, Chen B, Guo F, et al. Injectable silk fibroin/polyurethane composite hydrogel for nucleus pulposus replacement. *J Mater Sci Mater Med*. 2012;(111):711-722. doi:10.1007/s10856-011-4533-y.
30. An HS, Takegami K, Kamada H, et al. Intradiscal administration of osteogenic protein-1 increases intervertebral disc height and proteoglycan content in the nucleus pulposus in normal adolescent rabbits. *Spine (Phila Pa 1976)*. 2005;30(1):25-31-2. http://www.ncbi.nlm.nih.gov/pubmed/15626976.
31. Heuer F, Ulrich S, Claes L, Wilke HJ. Biomechanical evaluation of conventional anulus fibrosus closure methods required for nucleus replacement. *J Neurosurg Spine*. 2008;9(3):307-313. doi:10.3171/SPI/2008/9/9/307.
32. Chiang C-J, Cheng C-K, Sun J-S, Liao C-J, Wang Y-H, Tsuang Y-H. The Effect of a New Anular Repair After Discectomy in Intervertebral Disc Degeneration: An Experimental Study Using a Porcine Spine Model. *Spine (Phila Pa 1976)*. 2010;36(10):1-9. doi:10.1097/BRS.0b013e3181e08f01.
33. Chiang Y-F, Chiang C-J, Yang C-H, et al. Retaining intradiscal pressure after annulotomy by different annular suture techniques, and their biomechanical evaluations. *Clin Biomech (Bristol, Avon)*. 2011;27(3):241-248. doi:10.1016/j.clinbiomech.2011.09.008.

34. Heuer F, Ulrich S, Claes L, Wilke H-J. Biomechanical evaluation of conventional anulus fibrosus closure methods required for nucleus replacement. Laboratory investigation. *J Neurosurg Spine*. 2008;9(3):307-313. http://www.ncbi.nlm.nih.gov/entrez/query.fcgi?cmd=Retrieve&db=PubMed&dopt=Citation&list_uids=18928230.

35. Bron JL, Van Der Veen AJ, Helder MN, Van Royen BJ, Smit TH. Biomechanical and in vivo evaluation of experimental closure devices of the annulus fibrosus designed for a goat nucleus replacement model. *Eur spine J Off Publ Eur Spine Soc Eur Spinal Deform Soc Eur Sect Cerv Spine Res Soc*. 2010;19(8):1347-1355. http://www.ncbi.nlm.nih.gov/entrez/query.fcgi?cmd=Retrieve&db=PubMed&dopt=Citation&list_uids=20401620.

36. Parker SL, Grahovac G, Vukas D, et al. Effect of An Annular Closure Device (Barricaid) on Same Level Recurrent Disc Herniation and Disc Height Loss After Primary Lumbar Discectomy. *J Spinal Disord Tech*. April 2013:1. doi:10.1097/BSD.0b013e3182956ec5.

37. Gorensek M, Vilendecic M, Eustacchio S, et al. P126.Clinical Investigation of the Intrinsic Therapeutics Barricaid, A Novel Device for Closing Defects in the Annulus. *Spine J*. 2006;6(5):143S-144S. doi:10.1016/j.spinee.2006.06.334.

38. Nerurkar NL, Baker BM, Sen S, Wible EE, Elliott DM, Mauck RL. Nanofibrous biologic laminates replicate the form and function of the annulus fibrosus. *Nat Mater*. 2009;8(12):986-992. doi:10.1038/nmat2558.

39. Bowles RD, Williams RM, Zipfel WR, Bonassar LJ. Self-assembly of aligned

tissue-engineered annulus fibrosus and intervertebral disc composite via collagen gel contraction. *Tissue Eng Part A*. 2010;16(4):1339-1348. doi:10.1089/ten.TEA.2009.0442.

40. Grad S, Fortunato G. Biodegradable Electrospun Scaffolds for Annulus Fibrosus Tissue Engineering : 2014;20:672-682. doi:10.1089/ten.tea.2012.0679.

41. Xu B, Du L, Zhang J, et al. Circumferentially oriented microfiber scaffold prepared by wet-spinning for tissue engineering of annulus fibrosus. *RSC Adv*. 2015;5(53):42705-42713. doi:10.1039/C5RA03347K.

42. Koepsell L, Remund T, Bao J, Neufeld D, Fong H, Deng Y. Tissue engineering of annulus fibrosus using electrospun fibrous scaffolds with aligned polycaprolactone fibers. *J Biomed Mater Res A*. 2011;99(4):564-575. doi:10.1002/jbm.a.33216.

43. Kang R, Quang Svend Le D, Li H, et al. Engineered Three Dimensional Nanofibrous Multi-lamellar Structure for Annulus Fibrosus Repair. *J Mater Chem B*. 2013;(DOI: 10.1039/c0xx00000x). doi:10.1039/b000000x.

44. Chang G, Kim H-J, Kaplan D, Vunjak-Novakovic G, Kandel R a. Porous silk scaffolds can be used for tissue engineering annulus fibrosus. *Eur Spine J*. 2007;16(11):1848-1857. doi:10.1007/s00586-007-0364-4.

45. Du L, Zhu M, Yang Q, et al. A novel integrated biphasic silk fibroin scaffold for intervertebral disc tissue engineering. *Mater Lett*. 2014;117:237-240. doi:10.1016/j.matlet.2013.12.029.

46. Vergroesen P-P a., Bochyn´ska AI, Emanuel KS, et al. A Biodegradable Glue for Annulus Closure. *Spine (Phila Pa 1976)*. 2015;40(9):622-628.

doi:10.1097/BRS.0000000000000792.

47. Kang R, Li H, Lysdahl H, et al. Cyanoacrylate medical glue application in intervertebral disc annulus defect repair: Mechanical and biocompatible evaluation. *J Biomed Mater Res - Part B Appl Biomater*. 2015:1-7. doi:10.1002/jbm.b.33524.

48. Schek R, Michalek A, Iatridis J. Genipin-crosslinked fibrin hydrogels as a potential adhesive to augment intervertebral disc annulus repair. *Eur cells & Mater*. 2011;21:373. http://www.www.ecmjournal.org/journal/papers/vol021/pdf/v021a28.pdf. Accessed April 11, 2012.

49. Pirvu T, Blanquer SBG, Benneker LM, et al. A combined biomaterial and cellular approach for annulus fibrosus rupture repair. *Biomaterials*. 2015;42:11-19. doi:10.1016/j.biomaterials.2014.11.049.

50. Omlor GW, Nerlich a G, Lorenz H, et al. Injection of a polymerized hyaluronic acid/collagen hydrogel matrix in an in vivo porcine disc degeneration model. *Eur Spine J*. 2012;(Ivd). doi:10.1007/s00586-012-2291-2.

51. Bertolo A, Häfner S, Taddei AR, et al. INJECTABLE MICROCARRIERS AS HUMAN MESENCHYMAL STEM CELL SUPPORT AND THEIR APPLICATION FOR CARTILAGE AND DEGENERATED INTERVERTEBRAL DISC REPAIR. 2015;29(i):70-81.

52. Chik TK, Ma XY, Choy TH, et al. Photochemically crosslinked collagen annulus plug: a potential solution solving the leakage problem of cell-based therapies for disc degeneration. *Acta Biomater*. 2013;9(9):8128-8139.

doi:10.1016/j.actbio.2013.05.034.

53. Kadler KE, Holmes DF, Trotter J a, Chapman J a. Collagen fibril formation. *Biochem J*. 1996;316 (Pt 1:1-11. http://www.pubmedcentral.nih.gov/articlerender.fcgi?artid=1217307&tool=pmcentrez&rendertype=abstract.

54. Stenzel KH, Miyata T, Rubin a L. Collagen as a biomaterial. *Annu Rev Biophys Bioeng*. 1974;3:231-253. doi:10.1146/annurev.bb.03.060174.001311.

55. Silver FH, Freeman JW, Seehra GP. Collagen self-assembly and the development of tendon mechanical properties. *J Biomech*. 2003;36(10):1529-1553. doi:10.1016/S0021-9290(03)00135-0.

56. Zeugolis DI, Paul RG, Attenburrow G. Factors influencing the properties of reconstituted collagen fibers prior to self-assembly: animal species and collagen extraction method. *J Biomed Mater Res A*. 2008;86(4):892-904. doi:10.1002/jbm.a.31694.

57. Van Der Rest M, Garrone R. Collagen family of proteins. *FASEB J*. 1991;5(60):2814-2823.

58. Shoseyov O, Amitai H, Posen Y, Yaari A, Shilo S, Roth S. Large-scale Molecular Farming of Recombinant Human Collagen in Transgenic Tobacco. *ISB News Rep*. 2010;(September):3-6.

59. Rajan N, Habermehl J, Coté M-F, Doillon CJ, Mantovani D. Preparation of ready-to-use, storable and reconstituted type I collagen from rat tail tendon for tissue engineering applications. *Nat Protoc*. 2006;1(6):2753-2758. doi:10.1038/nprot.2006.430.

60. Wood GC, Keech MK. The Formation of Fibrils from Collagen Solutions 2. A mechanism of collagen fibril formaiton. *Biochemistry*. 1960;75:598-605.

61. Yuan L, Veis A. The Self-Assembly of Collagen Molecules. *Biopolymers*. 1973;12:1437-1444.

62. Wallace D. Collagen gel systems for sustained delivery and tissue engineering. *Adv Drug Deliv Rev*. 2003;55(12):1631-1649. doi:10.1016/j.addr.2003.08.004.

63. Cross VL, Zheng Y, Won Choi N, et al. Dense type I collagen matrices that support cellular remodeling and microfabrication for studies of tumor angiogenesis and vasculogenesis in vitro. *Biomaterials*. 2010;31(33):8596-8607. doi:10.1016/j.biomaterials.2010.07.072.

64. Roeder B a., Kokini K, Sturgis JE, Robinson JP, Voytik-Harbin SL. Tensile Mechanical Properties of Three-Dimensional Type I Collagen Extracellular Matrices With Varied Microstructure. *J Biomech Eng*. 2002;124(2):214. doi:10.1115/1.1449904.

65. Wang MC, Pins GD, Silver FH. Collagen fibres with improved strength for the repair of soft tissue injuries. *Biomaterials*. 1994;15(7):507-512. http://www.ncbi.nlm.nih.gov/pubmed/7918903.

66. Ibusuki S, Halbesma GJ, Randolph M a, Redmond RW, Kochevar IE, Gill TJ. Photochemically cross-linked collagen gels as three-dimensional scaffolds for tissue engineering. *Tissue Eng*. 2007;13(8):1995-2001. doi:10.1089/ten.2006.0153.

67. Davidenko N, Schuster CF, Bax D V., et al. Control of crosslinking for tailoring collagen-based scaffolds stability and mechanics. *Acta Biomater*. 2015;25:131-

142. doi:10.1016/j.actbio.2015.07.034.

68. Wollensak G, Spoerl E, Seiler T. Riboflavin/ultraviolet-a–induced collagen crosslinking for the treatment of keratoconus. *Am J Ophthalmol*. 2003;135(5):620-627. doi:10.1016/S0002-9394(02)02220-1.

69. Olde Damink LH, Dijkstra PJ, van Luyn MJ, van Wachem PB, Nieuwenhuis P, Feijen J. Cross-linking of dermal sheep collagen using a water-soluble carbodiimide. *Biomaterials*. 1996;17(8):765-773. http://www.ncbi.nlm.nih.gov/pubmed/10353646.

70. Roy R, Boskey A, Bonassar LJ. Processing of type I collagen gels using nonenzymatic glycation. *J Biomed Mater Res A*. 2010;93(3):843-851. doi:10.1002/jbm.a.32231.

71. Stenzel K, Miyata T, Rubin A. Collagen as a biomaterial. *Cas Lek Cesk*. 1989;128(42):1313-1317. doi:10.1146/annurev.bb.03.060174.001311.

72. Avery NC, Bailey a J. Enzymic and non-enzymic cross-linking mechanisms in relation to turnover of collagen: relevance to aging and exercise. *Scand J Med Sci Sports*. 2005;15(4):231-240. doi:10.1111/j.1600-0838.2005.00464.x.

73. Reiser K, Mccormick RJ, Rucker RB. Enzymatic and nonenzymatic cross-linking of collagen and elastin. *FASEB J*. 1992;6:2439-2449.

74. Fessel G, Gerber C, Snedeker JG. Potential of collagen cross-linking therapies to mediate tendon mechanical properties. *J Shoulder Elbow Surg*. 2012;21(2):209-217. doi:10.1016/j.jse.2011.10.002.

75. Monnier VM, Mustata GT, Biemel KL, et al. Cross-linking of the extracellular matrix by the maillard reaction in aging and diabetes: an update on “a puzzle

nearing resolution". *Ann N Y Acad Sci*. 2005;1043:533-544. doi:10.1196/annals.1333.061.

76. Monnier VM, Glomb M, Elgawish a, Sell DR. The mechanism of collagen cross-linking in diabetes: a puzzle nearing resolution. *Diabetes*. 1996;45 Suppl 3(September 1995):S67-72. http://www.ncbi.nlm.nih.gov/pubmed/8674897.

77. Ulrich P, Cerami a. Protein glycation, diabetes, and aging. *Recent Prog Horm Res*. 2001;56:1-21. http://www.ncbi.nlm.nih.gov/pubmed/11237208.

78. Huebschmann AG, Regensteiner JG, Vlassara H, Reusch JEB. Diabetes and advanced glycoxidation end products. *Diabetes Care*. 2006;29(6):1420-1432. doi:10.2337/dc05-2096.

79. Paul RG, Bailey a J. Glycation of collagen: the basis of its central role in the late complications of ageing and diabetes. *Int J Biochem Cell Biol*. 1996;28(12):1297-1310. http://www.ncbi.nlm.nih.gov/pubmed/9022289.

80. Fujimori E. Cross-linking and fluorescence changes of collagen by glycation and oxidation. *Biochim Biophys Acta*. 1989;998(2):105-110. http://www.ncbi.nlm.nih.gov/pubmed/2506934.

81. Kamaev P, Friedman MD, Sherr E, Muller D. Photochemical kinetics of corneal cross-linking with riboflavin. *Invest Ophthalmol Vis Sci*. 2012;53(4):2360-2367. doi:10.1167/iovs.11-9385.

82. Ahearne M, Yang Y, Then KY, Liu K-K. Non-destructive mechanical characterisation of UVA/riboflavin crosslinked collagen hydrogels. *Br J Ophthalmol*. 2008;92(2):268-271. doi:10.1136/bjo.2007.130104.

83. Grewal DS, Brar GS, Jain R, Sood V, Singla M, Grewal SPS. Corneal collagen

crosslinking using riboflavin and ultraviolet-A light for keratoconus: one-year analysis using Scheimpflug imaging. *J Cataract Refract Surg*. 2009;35(3):425-432. doi:10.1016/j.jcrs.2008.11.046.

84. Brummer G, Littlechild S, McCall S, Zhang Y, Conrad GW. The role of nonenzymatic glycation and carbonyls in collagen cross-linking for the treatment of keratoconus. *Invest Ophthalmol Vis Sci*. 2011;52(9):6363-6369. doi:10.1167/iovs.11-7585.

85. Liang J-Y, Yuann J-MP, Cheng C-W, Jian H-L, Lin C-C, Chen L-Y. Blue light induced free radicals from riboflavin on E. coli DNA damage. *J Photochem Photobiol B*. 2013;119:60-64. doi:10.1016/j.jphotobiol.2012.12.007.

86. Dagenais S, Caro J, Haldeman S. A systematic review of low back pain cost of illness studies in the United States and internationally. *Spine J*. 2008;8(1):8-20. doi:10.1016/j.spinee.2007.10.005.

87. Elliott DM, Yerramalli CS, Beckstein JC, Boxberger JI, Johannessen W, Vresilovic EJ. The effect of relative needle diameter in puncture and sham injection animal models of degeneration. *Spine (Phila Pa 1976)*. 2008;33(6):588-596. doi:10.1097/BRS.0b013e318166e0a2.

88. Thompson RE, Pearcy MJ, Barker TM. The mechanical effects of intervertebral disc lesions. *Clin Biomech (Bristol, Avon)*. 2004;19(5):448-455. doi:10.1016/j.clinbiomech.2004.01.012.

89. Han B, Zhu K, Li F-C, et al. A simple disc degeneration model induced by percutaneous needle puncture in the rat tail. *Spine (Phila Pa 1976)*. 2008;33(18):1925-1934. doi:10.1097/BRS.0b013e31817c64a9.

90. Keorochana G, Johnson JS, Taghavi CE, et al. The effect of needle size inducing degeneration in the rat caudal disc: evaluation using radiograph, magnetic resonance imaging, histology, and immunohistochemistry. *Spine J*. 2010;10(11):1014-1023. doi:10.1016/j.spinee.2010.08.013.

91. Lotz JC. Animal models of intervertebral disc degeneration: lessons learned. *Spine (Phila Pa 1976)*. 2004;29(23):2742-2750. http://www.ncbi.nlm.nih.gov/pubmed/15564923.

92. Atlas SJ, Keller RB, Wu Y a, Deyo R a, Singer DE. Long-term outcomes of surgical and nonsurgical management of lumbar spinal stenosis: 8 to 10 year results from the maine lumbar spine study. *Spine (Phila Pa 1976)*. 2005;30(8):936-943. http://www.ncbi.nlm.nih.gov/pubmed/15834339.

93. Dai L-Y, Zhou Q, Yao W-F, Shen L. Recurrent lumbar disc herniation after discectomy: outcome of repeat discectomy. *Surg Neurol*. 2005;64(3):226-31; discussion 231. doi:10.1016/j.surneu.2004.11.003.

94. Singh K, Park D. Lumbar Anular Repair for Degenerative Disc Disease. *Contemp Spine Surg*. 2010;11(11):1-6. http://journals.lww.com/cssnewsletter/Abstract/2010/11000/Lumbar_Anular_Repair_for_Degenerative_Disc_Disease.1.aspx. Accessed May 16, 2011.

95. Ahlgren BD, Lui W, Herkowitz HN, Panjabi MM, Guiboux JP. Effect of anular repair on the healing strength of the intervertebral disc: a sheep model. *Spine (Phila Pa 1976)*. 2000;25(17):2165-2170. http://www.ncbi.nlm.nih.gov/pubmed/10973397.

96. Michalek AJ, Iatridis JC. Penetrating annulus fibrosus injuries affect dynamic

compressive behaviors of the intervertebral disc via altered fluid flow: an analytical interpretation. *J Biomech Eng*. 2011;133(8):84502. doi:10.1115/1.4004915.

97. Korecki CL, Costi JJ, Iatridis JC. Needle puncture injury affects intervertebral disc mechanics and biology in an organ culture model. *Spine (Phila Pa 1976)*. 2008;33(3):235-241. doi:10.1097/BRS.0b013e3181624504.

98. Fazzalari NL, Costi JJ, Hearn TC, et al. Mechanical and pathologic consequences of induced concentric anular tears in an ovine model. *Spine (Phila Pa 1976)*. 2001;26(23):2575-2581. http://www.ncbi.nlm.nih.gov/pubmed/11725238.

99. Zhuang Y, Huang B, Li CQ, et al. Construction of tissue-engineered composite intervertebral disc and preliminary morphological and biochemical evaluation. *Biochem Biophys Res Commun*. 2011;407(2):327-332. doi:10.1016/j.bbrc.2011.03.015.

100. Bron JL, Mulder HW, Vonk L a, Doulabi BZ, Oudhoff MJ, Smit TH. Migration of intervertebral disc cells into dense collagen scaffolds intended for functional replacement. *J Mater Sci Mater Med*. 2012;23(3):813-821. doi:10.1007/s10856-011-4545-7.

101. Wilke H-J, Heuer F, Neidlinger-Wilke C, Claes L. Is a collagen scaffold for a tissue engineered nucleus replacement capable of restoring disc height and stability in an animal model? *Eur Spine J*. 2006;15 Suppl 3:S433-8. doi:10.1007/s00586-006-0177-x.

102. Grunert P, Borde BH, Hudson KD, Macielak MR, Bonassar LJ, Härtl R.

Annular repair using high-density collagen gel: a rat-tail in vivo model. *Spine (Phila Pa 1976)*. 2014;39(3):198-206. doi:10.1097/BRS.0000000000000103.

103. Sheu MT, Huang JC, Yeh GC, Ho HO. Characterization of collagen gel solutions and collagen matrices for cell culture. *Biomaterials*. 2001;22(13):1713-1719. http://www.ncbi.nlm.nih.gov/pubmed/11396874.

104. Cross VL, Zheng Y, Won Choi N, et al. Dense type I collagen matrices that support cellular remodeling and microfabrication for studies of tumor angiogenesis and vasculogenesis in vitro. *Biomaterials*. 2010;31(33):8596-8607. doi:10.1016/j.biomaterials.2010.07.072.

105. Fawzy a, Nitisusanta L, Iqbal K, Daood U, Beng LT, Neo J. Characterization of riboflavin-modified dentin collagen matrix. *J Dent Res*. 2012;91(11):1049-1054. doi:10.1177/0022034512459053.

106. Wollensak G, Wilsch M, Spoerl E, Seiler T. Collagen Fiber Diameter in the Rabbit Cornea After Collagen Crosslinking by Riboflavin/UVA. *Cornea*. 2004;23(5):503-507.

107. Elsdale T. Collagen substrata for studies on cell behavior. *J Cell Biol*. 1972;54:626-637. http://jcb.rupress.org/content/54/3/626.abstract. Accessed April 11, 2012.

108. Masuda K, Aota Y, Muehleman C, et al. A novel rabbit model of mild, reproducible disc degeneration by an anulus needle puncture: correlation between the degree of disc injury and radiological and histological appearances of disc degeneration. *Spine (Phila Pa 1976)*. 2005;30(1):5-14. http://www.ncbi.nlm.nih.gov/pubmed/15626974.

109. Kim Y, Bonassar J, Grodzinsky AJ. The Role of Cartilage Streaming Potential, Fluid Flow and Pressure in the Stimulation of chondrocyte Biosynthesis During Dynamic Compression. *J Biomech*. 1995;28(9).

110. Elliott DM, Sarver JJ. Young investigator award winner: validation of the mouse and rat disc as mechanical models of the human lumbar disc. *Spine (Phila Pa 1976)*. 2004;29(7):713-722. http://www.ncbi.nlm.nih.gov/pubmed/15087791.

111. Masuda K, Aota Y, Muehleman C, et al. A novel rabbit model of mild, reproducible disc degeneration by an anulus needle puncture: correlation between the degree of disc injury and radiological and histological appearances of disc degeneration. *Spine (Phila Pa 1976)*. 2005;30(1):5-14. http://www.ncbi.nlm.nih.gov/pubmed/15626974.

112. Rohlmann A, Claes LE, Bergmannt G, Graichen F, Neef P, Wilke HJ. Comparison of intradiscal pressures and spinal fixator loads for different body positions and exercises. *Ergonomics*. 2001;44(8):781-794. doi:10.1080/00140130120943.

113. Hussain M, Natarajan RN, Chaudhary G, An HS, Andersson GBJ. Relative contributions of strain-dependent permeability and fixed charged density of proteoglycans in predicting cervical disc biomechanics: a poroelastic C5-C6 finite element model study. *Med Eng Phys*. 2011;33(4):438-445. doi:10.1016/j.medengphy.2010.11.011.

114. Guterl CC, See EY, Blanquer SBG, et al. Challenges and strategies in the repair of ruptured annulus fibrosus. *Eur Cell Mater*. 2013;25:1-21.

http://www.ncbi.nlm.nih.gov/pubmed/23283636.

115. Michalek AJ, Funabashi KL, Iatridis JC. Needle puncture injury of the rat intervertebral disc affects torsional and compressive biomechanics differently. *Eur Spine J*. 2010;19(12):2110-2116. doi:10.1007/s00586-010-1473-z.

116. Michalek AJ, Buckley MR, Bonassar LJ, Cohen I, Iatridis JC. Measurement of local strains in intervertebral disc anulus fibrosus tissue under dynamic shear: contributions of matrix fiber orientation and elastin content. *J Biomech*. 2009;42(14):2279-2285. doi:10.1016/j.jbiomech.2009.06.047.

117. Schroeder Y, Elliott DM, Wilson W, Baaijens FPT, Huyghe JM. Experimental and model determination of human intervertebral disc osmoviscoelasticity. *J Orthop Res*. 2008;26(8):1141-1146. doi:10.1002/jor.20632.

118. Barbir A, Michalek AJ, Abbott RD, Iatridis JC. Effects of enzymatic digestion on compressive properties of rat intervertebral discs. *J Biomech*. 2010;43(6):1067-1073. doi:10.1016/j.jbiomech.2009.12.005.

119. Cortes DH, Han WM, Smith LJ, Elliott DM. Mechanical properties of the extra-fibrillar matrix of human annulus fibrosus are location and age dependent. *J Orthop Res*. 2013;31(11):1725-1732. doi:10.1002/jor.22430.

120. O'Connell GD, Guerin HL, Elliott DM. Theoretical and uniaxial experimental evaluation of human annulus fibrosus degeneration. *J Biomech Eng*. 2009;131(11):111007. doi:10.1115/1.3212104.

121. Schutgens EM, Tryfonidou MA, Smit TH, et al. Biomaterials for intervertebral disc regeneration: Past performance and possible future strategies. *Eur Cells Mater*. 2015;30:210-231.

122. Puetzer JL, Bonassar LJ. High Density Type I Collagen Gels for Tissue Engineering of Whole Menisci. *Acta Biomater*. 2013;(May). doi:10.1016/j.actbio.2013.05.002.

123. Hudson KD, Alimi M, Grunert P, Härtl R, Bonassar LJ. Recent advances in biological therapies for disc degeneration: tissue engineering of the annulus fibrosus, nucleus pulposus and whole intervertebral discs. *Curr Opin Biotechnol*. 2013;24(5):872-879. doi:10.1016/j.copbio.2013.04.012.

Chapter 3

1. Bron JL, Helder MN, Meisel HJ, et al. Repair, regenerative and supportive therapies of the annulus fibrosus: achievements and challenges. Eur Spine J. 2009; 18:301–13. [PubMed: 19104850]

2. Lebow RL, Adogwa O, Parker SL, et al. Asymptomatic same-site recurrent disc herniation after lumbar discectomy: results of a prospective longitudinal study with 2-year serial imaging. Spine. 2011; 36:2147–51. [PubMed: 21343849]

3. Ambrossi GL, McGirt MJ, Sciubba DM, et al. Recurrent lumbar disc herniation after single-level lumbar discectomy: incidence and health care cost analysis. Neurosurgery. 2009; 65:574–8. discussion 8. [PubMed: 19687703]

4. McGirt MJ, Eustacchio S, Varga P, et al. A prospective cohort study of close interval computed tomography and magnetic resonance imaging after primary lumbar discectomy: factors associated with recurrent disc herniation and disc height loss. Spine. 2009; 34:2044–51. [PubMed: 19730212]

5. Carragee EJ, Spinnickie AO, Alamin TF, et al. A prospective controlled study

of limited versus subtotal posterior discectomy: short-term outcomes in patients with herniated lumbar intervertebral discs and large posterior anular defect. Spine. 2006; 31:653–7. [PubMed: 16540869]

6. Carragee EJ, Han MY, Suen PW, et al. Clinical outcomes after lumbar discectomy for sciatica: the effects of fragment type and anular competence. J Bone Joint Surg Am. 2003; 85-A:102–8. [PubMed: 12533579]

7. Carragee EJ, Don AS, Hurwitz EL, et al. 2009 ISSLS Prize Winner: Does discography cause accelerated progression of degeneration changes in the lumbar disc: a ten-year matched cohort study. Spine. 2009; 34:2338–45. [PubMed: 19755936]

8. Melrose J, Smith SM, Little CB, et al. Recent advances in annular pathobiology provide insights into rim-lesion mediated intervertebral disc degeneration and potential new approaches to annular repair strategies. European spine journal: official publication of the European Spine Society, the European Spinal Deformity Society, and the European Section of the Cervical Spine Research Society. 2008; 17:1131–48.

9. Bron JL, van der Veen AJ, Helder MN, et al. Biomechanical and in vivo evaluation of experimental closure devices of the annulus fibrosus designed for a goat nucleus replacement model. Eur Spine J. 2010; 19:1347–55. [PubMed: 20401620]

10. Fazzalari NL, Costi JJ, Hearn TC, et al. Mechanical and pathologic consequences of induced concentric anular tears in an ovine model. Spine. 2001; 26:2575–81. [PubMed: 11725238]

11. Hampton D, Laros G, McCarron R, et al. Healing potential of the anulus fibrosus. Spine. 1989; 14:398–401. [PubMed: 2718042]

12. Vadala G, Mozetic P, Rainer A, et al. Bioactive electrospun scaffold for annulus fibrosus repair and regeneration. Eur Spine J. 2012; 21(Suppl 1):S20–6. [PubMed: 22411039]

13. Ledet EH, Jeshuran W, Glennon JC, et al. Small intestinal submucosa for anular defect closure: long-term response in an in vivo sheep model. Spine. 2009; 34:1457–63. [PubMed: 19525836]

14. Schek RM, Michalek AJ, Iatridis JC. Genipin-crosslinked fibrin hydrogels as a potential adhesive to augment intervertebral disc annulus repair. Eur Cell Mater. 2011; 21:373–83. [PubMed: 21503869]

15. Borde, BH.; James, AR.; Härtl, R., et al. Repair of Defects in the Rat Tail Annulus Fibrosus Using Injectable High Density Collagen Gels; Orthopedic Research Society, ANNUAL MEETING 2012; San Francisco, CA. 2012.

16. Keorochana G, Johnson JS, Taghavi CE, et al. The effect of needle size inducing degeneration in the rat caudal disc: evaluation using radiograph, magnetic resonance imaging, histology, and immunohistochemistry. Spine J. 2010; 10:1014–23. [PubMed: 20970740]

17. Han B, Zhu K, Li FC, et al. A simple disc degeneration model induced by percutaneous needle puncture in the rat tail. Spine. 2008; 33:1925–34. [PubMed: 18708924]

18. Zou F, Jiang J, Lu F, et al. Efficacy of intradiscal hepatocyte growth factor injection for the treatment of intervertebral disc degeneration. Mol Med Rep.

2013; 8:118–22. [PubMed: 23632892]

19. Zhang H, Wang L, Park JB, et al. Intradiscal injection of simvastatin retards progression of intervertebral disc degeneration induced by stab injury. Arthritis Res Ther. 2009; 11:R172. [PubMed: 19912653]

20. Gullung GB, Woodall JW, Tucci MA, et al. Platelet-rich plasma effects on degenerative disc disease: analysis of histology and imaging in an animal model. Evid Based Spine Care J. 2011; 2:13–8. [PubMed: 23230401]

21. Sheikh H, Zakharian K, De La Torre RP, et al. In vivo intervertebral disc regeneration using stem cell-derived chondroprogenitors. J Neurosurg Spine. 2009; 10:265–72. [PubMed: 19320588]

22. Cross VL, Zheng Y, Won Choi N, et al. Dense type I collagen matrices that support cellular remodeling and microfabrication for studies of tumor angiogenesis and vasculogenesis in vitro. Biomaterials. 2010; 31:8596–607. [PubMed: 20727585]

23. Bowles RD, Williams RM, Zipfel WR, et al. Self-assembly of aligned tissue-engineered annulus fibrosus and intervertebral disc composite via collagen gel contraction. Tissue Eng Part A. 2010; 16:1339–48. [PubMed: 19905878]

24. Yu LP, Qian WW, Yin GY, et al. MRI assessment of lumbar intervertebral disc degeneration with lumbar degenerative disease using the Pfirrmann grading systems. PLoS One. 2012; 7:e48074. [PubMed: 23284612]

25. Lu DS, Shono Y, Oda I, et al. Effects of chondroitinase ABC and chymopapain on spinal motion segment biomechanics. An in vivo biomechanical, radiologic, and histologic canine study. Spine. 1997; 22:1828–34. discussion 34–5.

[PubMed: 9280018]

26. Cheng NC, Estes BT, Young TH, et al. Genipin-crosslinked cartilage-derived matrix as a scaffold for human adipose-derived stem cell chondrogenesis. Tissue Eng Part A. 2013; 19:484–96. [PubMed: 23088537]

27. Stewart JM, Schultz DS, Lee OT, et al. Collagen cross-links reduce corneal permeability. Invest Ophthalmol Vis Sci. 2009; 50:1606–12. [PubMed: 19060268]

28. Tirella A, Liberto T, Ahluwalia A. Riboflavin and collagen: New crosslinking methods to tailor the stiffness of hydrogels. Materials Letters. 2012; 74:58–61.

29. Guidry C, Grinnell F. Studies on the mechanism of hydrated collagen gel reorganization by human skin fibroblasts. J Cell Sci. 1985; 79:67–81. [PubMed: 3914484]

30. Staskowski PA, Ford CN, Inagi K. The histologic fate of autologous collagen injected into the canine vocal fold. Otolaryngol Head Neck Surg. 1998; 118:187–90. [PubMed: 9482550]

31. Harriger MD, Supp AP, Warden GD, et al. Glutaraldehyde crosslinking of collagen substrates inhibits degradation in skin substitutes grafted to athymic mice. J Biomed Mater Res. 1997; 35:137–45. [PubMed: 9135162]

32. Jarman-Smith ML, Bodamyali T, Stevens C, et al. Porcine collagen crosslinking, degradation and its capability for fibroblast adhesion and proliferation. J Mater Sci Mater Med. 2004; 15:925–32. [PubMed: 15477745]

33. Hashemi H, Seyedian MA, Miraftab M, et al. Corneal Collagen Cross-linking with Riboflavin and Ultraviolet A Irradiation for Keratoconus: Long-term

Results. Ophthalmology. 2013 [PubMed: 23583165]

Chapter 4

1. Andersson GB. Epidemiological features of chronic low-back pain. *Lancet* 1999;354:581-5.
2. Battie MC, Lazary A, Fairbank J, et al. Disc degeneration-related clinical phenotypes. *European spine journal : official publication of the European Spine Society, the European Spinal Deformity Society, and the European Section of the Cervical Spine Research Society* 2014;23 Suppl 3:S305-14.
3. Deyo RA, Weinstein JN. Low back pain. *The New England journal of medicine* 2001;344:363-70.
4. Bruske-Hohlfeld I, Merritt JL, Onofrio BM, et al. Incidence of lumbar disc surgery. A population-based study in Olmsted County, Minnesota, 1950-1979. *Spine* 1990;15:31-5.
5. Carragee EJ, Han MY, Suen PW, et al. Clinical outcomes after lumbar discectomy for sciatica: the effects of fragment type and anular competence. *The Journal of bone and joint surgery. American volume* 2003;85-A:102-8.
6. Laus M, Bertoni F, Bacchini P, et al. Recurrent lumbar disc herniation: what recurs? (A morphological study of recurrent disc herniation). *La Chirurgia degli organi di movimento* 1993;78:147-54.
7. Ambrossi GL, McGirt MJ, Sciubba DM, et al. Recurrent lumbar disc herniation after single-level lumbar discectomy: incidence and health care cost analysis. *Neurosurgery* 2009;65:574-8; discussion 8.

8. Frymoyer JW, Pope MH, Costanza MC, et al. Epidemiologic studies of low-back pain. *Spine* 1980;5:419-23.
9. Barth M, Diepers M, Weiss C, et al. Two-year outcome after lumbar microdiscectomy versus microscopic sequestrectomy: part 2: radiographic evaluation and correlation with clinical outcome. *Spine* 2008;33:273-9.
10. Frei H, Oxland TR, Rathonyi GC, et al. The effect of nucleotomy on lumbar spine mechanics in compression and shear loading. *Spine* 2001;26:2080-9.
11. O'Connell GD, Malhotra NR, Vresilovic EJ, et al. The effect of nucleotomy and the dependence of degeneration of human intervertebral disc strain in axial compression. *Spine* 2011;36:1765-71.
12. DePalma MJ, Ketchum JM, Saullo TR, et al. Is the history of a surgical discectomy related to the source of chronic low back pain? *Pain physician* 2012;15:E53-8.
13. Guterl CC, See EY, Blanquer SB, et al. Challenges and strategies in the repair of ruptured annulus fibrosus. *European cells & materials* 2013;25:1-21.
14. Ahlgren BD, Lui W, Herkowitz HN, et al. Effect of anular repair on the healing strength of the intervertebral disc: a sheep model. *Spine* 2000;25:2165-70.
15. Bron JL, Vonk LA, Smit TH, et al. Engineering alginate for intervertebral disc repair. *J Mech Behav Biomed Mater* 2011;4:1196-205.
16. Bron JL, Helder MN, Meisel HJ, et al. Repair, regenerative and supportive therapies of the annulus fibrosus: achievements and challenges. *European spine journal : official publication of the European Spine Society, the European*

Spinal Deformity Society, and the European Section of the Cervical Spine Research Society 2009;18:301-13.

17. Bailey A, Araghi A, Blumenthal S, et al. Prospective, multicenter, randomized, controlled study of anular repair in lumbar discectomy: two-year follow-up. *Spine* 2013;38:1161-9.
18. Bhattacharjee M, Miot S, Gorecka A, et al. Oriented lamellar silk fibrous scaffolds to drive cartilage matrix orientation: towards annulus fibrosus tissue engineering. *Acta biomaterialia* 2012;8:3313-25.
19. Chang G, Kim HJ, Vunjak-Novakovic G, et al. Enhancing annulus fibrosus tissue formation in porous silk scaffolds. *Journal of biomedical materials research. Part A* 2010;92:43-51.
20. Nerurkar NL, Baker BM, Sen S, et al. Nanofibrous biologic laminates replicate the form and function of the annulus fibrosus. *Nat Mater* 2009;8:986-92.
21. Schek RM, Michalek AJ, Iatridis JC. Genipin-crosslinked fibrin hydrogels as a potential adhesive to augment intervertebral disc annulus repair. *European cells & materials* 2011;21:373-83.
22. Vadala G, Mozetic P, Rainer A, et al. Bioactive electrospun scaffold for annulus fibrosus repair and regeneration. *European spine journal : official publication of the European Spine Society, the European Spinal Deformity Society, and the European Section of the Cervical Spine Research Society* 2012;21 Suppl 1:S20-6.

23. Ledet EH, Jeshuran W, Glennon JC, et al. Small intestinal submucosa for anular defect closure: long-term response in an in vivo sheep model. *Spine* 2009;34:1457-63.

24. Duncan TJ, Tanaka Y, Shi D, et al. Flow-manipulated, crosslinked collagen gels for use as corneal equivalents. *Biomaterials* 2010;31:8996-9005.

25. Schneider U, Rackwitz L, Andereya S, et al. A prospective multicenter study on the outcome of type I collagen hydrogel-based autologous chondrocyte implantation (CaReS) for the repair of articular cartilage defects in the knee. *The American journal of sports medicine* 2011;39:2558-65.

26. Grunert P, Borde BH, Hudson KD, et al. Annular repair using high-density collagen gel: a rat-tail in vivo model. *Spine* 2014;39:198-206.

27. Grunert P, Borde BH, Towne SB, et al. Riboflavin crosslinked high-density collagen gel for the repair of annular defects in intervertebral discs: An in vivo study. *Acta biomaterialia* 2015;26:215-24.

28. Bowles RD, Gebhard HH, Hartl R, et al. Tissue-engineered intervertebral discs produce new matrix, maintain disc height, and restore biomechanical function to the rodent spine. *Proc Natl Acad Sci U S A* 2011;108:13106-11.

29. Mueller SM, Shortkroff S, Schneider TO, et al. Meniscus cells seeded in type I and type II collagen-GAG matrices in vitro. *Biomaterials* 1999;20:701-9.

30. Yu LP, Qian WW, Yin GY, et al. MRI assessment of lumbar intervertebral disc degeneration with lumbar degenerative disease using the Pfirrmann grading systems. *PloS one* 2012;7:e48074.

31. Grunert P, Hudson KD, Macielak MR, et al. Assessment of intervertebral disc degeneration based on quantitative magnetic resonance imaging analysis: an in vivo study. *Spine* 2014;39:E369-78.

32. Lu DS, Shono Y, Oda I, et al. Effects of chondroitinase ABC and chymopapain on spinal motion segment biomechanics. An in vivo biomechanical, radiologic, and histologic canine study. *Spine* 1997;22:1828-34; discussion 34-5.

33. Oehme D, Ghosh P, Shimmon S, et al. Mesenchymal progenitor cells combined with pentosan polysulfate mediating disc regeneration at the time of microdiscectomy: a preliminary study in an ovine model. *Journal of neurosurgery. Spine* 2014;20:657-69.

34. Sato M, Kikuchi M, Ishihara M, et al. Tissue engineering of the intervertebral disc with cultured annulus fibrosus cells using atelocollagen honeycomb-shaped scaffold with a membrane seal (ACHMS scaffold). *Medical & biological engineering & computing* 2003;41:365-71.

35. Vadala G, Russo F, Pattappa G, et al. The transpedicular approach as an alternative route for intervertebral disc regeneration. *Spine* 2013;38:E319-24.

36. Vadala G, Sowa G, Hubert M, et al. Mesenchymal stem cells injection in degenerated intervertebral disc: cell leakage may induce osteophyte formation. *Journal of tissue engineering and regenerative medicine* 2012;6:348-55.